This is to certify that the

thesis entitled

Fluidity And Chromophore Interactions In Purple Membrane: Electron Spin Resonance, Fluorescence And Circular Dichroism Study

presented by

SHARMILA SHARAD GUPTE

has been accepted towards fulfillment
of the requirements for

Ph.D. degree in Biophysics

M. A. V. Sayeem
Major professor

Date Jul 23 1978

O-7639

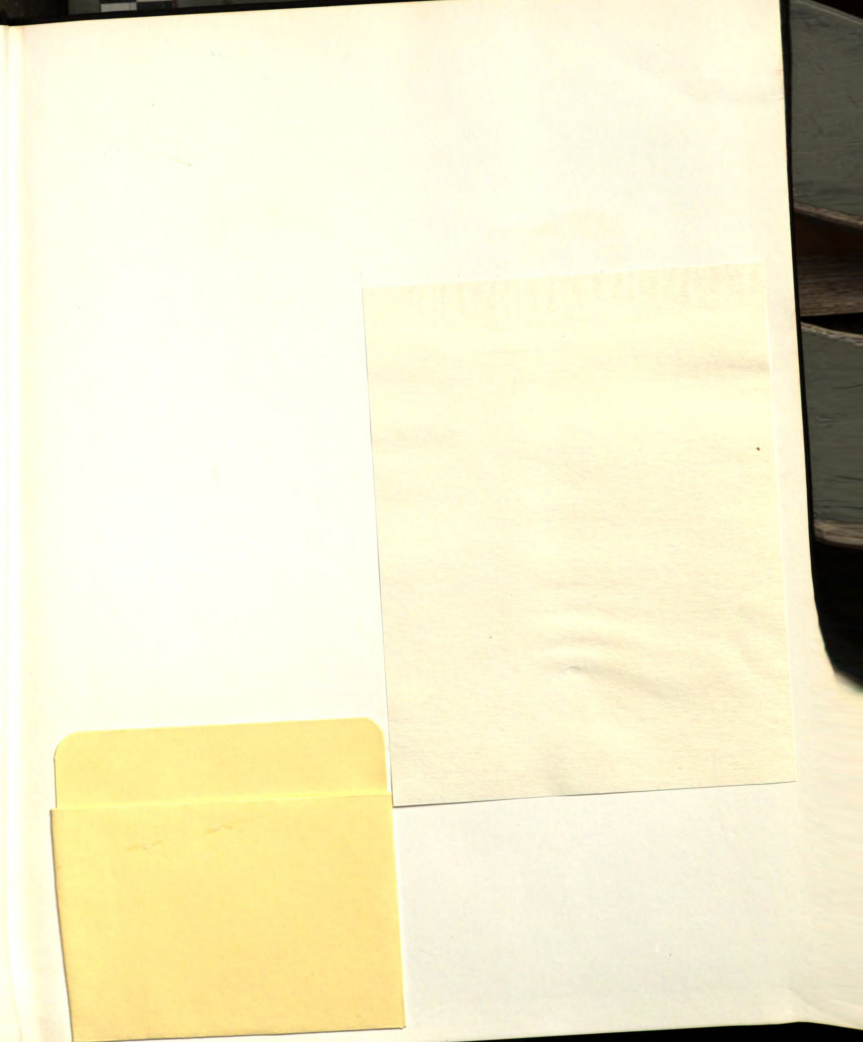

FLUIDITY AND CHROMOPHORE INTERACTIONS IN PURPLE MEMBRANE: ELECTRON SPIN RESONANCE, FLUORESCENCE AND CIRCULAR DICHROISM STUDY

By

Sharmila Sharad Gupte
(Shaila Kamalakar Karkhanis)

A DISSERTATION

Submitted to
Michigan State University
in partial fulfilment of the requirements
for the degree of

DOCTOR OF PHILOSOPHY

Department of Biophysics

1978

FLUIDITY AND CHROMOPHORE INTERACTIONS IN PURPLE MEMBRANE: ELECTRON SPIN RESONANCE, FLUORESCENCE AND CIRCULAR DICHROISM STUDY

By

Sharmila Sharad Gupte
(Shaila Kamalakar Karkhanis)

AN ABSTRACT OF A DISSERTATION

Submitted to
Michigan State University
in partial fulfilment of the requirements
for the degree of

DOCTOR OF PHILOSOPHY

Department of Biophysics

1978

ABSTRACT

FLUIDITY AND CHROMOPHORE INTERACTIONS IN PURPLE MEMBRANE: ELECTRON SPIN RESONANCE, FLUORESCENCE AND CIRCULAR DICHROISM STUDY

By

Sharmila Sharad Gupte

(Shaila Kamalakar Karkhanis)

Halobacterium halobium is a halophilic bacterium which requires 4 M NaCl in its growth medium. It exhibits differentiated purple membrane (pm) regions in the cytoplasmic membrane. The pm forms a rigid lattice of two-dimensional crystalline array. Bacteriorhodopsin is the only protein in the pm, its chromophore is a retinal covalently bound to an ϵ-amino group of a lysine via a Schiff base. The circular dichroism (CD) spectrum of pm shows a positive and a negative band, indicating exciton interaction between the chromophores of protein trimer.

In this study, we have examined the fluidity of the pm and cell membrane vesicles (cmv) using spin and fluorescence probe fatty acids. These probes have shown that the cmv are rigid, although less rigid than pm. Nitroxyl labelled (5-NS) pm exhibits a phase transition at about 31°C whereas the cmv show a phase transition at about 22°C. In cmv, the rigidity extends at least to the twelfth carbon position reflecting a tight packing. Relative fluidities of the pm and the cmv can be measured also using changes in the fluorescence wavelength maxima of anthroyl stearate (AS) probe. The emission maxima of AS probe in phosphatidyl choline vesicles, cmv and pm occur at 446, 437 and 435 nm respectively. The blue shift in the emission maxima reflect an increasing degree of rigidity of the membrane. In the pm, there is an additional peak at 417 nm. This probably arises from AS probe molecules in the pm which are tightly packed such that the anthracene moiety is twisted out of plane with respect to the carboxyl group. There are two populations of AS molecules in the pm as detected by fluorescence decay measurements, one near bacteriorhodopsin and undergoes efficient energy transfer to the chromophore. The other population lies in the bulk lipid phase. The rigidity of the pm seems to be due to a high ratio of protein:lipid and interdigitation of protein in the membrane.

Our studies of chromophore-chromophore exciton interaction using absorption spectroscopy confirms published

CD data. Stepwise reconstitution of a bleached pm shows that the absorption spectrum of the monomer lies at shorter wavelength compared with the trimer. The orientation of retinal seems to be head to tail at about 20° from the plan plane of the membrane. We interpret the optical activity around 355 nm in bleached pm as that retinal oxime occupies the cavity even after bleaching. Our results show that the retinal oxime can be removed by retinal during the reconstitution. We have succeeded in obtaining a fluorescence analog of bacteriorhodopsin by incorporating diphenyl hexatriene (DPH) in bleached pm. The DPH replaces the retinal oxime. Such an approach may prove valuable in exmining the nature of the chromophore cavity.

A photophysical study of a fluorescence polarity probe (dansyl sulfanoamide) provides data on its emission properties (quantum yield, emission maximum, fluorescence lifetime) in media of different polarities and in ethanol as a function of temperature. This study required us to obtain solvent contraction factors at different temperatures. Our study of the emission properties of anthroyl stearate in different solvents at room temperature and at 77°K show that in addition of being a polarity probe, it is also a fluidity and a "packing" probe.

Our study has pointed out numerous new directions for future work on H. halobium and its purple membrane.

To
my parents, family
and friends
who helped to be
what I am today

ACKNOWLEDGMENTS

I would like to express my deep appreciation to my adviser, Dr. M. A. El-Bayoumi, for his guidance and understanding. Without his support and parental affection, this study might not have been completed. I appreciate the freedom given for the selection of the dissertation topic. Part of this work was done in Dr. Haug's laboratory. I am indebted to Dr. Haug for his guidance, support and use of the PRL facilities. Also, I would like to thank Dr. McGroarty for her advice on various matters and her friendship and understanding during the course of the study. I would like to thank my dissertation committee composed of Drs. El-Bayoumi, Haug, McGroarty and Popov for their useful suggestions. I would like to thank Dr. J. I. Johnson, Chairman, Biophysics dept for his advice on departmental matters.

I would like to thank my colleagues and friends David Carr, Dr. Chang Chen, Dr. David Johnson, Barbara Kennedy, Denise Mazorow, Gary Smith and Herman Weller for making this study memorable. Special thanks to David Carr for his expert assistance with Time Resolved Spectrofluorimeter

and sptropolarimeter and to Denise Mazorow for typing the rough draft of the dissertation.

I would like to thank Dr. Zand, University of Michigan for the use of the Spectropolarimeter.

I wish to express thanks to my husband, Dr. Sharad Gupte for his patience and understanding. Without his efforts, this study could not have been initiated. Also to my brother, Rajiv Karkhanis for his help. Finally, very special thanks to a very special person, my son, Naren for enduring through the course of this work.

This work was supported by Department of Human Medicine and Department of Osteopathic medicine, Michigan State University.

TABLE OF CONTENT

LIST OF FIGURES

LIST OF TABLES

CHAPTER 1

INTRODUCTION

A gram negative bacterium, Halobacterium halobium grows optimally in near saturating salt concentrations. In the presence of light and at low rates of aeration, the bacterium forms distinct purple patches contiguous with the cytoplasmic membrane. When the NaCl concentration of the suspending medium is lowered to 1.0 M NaCl, the cell wall, which is made of two layers of protein, disintegrates and closed cytoplasmic membrane (cmv) remain intact. Dialysis against deionized, distilled water yields purple membrane (pm) patches, rest of cytoplasmic membrane solubilizes (Oesterhelt & Stoeckenius, 1971),(Stoeckenius & Rowen, 1967),(Blaurock et al, 1976).The difference in the stability of pm and cmv to water was investigated in this study by using spin and fluorescence probes. The pm is a very interesting biological membrane to study. It has only one protein bacteriorhodopsin (bR) which makes it uniform in structure compared with other biological membranes. Therefore, X-ray diffraction and electron microscopy of the architecture of pm have yielded valuable information about this membrane which may be extended to other membranes. These techniques show that the pm is composed of a rigid lattice of two dimensional crystalline array of P3 symmetry. The crystalline lattice of pm indicates rigid

membrane which is substantiated by our ESR and fluorescence study of pm using fatty acid probes. Electron microscopy of tilted unstained pm shows that 70%-80% of the protein of the purple membrane, bR, consists of 7 α-helices, almost perpendicular to the plane of the membrane. Three molecules pf bR form a trimeric unit which may be responsible for the hexagonal lattice structure of pm seen with electron microscopy (Henderson & Unwin, 1975). Recent studies with freeze-fracture of pm show that the interaction between protein entities may extend to between 9 or 12 protein molecules (Fisher & Stoeckenius, 1977). Our studies of the pm in solution also indicate that the pm is a very rigid membrane and most of the lipids seem to be boundary lipids. The chromophore of bR, which absorbs at 560 nm, is a retinal covalently bound to an ϵ-amino group of a lysine, forming a protonated Schiff base with the protein (Oesterhelt & Stoeckenius, 1971). In native conformation, the retinal can occur as a 13-cis or an all-trans isomer. Absorption of a photon causes some conformational change in the protein, the Schiff base becomes unprotonated and a vectorial translocation of the proton takes place. This intermediate absorbs at 412 nm, and is called "bleached" pm as its purple color disappears. Within milliseconds, the pm converts to its native conformation, therefore, at moderate intensities, the 412 nm complex is undetectable. (Oesterhelt & Hess, 1973).Irradiating the pm with high intensity light between 500 nm and 700 nm and in the

presence of 0.2 M NH_2OH, pH 7.0 causes breaking of the covalent bond of retinal from the protein. The complex can be reconstituted by the addition of retinal in the absence of NH_2OH. Retinal is thought to be in a protein cavity which is unaccessible to solvent without light. Light induced conformational change makes it accessible (Konishi & Packer,1976). Our results indicate that retinal oxime occupies the "cavity" even after bleaching, however, it is displaced by retinal during reconstitution. We have succeeded in substituting retinal by a linear polyene, diphenyl hexatriene (DPH) which can be used as a fluorescence analog of bR.

Another important aspect of pm is the chromophore-chromophore exciton interaction between adjacent retinals (Bauer et al, 1976). Our results from absorption studies of stepwise reconstitution agree with the circular dichroism data. This interaction may be important in increasing the efficiency of photon absorption. The absorption of a photon causes a vectorial translocation of protons across the membrane, resulting in a proton gradient making the medium acidic. The light induced proton gradient is used by the cells for ATP synthesis.

The author is intrigued by various aspects of the H. halobium membrane, particularly pm. The complexity of the biological membranes and various functions performed by them are, in author's opinion, most important and contain interesting facts in terms of understanding a "living"

cell. Especially the pm, the degree of sophistication of its structure and function compared even with the visual pigments makes her wonder whether H. halobium (as well as other halobacteria species with a purple membrane) has evolved further compared with the rod outer segments.

Different probe molecules have been used to understand the structure and function of various biological macromolecules and membrane systems. An extensive study of the photophysics of fluorescence probes under various conditions is essential in order to extract meaningful information from the fluorescence studies of biological membranes.

According to the above rationale, the research reported here is divided into three parts: (A) A photophysical study of (i) a polarity fluorescence probe, dansyl sulfanoamide (DNSA) and (ii) a packing fluorescence probe, 12-(9anthroyl) stearate (AS) (Chapter 5). (B) The relative fluidity studies of pm and cmv using ESR and fluorescence probes (Chapter 6). (C) The investigation of the chromophore binding site and chromophore-chromophore interactions using fluorescence, absorbance and circular dichroism (CD) techniques (Chapter 7). Future directions for the continuation of these studies are outlined in Chapter 8.

In addition, a chapter on the membrane structure-function and a brief description of the techniques used in this study (Chapter 2) is included. A comprehensive literature review seems a necessity and, therefore, is included as Chapter 3.

CHAPTER 2

SECTION I

STRUCTURE AND FUNCTIONS OF BIOLOGICAL MEMBRANES

(a) Introduction:

Biological membranes play a crucial role in almost all cellular phenomena, yet, the understanding of the molecular organization of the membranes is still rudimentary. Once the plasma membranes were thought merely to be a barrier between the cytoplasm and the outside environment of the cell. However, now it is widely known that the plasma membrane is one of the most essential component of the cell.

(b) Functions of membranes:

Some functions attributed to the procaryote plasma membrane are (i) active transport (ii) electron trnasport and oxidative phosphorylation (iii) secretion of exocellular proteins, toxins and enzymes (iv) protein synthesis and membrane associated ribosomes (v) phospholipid and glycolipid biosynthesis (vi) DNA anchoring, replication and cell division (Salton, 1971). In addition to these functions, specialized membranes of eucaryote cell participate in functions such as cell-differentiation, cell-cell recognition, contact inhibition, density inhibition, synaptic transmission, drug and/or hormone interaction etc. (Edelman, 1976). The diversity of the functions of these membranes reflects the structural differences, i. e. the variation of the components of the membranes. For example,

the erythrocyte plasma membrane, which is a well-studied fluid mosaic membrane, contains 40% lipids, 52% proteins and 8% carbohydrates by weight (Steck, 1974). On the other hand, highly ordered structures of mitochondria and chloroplasts contain 80% proteins and 20% lipids. These membranes are responsible for the energy transduction mechanism. Similarly, the purple membrane contains 75% protein and 25% lipids (Oesterhelt & Stoeckenius, 1971) and is a highly ordered two dimensional crystalline structure which probably correlates to its photocoupling (Oesterhelt & Stoeckenius, 1973) and photosensing (Hildebrand & Dencher, 1975) function. From these examples, it seems that the higher the percentage of proteins in the cell membrane, the more specialized its function becomes. The matrices of these specific membranes must be highly organized to perform certain functions. In other words, there is likely to be a relationship between the high content of proteins and specialized membrane function.

(c) Membrane asymmetry:

Another aspect of structure-function correlation of biological membranes which has been emerging in recent years is the asymmetry in the membrane lipids (Gordesky, 1976) and proteins which may in turn be related to its function (Rothman & Lenard, 1977),(Wisnieski & Iwata, 1977). Although the membrane asymmetry has been discussed for many years, it is only recently that direct evidence has been obtained confirming the asymmetry at the molecular level.

Chemical modifications of exposed residues of the membrane proteins in the intact cells by some impermeable molecules shows that only the external surface of the cell is labelled. However, similar chemical modifications of leaky cells (permeable) show labelling of some other proteins in addition to the proteins in the intact cells. Also, the chemical modification of right-side-out and inside-out vesicles shows that different proteins are labelled in the two cases. These experiments indicate that some proteins on the external surface of the membrane are diffirent than the ones on the internal surface. In addition, the histochemical labels which can be visualized in an electron microscope and are specific for a particular enzyme can be used to investigate the sidedness of its active site. Ferritin labelled antibodies can be used to determine the location and orientation of antigenic determinants in the membrane(Singer, 1974). These studies have shown that the asymmetry of the membrane proteins (i) may be an important factor for Peter Mitchell's chemiosmotic hypothesis of vectorial ion transport across the membrane (ii) may be utilized in transport of metabolites across the membrane. (iii) may play an important role in membrane biogenesis (iv) may have different control mechanisms for a normal and a transformed cell (Nicolson, 1976). The glycoproteins and glycolipids are detected exclusively on the outer monolayer of the plamsa membrane where they serve as a link between the cell and its environment. In addition to

protein and carbohydrate asymmetry, the phospholipid asymmetry is also becoming evident in lipid bilayers and in natural membranes (Gordesky, 1976). The phospholipid asymmetry may be due to the difference in the charge of the polar group, however, its function in the biological membranes is still obscure.

(d) Nature of protein association with membranes:

In general, the proteins associated with a membrane can be classified into two broad categories. (i) Peripheral or extrinsic : The extrinsic proteins are mainly bound to the membrane by the 'ionic' forces, therefore, they can be isolated by changes in the ionic strength, pH, etc. (ii) Integral or intrinsic proteins: These integral proteins are essentially lipoproteins in which the lipids are closely associated with the protein and are essential for its function or conformation (Capaldi, 1974), (Singer & Nicolson, 1972),(Farias et al, 1975). Depending on the asymmetry of the membrane, the intrinsic proteins may be further classified as (1) ectoproteins which have their hydrophilic mass projecting beyond the extracytoplasmic surface (outside of plamsa membrane) of the lipid bilayer, (2) endoproteins which have most of their mass associated with the cytoplasmic side of the membrane (Rothman & Lenard, 1977) and (3) transmembrane proteins which asymmetrically span the bilayer from the intracellular to extracellular space (Henderson & Unwin, 1975), (Singer, 1974). The function of these transmembrane

proteins seems to be mainly the transport of ions and metabolites across the membrane by either conformational change or by a 'pore' mechanism.

(e) Membrane models:

From the above discussion, one may get a glimpse of the diversity of the membrane structure. Membrane models which may account for most of the experimental observations are discussed briefly.

The early membrane models consisted of a 'unit membrane' hypothesis in which all the lipids were in a thermodynamically favorable bilayer and the proteins were composed mainly of β-sheets which may extend in the bilayer to form a 'pore'. Although birefringence and small angle X-ray diffraction studies supported the notion of the unit membrane and stained electron micrographs of various specimens showed characteristic double tracks of unit membrane, later studies have questioned the validity of the methods used (Wallach & Winzler, 1974). The interaction of the intrinsic proteins with surrounding lipids is mainly hydrophobic contrary to the ionic interaction of the β-sheets.

Singer-Nicolson's fluid mosaic model (Singer & Nicolson, 1972) hypothesizes a fluid lipid bilayer interdigitated by proteins. On thermodynamic grounds, the noncovalent hydrophilic interaction among the polar heads of the phospholipids and the polar residues of the proteins and the hydrophobic interaction between the fatty acid

chains of lipids and the non-polar residues of the proteins, seem favorable. Also, lipids, (mainly their hydrophobic interaction) are essential for the activation of some, if not all, of the intrinsic enzymes which seem to stabilize the active conformation of the enzyme (Overath et al, 1976). According to the fluid mosaic model, most of the lipids and proteins are capable of rotational and translational diffusion in the membrane matrix (Lee, 1975). A major contribution to this model has been made by Frye and Edidin (1970) who investigated the membrane receptor properties of a cell-fusion heterokaryon. Individual cell antigens were labelled with different antibodies and allowed to diffuse after fusion. After 40 minutes, intermixing of two labels occured indicating fast diffusion of two types of antigen at growth temperature due to a fluid, mosaic membrane. Even in the fluid membrane, as much as 30% of the lipids may be immobolized (boundary lipids) due to a strong hydrophobic interaction with the proteins (Stier & Sackmann, 1973).

Although some membranes seem to fit in the fluid mosaic membrane model (e. g. rod outer segment membrane), others seem to be highly ordered membranes in a rigid crystalline lattice. The electron micrographs of a gap junction between the cells of mouse liver and the purple membrane of Halobacterium halobium both show a two-dimensional, rigid, hexagonal crystalline lattice (Goodenough & Stoeckenius, 1972),(Blaurock & Stoeckenius, 1971). The

boundary lipids of these membranes may comprise most or all of the lipids restricting the diffusion of both proteins and lipids. The polarization studies of the protein mobility in the purple membrane have shown that the protein appears to be particularly immobilized and has a rotational relaxation time of at least 20 msec (Naqvi et al, 1973). This is contrasted with the rotational relaxation time of rhodopsin of about 20 μsec (Cone, 1972).

(f) Mobility of proteins in the membrane:

In addition to the immobilization of proteins and lipids due to ordered structure, other mechanisms also alter the mobility of the membrane components. These are (i) Supramolecular functional aggregates: In case of erythrocyte ghosts, spetrin forms supramolecular aggregates which move as an aggregate due to cross-linking by spectrin's antibody. Also, in the mitochondrial inner membrane, a tight association between five different proteins makes uniform arrays throughout the membrane. This supramolecular association may increase the efficiency of electron transfer and its coupling to ATP synthesis (Capaldi, 1974). (ii) Ligand-induced rearrangement of proteins: 'capping' of cell surface receptors by lectins or antibodies may change the diffusion properties of the receptor proteins (Bretscher, 1976). (iii) The glycoproteins and glycolipids may have carbohydrate crosslinking and extensive ionic and hydrophobic interactions at the outer monolayer of the asymmetric membrane. These

interactions may change the diffusion of the membrane components significantly. If this is the case, the diffusion of an endoprotein may be higher than that of an ectoprotein and the diffusion of a transmembrane proteins of similar dimensions may represent an average diffusion. (iv) Divalent cations interact with lipids and proteins which causes crosslinking and structure fomring (Hauser et al, 1976). These effects decrease the mobility of the membranes such as rat synaptic plasma membrane (Breton et al, 1977). (v) Finally, the cytoskeletal attachment of microfilaments and microtubules may restrict and regulate the movement of proteins in the membrane (Linden & Fox, 1975). The cytoskeletal attachment exhibits a transmembrane control of the cell-surface receptors and may be very important for the surface modulation in cell-recognition and in cell-growth (Edelman, 1976).

SECTION II

FLUORESCENCE AND ELECTRON SPIN RESONANCE PROBES OF MEMBRANE

(a) Spectroscopic techniques:

It is evident from the discussion in the preceding section that the biological membranes are very complex and that various techniques need to be combined to investigate the structure and the function of the membranes. These techniques range from electron microscopy to the chemical analysis of the lipids. Spectroscopic techniques have been used widely to gain information about the membranes. X-ray diffraction and recently, electron diffraction of tilted, unstained specimens have been most successful for structure determination. However, the information obtained by these techniques is mainly static and time-averaged. The mechanism by which the structure enables the function cannot be determined by these techniques. Spectroscopic probe techniques provide insight into the correlation of the biological structure with its function. The techniques involved in the membrane structure-function relationship are (i) absorption (ii) emission (iii) optical rotation (iv) Raman and resonance Raman (v) nuclear magnetic resonance (NMR) (vi) electron spin resonance (ESR) and (vii) various aspects of the magnetic resonance techniques e. g. ENDOR, FDMCD (fluorescence detected magnetic (or natural) circular dichroism) etc.. The time domains

investigated by these techniques range from picosecond to infinitely long time on the molecular scale. Out of all the techniques mentioned here, the fluorescence and the electron spin resonance techniques are very sensitive. Also, the number of parameters that can be used to obtain meaningful information is very large. Probes of various specificities can be used with these techniques. The term 'probe' implies the penetration of a region by the molecule with no or minimal disturbance of that region. The spectroscopic probes can be divided into (i) intrinsic and (ii) extrinsic categories. Intrinsic probes are the naturally occuring chromophores, e. g. tryptophan retinal, chlorophyll, heme proteins (paramagnetic ferric ion), dopamine β-hydroxylase (paramagnetic copper). Extrinsic probes are the molecules which are sensitive to its local environemt. These are inserted in a system and the local parturbation is measured by the suitable spectroscopic technique.

Some of the physical parameters that can be measured with the fluorescence and the ESR techniques is discussed in the next two parts.

(b) Physical parameters of fluorescence probes:

(i)Emission maxima: If the dipole moment of a fluorescent molecule in the excited state is different than that in the ground state, the solvent molecules can relax around the excited state molecule prior to the emission. This results in the emission maximum shifting to a different energy. This type of molecule e. g. 2,6 anilino-

naphthalene sulfonate (ANS) shifts its emission maximum from 465 nm for a non-polar solvent to 515 nm for apolar solvent like water.

(ii) Quantum yield: Change in the quantum yield from non-polar to polar solvent is parallel to the emission maximum.

(iii) Life-time of the excited state: Total light emitted after a delta pulse of light is stopped depends on the rates of transitions which depopulate the lowest excited singlet state. For the probes in a homogeneous environment, the decay of the intensity is given by

$$F(t) = F_o e^{-t/\tau} \quad \text{.....2.1}$$

If the fraction of molecules have different degrees of the solvent relaxation, the decay of the intensity is given by

$$\frac{F(t)}{F_o} = F\sum_{i=1}^{n} a_i e^{-t/\tau_i} \quad \text{.....2.2}$$

where a_i is the fraction of the molecules which have the life-time of τ_i. A semi-logarithmic plot of the first equation is a straight line whereas for the second equation, it represents a superposition of each straight line components making it non-linear. The individual life-times can be resolved by deconvoluting the curve by various methods currently available (Ware, 1973),(Kennedy & El-Bayoumi, in preparation).

(iv) Polarization: If a fluorescent probe is excited by polarized light, its emission is maximally polarized if, during the life-time of the excited state, it will not have to rotate or change the position. For example, in a very viscous solution or if the probe is rigidly bound by hydrophobic and/or inoic interaction. The anisotropy is given by

$$A = \frac{I_{//} - I_{\perp}}{I_{//} + 2I_{\perp}} \quad \ldots\ldots\ldots\ldots\ldots\ldots 2.3$$

In the case of macromolecules which are rigid sphere and th the probe is firmly attached to it, the decay of anisotropy is given by

$$A(t) = A_o e^{-t/\phi} \quad \ldots\ldots\ldots\ldots\ldots\ldots 2.4$$

where ϕ = rotation correlation time,

$$\phi\,(\text{sec}) = \frac{\eta V}{K T} \quad \ldots\ldots\ldots\ldots\ldots\ldots 2.5$$

V = hydrated volume of sphere, η = viscosity,

$$V = \frac{M\,(v + h)}{N} \quad \ldots\ldots\ldots\ldots\ldots\ldots 2.6$$

M = molecular weight, v = specific volume,

h = hydration, N = Avogadro's number

In the case of rigid ellipsoidal molecules,

$$\frac{A(t)}{A_o} = \sum f_i \, e^{-(t/\phi)\Omega_i} \quad \text{.....2.7}$$

where Ω_i 's are related to the rotational diffusion about major and minor axes of the ellipoid.

(v) Quenching: Two types of fluorescence quenching can be observed.

(a) Static quenching which is an interaction between the probe and other molecule/molecules in the ground state to form non-fluorescent complexes.

$$\frac{F_o}{F} = 1 + K_s \left[Q\right] \quad \text{.....2.8}$$

Where F_o and F are the intensities in the absence and in the presence of the quencher and $\left[Q\right]$ is the concentration of the quencher. This type of quenching reduces the intensity without changing emission properties.

(b) Dynamic quenching: This process competes with the emission for the depopulation of the excited state, thereby, decreasing the intensity and the life-time of the excited state. In the case of the dynamic quenching,

$$\frac{F_o}{F} = 1 + K_D \left[Q\right] \quad \text{.....2.9}$$

Where $K_D = k\tau$, $k = 4\pi a D N'$ 2.10

a = sum of the molecular radii

N' = number of molecules/millimole

D = sum of diffusion constants

When both processes are present,

$$\frac{F_o}{F} = (1 + K_D [Q])(1 + K_S [Q]) \quad .....2.11$$

(vi) Energy transfer by Forster Mechanism: The electronic excitation energy can be transfered from a singlet excited molecule (donor) to an unexcited molecule (acceptor) if the fluorescence of the donor overlaps with the absorption of the acceptor. This type of energy transfer occurs by a transition dipole-dipole interaction. The rate of the energy transfer is given by

$$k_{DA} = 8.7 \times 10^{23} J K^2 n^{-4} k_e R^{-6} \text{ sec}^{-1} \quad .....2.12$$

Where J is the overlap integral

$$J = \frac{\int F_D(\lambda) \epsilon_A(\lambda) (\lambda)^4 d\lambda}{\int F_D(\lambda) d\lambda} \quad .....2.13$$

K = orientation factor, is 2/3 for random distribution of the donor and the acceptor.

n = refractive index of the medium

k_e = rate of donor emission.

$$k_{DA} = 1/\tau_D - 1/\tau_{D'} \quad .....2.14$$

$$k_e = \phi_{D'} \gamma_{D'} \quad \ldots\ldots\ldots\ldots\ldots\ldots\ldots\ldots \quad 2.15$$

D' = emission in the absence of the acceptor.
The distance R between the donor and the acceptor can be calculated by the above mechanism.

Other parameters that can be used to obtain meaningful information are (vii) excimer formation (viii) exciplex formation etc..

(c) Physical parameters of the electron spin resonance probes:

General discussion: The resonance condition of an unpaired electron in the magnetic field is describes by

$$\Delta E = h\nu = g \mu_\beta H \quad \ldots\ldots\ldots\ldots\ldots\ldots\ldots\ldots 2.16$$

With an appropriate condition of the external magnetic field and the corresponding resonance frequency, the energy is absorbed by a paramagnetic sample (Keith et al, 1973). (Fig. 2.1a). For the nitroxide spin probes, the ^{14}N nucleus has a spin value of 1 therefore, can take the nuclear spin quantum value of 1, 0, & -1. Consequently, the unpaired electron signal is split into three equal components called low-, mid-, and high-field lines. The absorption of energy is shown in Fig. 2.1b. The spectral parameters are normally measured from the first derivative spectrum, g denotes the center of the spectrum and a is the hyperfine coupling (Fig. 2.1c).

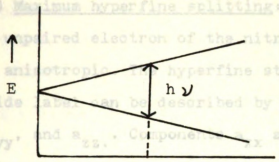

$$\Delta E = h\nu = g\mu_\beta H$$

Figure 2.1a Resonsnce condition for electron spin resonance

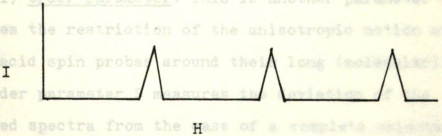

Figure 2.1b Absorption of energy by nitroxyl radical

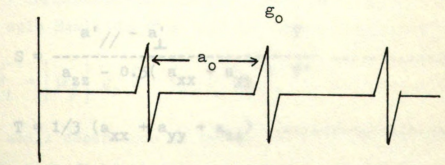

Figure 2.1c First derivative of absorption of nitroxyl radical, g_o is mid-field splitting and a_o is width of separation of signal.

Figure 2.1 Spectral parameters of electron spin resonance

(i) Maximum hyperfine splitting: The orbital geometry of the unpaired electron of the nitroxide spin labels is highly anisotropic. The hyperfine structure tensor of nitroxide label can be described by three components of a_{xx}, a_{yy}, and a_{zz}. Components a_{xx} and a_{yy} are in the direction of the nitroxyl ring and are small compared with a_{zz}. The component a_{zz} is in the direction of the fatty acid chain by convention. The maximum hyperfine splitting a_{zz} is the measure of the restriction of the motion (Fig. 2.2a).

(ii) Order parameter: This is another parameter that measures the restriction of the anisotropic motion of the fatty acid spin probes around their long (molecular) axis. The order parameter S measures the deviation of the observed spectra from the case of a complete orientation of the probe. For a completely oriented sample, S = 1, for a random sample, S = 0.

$$S = \frac{a'_{//} - a'_{\perp}}{a_{zz} - 0.5(a_{xx} + a_{yy})} \cdot \frac{T}{T'} \quad \text{.....2.17}$$

where $T = 1/3\ (a_{xx} + a_{yy} + a_{zz})$ 2.18

and $T' = 1/3\ (a'_{//} + a'_{\perp})$ 2.19

The parameters a_{xx}, a_{yy}, and a_{zz} are obtained from crystal (rigid lattice)measurements. $a'_{//}$ and $a'_{\perp}$ correspond to

the separation of the outer and inner hyperfine maxima (Fig. 2.2b). One can write the equation 2.17 as (Esser & Lanyi, 1973)

$$S = 0.568 \frac{a'_{//} - a'_{\perp}}{T'} \quad \ldots\ldots\ldots\ldots\ldots\ldots\ldots\ldots 2.20$$

(iii) Rotational correlation time: ESR spectrum of a spin label is extremely sensitive to the rate and the nature of motions the label undergoes. The rate of the molecular rotation can range from 10^{-10} seconds for small molecules in an isotropic, fluid medium to 10^{-7} seconds for fatty acid spin probe in an anisotropic, rigid lattice. For the nitroxyl spin moiety, the rotational correlation time τ_c is given by (Esser & Lanyi, 1973) (Fig. 2.2c):

$$\tau_c = 6.5 \times 10^{-10} W_o \left[\left(\frac{h_o}{h_{-1}} \right)^{1/2} - 1 \right] \quad \ldots\ldots 2.21$$

(iv) Partition coefficient: The g_o and the a_o tensors in the spin Hamilton of a rapidly tumbling nitroxide

$$\hat{H} = \left| \mu_\beta \right| g_o \hat{H} \cdot \hat{S}_z + a_o \hat{I} \cdot \hat{S} \quad \ldots\ldots\ldots\ldots 2.22$$

show a small dependence on the polarity of the solvent. Only the high field line is resolved at the 9.5 GH_z frequency. Nitroxides like TEMPO with appropriate solubility properties partition between the aqueous and the lipid regions of the wet, biological samples. The ratio of the

intensities A and B in the Fig. 2.2d is proportional to the relative amounts of nitroxides in the two environments.

(v) Proximity effects: These can be measured by two parameters (a) spin-spin interaction: Theoretical estimates show that when two nitrogen atoms containing two unpaired 2p electrons approach to within 15 Å of each other, the rate of the interchange of their electrons exceeds 10^7 per second. This rate is rapid enough to cause very pronounced changes in the ESR hyperfine splitting pattern. (b) reduction of the spin label by suitable agents: Suseptibility of the spin probes to the reducing agents depends on the accessibility of the probe. Normally, the fatty acid spin probe in the hydrocarbon medium is non-accessible to the reducing agents, however, if the probe is in the aqueous environment or if the membrane is leaky, the spin probe can get reduced.

(d) Applications of fluorescence and electron spin resonance probes for membrane studies:

The physical parameters for the fluorescent and ESR probes described in the previous section can be used to determine (i) membrane polarity (ii) membrane fluidity (iii) accessibility (iv) distances (v) electrical potentials.

(i) Membrane polarity: The most common fluorescent probe used to investigate the membrane polarity is ANS. As discussed earlier, the emission maximumaand quantum yield of fluorescence are the parameters used to determine

Figure 2.2a Anisotropy of hyperfine splitting

Figure 2.2b

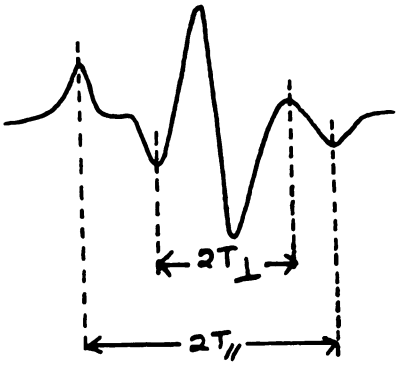

Figure 2.2c

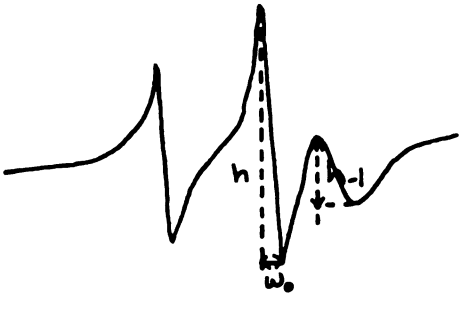

Figure 2.2d

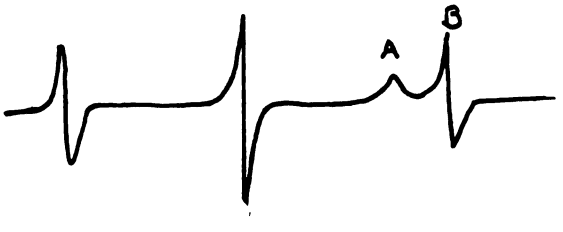

Figure 2.2 Spectral parameters of electron spin resonance

the polarity and the change in the polarity for a variety of membranes, e. g. erythrocytes, mitochondrial membranes, bacterial inner and outer membranes, excitable membranes etc. (Azzi, 1975). The location of ANS is shown to be below the polar heads of the lipids. However, ANS has no anchorage in the membrane, making the interpretation ambiguous. Most widely used ESR probes to investigate the polarity are TEMPO or TEMPENE which measure the partition coefficient for the membrane.

(ii) Fluidity: Fluidity of the lipids or the biological membrane is a measure of the extent of the packing of the neighbouring molecules which make the membrane matrix. Therefore, it represents the physical state of the lipids. Lipids, especially phospholipids exhibit interesting behavious in the presence of water. The order -▷ fluid or gel + liquid crystalline -▷ liquid cryastalline transition of the hydrated, lamellar phospholipids can be described as follows: In gel state below critical temperature, $T < T_l$, the hydrocarbon chains are in the all-trans conformation, perpendicular to the plane of the bilayer. On increasing the temperature, an endothermic transition occurs which is accompanied by a lateral expansion and a decrease in the thickness of the bilayer. In the liquid crystalline state, $T > T_h$, the hydrocarbon chains maintain an average orientation perpendicular to the plane of the bilayer but are disordered by a rapid trans/gauche rotational isomerization along the chains. Also, there is a simultaneous

dissociation of the ionic lattice of the phospholipids by the penetration of water. The temperature of the phase transition in the pure phospholipids-water system depends on the chain length and on the extent of unsaturation. Although the principle is similar, gel-liquid crystalline phase transitions in the lipids of the biological membranes are more complex than the hydrated phospholipids due to (a) the heterogeneity of the chain length and the degree of unsaturation of the fatty acids (b) different polar groups comprising the membrane (c) the presence of intrinsic membrane proteins (d) presence of cholesterol, lipopolysaccharides etc. (e) asymmetry of the membrane. To complicate the matter further, different lipids in the lipid mixtures 'melt' at different temperatures causing phase separation rather than phase transitions. In such a case, the ordered and the fluid lipids form seggregated domains.

Spin probes are most widely used to investigate the fluidity of the membranes. The physical parameters used are: the maximum hyperfine splitting $2T_{//}$, the rotational correlation time τ_c and the order parameter S. Most widely used ESR probes are nitroxide labelled fatty acids, phospholipids, cholestane etc.. The parameters determined for a fluorescence probe are the emission maximum, polarization of fluorescence, time resolved emission anisotropy, excimer emission and fluorescence quenching. The fluorescent probes used to investigate the lipid matrix of the membranes are

dissociation of the ionic lattice of the phospholipids by the penetration of water. The temperature of the phase transition in the pure phospholipids-water system depends on the chain length and on the extent of unsaturation. Although the principle is similar, gel-liquid crystalline phase transitions in the lipids of the biological membranes are more complex than the hydrated phospholipids due to (a) the heterogeneity of the chain length and the degree of unsaturation of the fatty acids (b) different polar groups comprising the membrane (c) the presence of intrinsic membrane proteins (d) presence of cholesterol, lipopolysaccharides etc. (e) asymmetry of the membrane. To complicate the matter further, different lipids in the lipid mixtures 'melt' at different temperatures causing phase separation rather than phase transitions. In such a case, the ordered and the fluid lipids form seggregated domains.

Spin probes are most widely used to investigate the fluidity of the membranes. The physical parameters used are: the maximum hyperfine splitting $2T_{//}$, the rotational correlation time τ_c and the order parameter S. Most widely used ESR probes are nitroxide labelled fatty acids, phospholipids, cholestane etc.. The parameters determined for a fluorescence probe are the emission maximum, polarization of fluorescence, time resolved emission anisotropy, excimer emission and fluorescence quenching. The fluorescent probes used to investigate the lipid matrix of the membranes are

AS, ONS, DPE, NPN, ANS, pyrene, perylene DPH etc.. Various probes and techniques described so far have shown that the membrane fluidity is the single most important parameter used to investigate membrane structure, contribution of the different components of the membrane, effect of adding or removing ions, ligands, state of energization of the membrane etc.. The resulting changes in the fluidity due to these factors are interpreted accordingly.

(iii) Accessibility: The probes bound to the membrane can be used as a possible measure of the accessibility of their binding sites by a number of molecules. Reduction of an ESR signal of a spin probe labelled at the different carbons along the fatty acid carbon backbone has been used to determine the 'leakiness' of the membrane by various agents. The extent of the fluorescence quenching of pyrene by oxygen is used as a measure of the penetration of the lipid matrix by polar molecules. A spin label analog of a local anesthetic was able to quench ANS fluorescence in the erythrocyte membrane indicating a close proximity of the fluorescence probe and the local anesthetic binding site.

(iv) Distances: The energy transfer between two fluorescent probes and the saturation effect or the use of biradical spin probes are the two approaches used to determine the distances in a membrane. The aromatic amino acid tryptophan of the membrane proteins is an energy donor for avariety of acceptor probes. The proximity between the protein moiety of the membrane and the DNS-choline in the

cholinergic receptor protein purified from the electric organ of Torpedo Marmorate has been established by the energy transfer.

(v) Lipid-protein interaction: This is another approach to investigate the membrane structure. The effect of detergents, bleaching etc. on rhodopsin has been studied by using meleimide spin probe covalently attached to the protein. Immobilization of the lipids, especially boundary lipids by the perturbation is also investigated using fatty acid spin probes.

CHAPTER 3

A LITERATURE REVIEW OF THE PURPLE MEMBRANE

(a) Characterization of H. halobium: An unusual purple membrane is a specialized part of the cell membrane of some extremely halophilic bacteria e. g. Halobacterium halobium (Bergy, 1974), (Larson, 1967). These bacteria need at least 3 M NaCl to be viable, and grow optimally at higher salt concentrations, even in salt crystals. Halobacteria are gram-negative. In normal growth conditions, these bacteria are rod shaped, about one micron in diameter and about 4 - 10 microns long, and have a bundle of flagella at each end. The wild type cells have vacuole membranes which are made up only of proteins. The vacuole membrane has a buyant density similar to pm (Stoeckenius & Kanau, 1968). The envelope of H. halobium consists of a cell wall made of two layers of protein and a cytoplasmic membrane. The cell wall shows a regular arrangement about 45 Å in diameter, possibly of a glycoprotein, from electron micrographs (Blaurock et al, 1976). In the case of another halobacterium H. salinarium, at least 50% of the cell wall protein is composed of a glycoprotein. This glycoprotein is very acidic and has N-and O-linked glysidic linkages (Mescher & Strominger, 1976). These authors claim that the cell-wall glycoprotein of H. salinarium is the first one of such linkage of a glycoprotein to be found in

procaryotes. Also, the sugars of the cell wall of this halobacterium are lipid linked indicating an envolvement of a cyclic biosynthetic pathway (Mescher et al, 1976). The halobacterium needs about 20 mM Mg^{2+} for normal growth, however, bacteria of aberrent shapes have been shown to grow and divide at lower Mg^{2+} concentrations (Henning, 1975). It seems that the divalent cation Mg^{2+} is needed to stabilize the cell wall proteins.

The intracellular physiology of the extreme halophiles is dominated by the massive accumulation of K^+ and Cl^- ions and by the effective exclusion of Na^+ (Brown, 1976). In general, enzymes associated with the cell membrane are most active at concentrations of 4 M NaCl or KCl, ribosomal enzymes have a specific requirement for 4 M KCl, and soluble enzymes have a wide range of salt optima (Brown, 1976). One interesting example of halophilic enzymes is alanine dehydrogenase from H. cutirubrum which has two specificities. As a reductive deaminase, the enzyme is fully active in the presence of high concentrations of K^+, Na^+, and NH_4, and also partially active with Cs^+ or Li^+. However, as an oxidative deaminase, it has an absolute requirement for K^+. In addition, its activity increases with the temperatures upto 70 ^oC, although the enzyme is not thermostable (Kim & Pitt, 1977).

The halobacteria are customarily grown in a complex media containing peptone and basal salts (see methods and materials) (Oesterhelt and Stoeckenius, 1974). A synthetic

medium containing sixteen amino acids and a variety of metal ions has been successfully used by various researchers with a few modifications (Gray & Pitts, 1976). Addition of 0.1% glycerol to the medium dramatically increases the biosynthesis of non-polar lipids e. g. carotenoids, squalenes, and retinal in the halophilic bacteria (Gochner et al, 1972).

The colonies of H. halobium are characterized by their transluscent orange color which is due to a high content of carotenoid pigments in the cell. The harvested pellets of cells grown at a high rate of aeration are orange compared with the grayish purple cells grown at low rate of aeration. It seems that there is a branching in the carotenoid pathway leading to retinal biosynthesis (Gouchner et al, 1972). The significance of retinal biosynthesis in conjunction with purple membrane formation is discussed at the end of this chapter. The non-purple or 'red' cell membrane contains enzymes for oxidative phosphorylation and other cellular functions. By using SDS-gel electrophoresis technique, the 'red' membrane of H. cutirubrum has been shown to contain at least 25 different bands indicating as many or more membrane polypeptides (Kushwaha et al, 1975). On the other hand, proteins of pm migrates as a single band. The molecular weight of this protein is 26,000 daltons. The lipids of the red membrane and pm are also different. In general, the lipids of extreme halophiles are very acidic(Brown, 1976). These

are diphytanyl ether linkages having sulfate, phosphate, or sugar polar groups. The lipids are branched and have a methyl group at every fourth carbon. However, only the pm lipids are sulfated (Kushwaha et al, 1975). A detailed discussion about red mebrane and pm lipids is presented in chapter 6.

As discussed in the introduction, the dialysis of H. halobium with deionized, distilled water yields purple patches (Stoeckenius & Rowen, 1967). Until Oesterhelt and Stoeckenius (1971) and Blaurock and Stoeckenius (1971) reported the existance of the unique purple membrane protein, bR, its similarities with the visual pigment and the hexagonal lattice structure, these bacteria were studied only for their ability to survive in a harsh environment (Oesterhelt & Stoeckenius, 1971), (Blaurock & Stoeckenius 1971). The observation that the pm has simple chemical composition and a repeating physical structure established it as a simple experimental system amenable to several approaches in various directions.

(b) Structure of purple membrane: The structure of pm has been studied extensively in recent years. The early freeze-fracture electron micrographs (Bluarock & Stoeckenius, 1971) show two types of structures in the cytoplasmic membrane. One shows an irregular structure and the other shows a regular structure. Comparison of these structures with isolated pm shows that the smoother, regular pattern is the pm part of the cytoplasmic membarne. X- ray diffaction

studies of dried and/or oriented films of pm show a regular hexagonal pattern having a P3 symmetry. An initial conclusion about the organization of the protein was that a continuous 34 Å layer was formed by the protein, lipids comprising the remaining 15 Å, separating pm into two domains (Bluarock & Stoeckenius, 1971). More data on the structure of pm have, however, shown that the protein-lipid distribution is different. According to newer models, which take into account the function of the bR as a light driven proton pump, spans the entire width of the lipid bilayer (Blaurock, 1975), (Henderson, 1975). These models describe pm as a symmetric unit of hexagonal P3 symmetry is composed of three asymmetric units. The electronmicrographs of tilted, unstained specimen show that there are seven 'rods' in each asymmetric unit and they are 10-12 Å apart. Adjacent rods are slightly inclined to one another at various angles from 0^{o} to 20^{o}. These rods seem to be 30 Å -40 Å long (Henderson, 1975). The X-ray diffaction pattern leaves little doubt that these rods are α-helices. Since bR has a molecular weight of 26,000, the α-helices make about 70-80% of the polypeptide. Incidentally, the corrected circular dichroism spectra of pm in the peptide bond absorbance region of 190 nm-240 nm range also show that the α-helical content of bR is 75% (Long et al, 1977). The overall dimensions of bR in the model based of seven α-helices are 25X35X45 Å. The longest of these dimension (45 Å) is perpendicular to

the plane of the membrane and parallel to the helices. The inner three helices from each protein almost touch each other; the outer twelve helices (four for each protein) make an outer ring which are slightly more inclined. The direction of the tilting of the outer helices is consistent with the interlocking of the amino acid side chains from adjacent α-helices -- that is the structure is a left-handed supercoil (Fig. 3.1). It appears from these studies that the protein is globular, is almost certainly exposed on both sides of the membrane and surrounded by lipids which are arranged in separate areas with a bilayer configuration (Henderson & Unwin, 1975). The region between the inner nine helices is presumed to be a lipid bilayer as UO_2^{2+} ions can bind to it (UO_2^{2+} binds to the phosphate groups of the lipid region similar to Mg^{2+}). This space between the three protein molecules is approximately 20 Å^2. Also, the three protein complex of the unit cell (dimension of 62 Å) is surrounded by lipids which are arranged in separate areas with a bilayer configuration (Henderson & Unwin, 1975). However, as discussed in chapter 5, the number of lipid molecules in pm seems insufficient to form a lipid domain. Packing of dihydrophytanyl chains warrants some discussion. From the monolayer studies, it has been shown that an average fatty acid phospholipid occupoes 45-50 Å^2. This area causes a 4.5 Å diffraction. The diphytanyl ether lipid occupies 60 Å^2 area, therefore, it should have a 5.1 Å diffraction. However, the X-ray diffraction data of

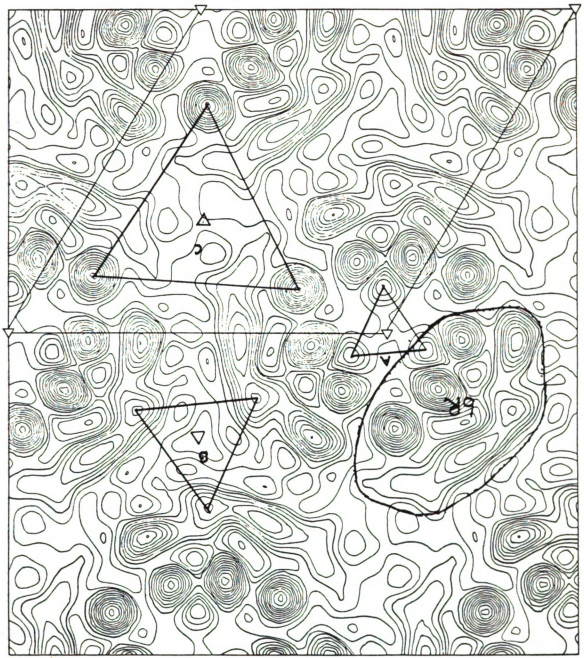

Figure 3.1 X-ray diffraction data for the structure of purple membrane.

Three axes of symmetry A, B, C can be seen: A seems to be the structural unit. Seven α-helices of a bacteriorhodopsin, an inner ring of nine helices and outer twelve helices can be detected (Henderson & Unwin, 1975).

extracted lipids show (Blaurock, 1975) that the packing distance of diphytanyl ethers in pm is smaller, showing a 4.9 Å diffraction instead of 5.1 Å. This indicates that the pm lipids are more tightly packed compared with their geometrically relaxed conformation lacking hindrance.

(c) Comparison of bacteriorhodopsin with visual pigment (rhodopsin):

The chromophore of the protein discussed above is a retinal which is covalently bound to the ϵ-amino group of a lysine, forming a Schiff base with the protein, similar to rhodopsin (R). Hence the name bacteriorhodopsin (bR). The similarities and differences in bR and R are listed below:

Similarities:

(1) Membrane bound protein, undergoes reversible conformational changes upon absorption of a photon.

(2) Retinal is covalently bound to an ϵ-amino group of a lysine.

(3) Schiff base is protonated in native conformation and unprotonated in bleached state.

(4) Considerable red shift in the retinal-Schiff base absorption due to the interaction with protein.

(5) Chromophore is all-trans in bleached conformation.

(6) Acts as a photoreceptor.

Differences between bacteriorhodopsin(bR) and rhodopsin(R):

bR	R
1) Mol. wt. 26,000, 75% protein	Mol. wt. 40,000, 60% protein
2) Absorption peak around 565 nm.	absorption peak around 500 nm.
3) Rigid membrane matrix of two dimensional crystalline array	Fluid membrane, protein free to rotate and translocate within plane of the membrane
4) Exists in trimeric units, exciton interaction between chromophores of neighbouring proteins	No such interaction documented
5) Chromophore can be 13-cis or all-trans in native bR	Chromophore is 11-cis in native R
6) Chromophore is covalently bound in all intermediates	Chromophore leaves the protein during bleaching
7) Proton gradient leading to ATP synthesis	Overall change in membrane permeability leading to action potential

In addition, the amino-acid sequence near the retinal binding site of bR is known (Bridgen & Walker, 1976). That sequence has been shown to be Val-Ser-Asp-Pro-Asp-Lys-Lys*-Phe-Tyr-Ala-Ile-Met-. The retinal binding site is at the seventh lysine which is not homologous to animal rhodopsin.

Also, it seems possible that the hydrophilic sequence Ser-Asp-Lys-Lys represents a link between two helices and the latter sequence is a beginning of the next helix penetrating in the membrane. However, the retinal binding site speculated by this argument does not agree with the bleaching and linear dichroism studies on investigation of the 'cavity' of retinal (see below). Amino acid analysis of bR shows that the protein is mostly in the hydrophobic region (Keefer & Bradshow, 1977). In contrast, the rhodopsin amino acid sequence and rotational relaxation studies show that a third of the polypeptide is hydrophilic. Hydrogen excahnge studies of bR and R show that 75% of the bR peptides are hydrogen bonded (180 H-bonded, 60 free) compared with 33% of the R peptides (100 H-bonded, 200 free) (Englander & Englander, 1977).

(d) Intermediates of bacteriorhodopsin:

The similarities between bR and R extend to the formation of the intermediates upon absorption of a photon. The initial studies showed that a suspension of pm in basal salts saturated with diethyl ether was bleached and absorbed maximally at 412 nm (412 nm complex or M_{412}) in the presence of light. This photochemical reaction was shown to be accompanied by the release of a proton during bleaching due to illumination and subsequent dark uptake (Oesterhelt & Hess, 1973). Other organic solvents e. g. dimethyl sulfoxide were similarly used (Oesterhelt et al, 1973). Low temperature and flash spectroscopy have been

used to gain insight into the photochemical intermediates of bR. Since bR cannot be bleached using ordinary light intensities, a high intensity laser beam has been employed for such studies. Stoeckenius and Lozier (1974) have shown the presence of at least four cyclic intermediates at low temperatures. Only the first intermediate bR_{570} -▷ bR_{610} requires light, the rest of them are thermal transitions. Similar work, including studies of the state of protonation of retinal-Schiff base has appeared later (Hess & Oesterhelt, 1974),(Oesterhelt 1974),(Chance et al, 1975), (Tokunaga et al, 1976),(Kung et al, 1975),(Lozier et al, 1975),(Lozier & Niederberger 1977). The quantum efficiency of the first intermediate is shown to be 0.4 for the forward process (Goldschmidt et al, 1976). According to these studies, at -196°C, bR_{570} can be converted into a roughly equal mixture of itself and a red-shifted photoproduct K_{610} by illumination with 500 nm light. This batho-bacteriorhodopsin (K_{610}) forms in less than 6 psec (Kaufman et al, 1976) and decays with a half-time of 2 μsec to L_{550} in the dark. The next intermediate, M_{412} has a formation time of approximately 40 μsec at room temperature. This intermediate, M_{412}, can be trapped in the salt-ether system by cooling to -196°C during illumination.A further intermediate, O_{640} is observed in experiments at 40°C but not at 0°C because of the temperature dependence of the rate constants (Dencher & Wilms, 1975),(Lozier et al, 1975). Also, an intermediate N_{520} is suspected because the

spectrum derived for M_{412} seems to vary with the temperature of the experiment. The half-time of N_{520} and O_{640} seems to be of the order of 5 μsec each (Lozier & Niederberger, 1977). Figure 3.2 gives a summary of the present understanding of the photochemical bleaching.

(e) Conformation of retinal in bacteriorhodopsin:

(i) Extraction of the chromophore: Most of the above experiments of the photochemical bleaching were performed using a 'light adapted' bR which absorbs maximally at 570 nm (LA_{570}). If the pm suspension is kept in the dark, its absorption maximum occurs at 560 nm (dark adapted, DA_{560}, also see Chapter 7, page 115). The chromophore of LA_{570} has been shown to be all-trans retinal, however, there is no agreement about the chromophore of DA_{560}. It was shown to be 1:1 mixture of all-trans and 13-cis by Pettei et al (1977) and Oesterhelt et al (1973); and excusively 13-cis by Jan (1975). Also, one of these studies have shown (Pettei et al, 1977) that the photointermediate M_{412} in a membrane modified by ether yields a 1:1 mixture of 13-cis and all-trans, whereas the M_{405} species produced by illumination of pm in 2M guanidine hydrochloride at high pH yields mainly 13-cis retinal (irreversible bleaching). It seems that the photochemical cycle of LA_{570} may involve an isomerization of the retinal chromophore from the all-trans to the 13-cis form. This is consistent with the observation that the interaction between the apoprotein and retinal seems more pronounced when the retinal is in

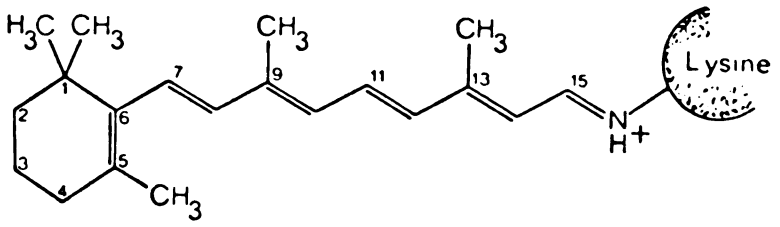

Figure 3.2a Chromophore of bacteriorhodopsin.

The chromophore all-trans retinal is covalently bound to an ε-amino group of a lysine of bacteriorhodopsin via a Schiff base.

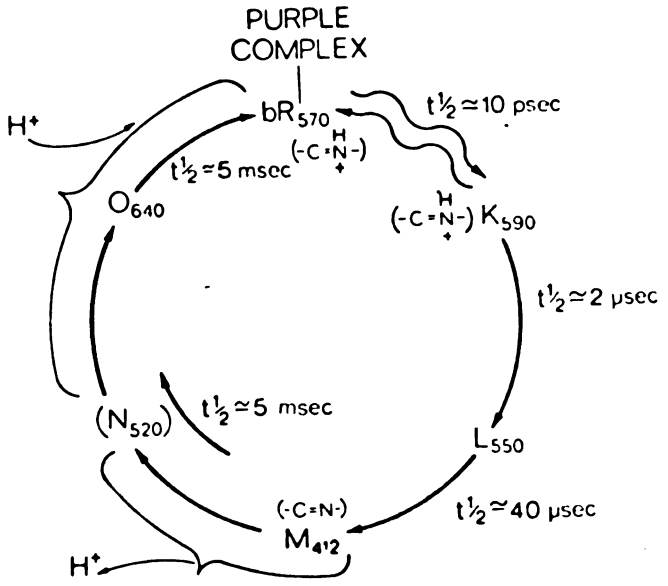

Figure 3.2b Model of bacteriorhodopsin intermediates.

A current model showing the intermediates detected in the photochemical cycle of the purple membrane by low temperature spectroscopy. One hydrogen ion is released and taken up again near the positions shown.

the all-trans form than when it is in the 13-cis form and also the apoprotein seems to impose more pronounced asymmetric constraints on the retinal in the all-trans form than in the 13-cis form (Becher & Cassim, 1976). Also, DA_{560} bleached in the dark with dimethyl sulfoxide and hydroxylamine produces only one isomer of the all-trans form, either syn or anti. In contrast, LA_{570} bleached with light and hydroxylamine (NH_2OH) produces both syn and anti isomers of all-trans retinal (Oesterhelt et al, 1973). These observations reflect changes, at the atomic level in the conformation of the protein or the retinal or both, near the Schiff base during illumination.

(ii) Resonance Raman spectroscopy of retinal in bR: The extraction of retinal has a conformation close to all-trans when it is bound to the protein. The problem remains as to how to explain the difference in the spectral properties of the bR intermediates upon absorption of a photon. Knowledge of the structure of retinal-protein complex and the state of isomerization of retinal induced by the conformational changes that follow the absorption of light seems to be the next step. Resonsnce Raman spectroscopy of pm and its photochemical intermediates offers an experimental approach to the analysis of the retianl conformations (Mendelsohn, 1973),(Lewis et al, 1974), (Marcus & Lewis, 1977),(Campion et al, 1977). Lewis et al have shown that in the pm complex bR_{570}, the Schiff base linkage is protonated and , that in the M_{412} complex, it is

unprotonated. Also, the first intermediate K_{590} has been shown to be protonated.(Lewis, 1976). The flash spectroscopic results showing that the release of a proton into solution is most closely correlated in time with the formation of M_{412} is in agreement with this. It seems from these experiments that the Schiff base may be directly involved in proton uptake and release , although the exact timing and involvement of other groups (residues) in the protein is not yet known. Kinetic resonsnce Raman data suggest (Marcus & Lewis, 1977) that there might be another intermediate, which contains the unprotonated Schiff base before M_{412} formation. Thus the release of the Schiff base proton can only be indirectly tied to the protein. The proton is eventually released forming a vectorial proton gradient across the membrane.

(f) Fluorescence of the chromophore in bR:

Excitation of bR in the 560-570 nm region shows very weak fluorescence around 740 nm (Alfano et al, 1976). The kinetics of fluorescence has been obtained by using picosecond laser pulses. At room temperature the life-time of fluorescence decay is estimated to be less than 3 psec (Alfano et al, 1976), however, Lewis et al (1977) estimate the life-time at room temperature to be 15 ± 3 psec amd have a quantum efficiency of 2.5×10^{-4}. The observation of fluorescence from the chromophore in bR is expected to provide some information about the character of an excited state that is produced before the K_{590} intermediate ,

presumably that particular excited state from which K_{590} is formed (Lewis et al, 1977). Also, the picosecond absorption measurements suggest (Kaufmann et al, 1976) the existence of a transient intermediate between bR_{570} and K_{590}.

(g) Chromophore interaction in bacteriorhodopsin:

The interaction of the chromophores of neighbouring bR molecules produces an exciton coupling which can be detected by absorption and by circular dichroism of the chromophore (Heyn et al, 1975),(Becher & Ebery 1976), (Kriebel & Albrecht, 1976). Different theories have been presented by various researchers and are discussed in detail in chapter 7. The model that accounts for the most of the data is a head to tail packing of three chromophores lying at about 20^{o} from the plane of membrane. The results of this model are in agreement with the linear dichroism studies (King et al, 1977). The distance between two β-ionone rings, calculated using this technique, is about 18.6 Å and the position of the ring is about one-third of the membrane from one surface.

(h) Light induced conformational changes in bacteriorhodopsin investigaed by cross-linking technique:

Cross-linking reagents like gluteraldehydes (Length= 7.5 Å) or more specific reagents dimethyl adipimidate, DMA (length=8.5 Å), dimethyl suberimidate, DMS (length=11.5 Å) have been used to cross-link bR in the presence and in the absence of light (Konishi & Packer, 1976),(Packer et al

1977). This type of cross-linking can be used to determine the degree of exposure of various residues due to light induced conformational changes. These experiments indicate that the cross-linking of DMA is substantially different in the presence of light. Liposomes made from the cross-linked pm show a difference in proton transport in the dark vs light treated samples. These researchers conclude that proton may be transferred through a channel or a pore.

(i) Proton gradient across the cell membrane of H. halobium:

The structure of pm and the conformational changes in bR have been discussed in the preceding sections. It has been pointed out that the conformational changes in bR cause deprotonation and reprotonation of the Schiff base via a complex mechanism which is not yet understood. However, this cyclic change in the retinal Schiff base causes the vectorial translocation of a proton in the cell from the cytoplamsic side to the outside causing net acidification of the medium. The net acidification of the medium can be explained as a protonmotive force (pmf) according P. Mitchell's chemiosmotic gradient hypothesis (Mitchell, 1961). Initial observations by Oesterhelt and Stoeckenius (1973) show that (i) H. halobium cells synthesize pm patches in the presence of light coupled with low oxygen supply and/or loss of other metabolites. (ii) oxygen consumption of the bacterium is reduced if it contains pm (iii) light lowers the pH of the medium in

which pm containing bacteria are suspended, led these and other researchers to postulate the pm as an alternate photosynthetic pigment. It was further shown (Danon & Stoeckenius, 1974) that light increases the ATP content of anaerobic, pm containing cells.

Early studies using liposomes containing pm and mitochondrial ATPase (Racker & Stoeckenius, 1974) showed that the protons can be translocated vectorially across the membrane. However, the direction of translocation of the protons observed in this study was opposite (medium alkaline) compared with whole cells (medium acidic) due to inside out incorporation of pm. These lipsomes were shown to phosphorylate ADP in the presence of light. This study and similar recent experiments using purified ATPase from a thermophile and well defined lipids instead of original mitochondrial hydrophobic fractions which contained electron transport chain proteins (Kagawa et al, 1977), supports the chemiosmotic theory of energy transduction in cell membranes. The liposomes generate a protonmotive force (pmf). The pmf consists of a potential gradient ($\Delta\psi$) and a pH gradient (Δ pH). The potential gradient is explained as an ionic gradient other protons and is given as follows:

$$p = \Delta\psi - \Delta \text{ pH} \quad \text{.....3.1}$$

$$\Delta\psi = \frac{RT}{F} \ln\left[\frac{I_o}{I_i}\right] \quad \text{.....3.2}$$

$$\text{Therefore, } \Delta p = \frac{RT}{F}\left[\ln\left[\frac{I_o}{I_i}\right] + \ln\left[\frac{H_o}{H_i}\right]\right] \quad \text{.....3.3}$$

Both the magnitude of the pH gradient (Δ pH) and the membrane potential ($\Delta\psi$) in cells and in resealed envelopes have been estimated using lipophilic ions e. g. tetraphenyl phosphonium (TPP^+), or triphenyl methyl phosphonium ($TPMB^+$) cation (Bogomolni, 1977) or fluorescence probes e. g. cyanine dye 3,3-dipentyloxadicarbocyanine (Renthal & Lanyi, 1976) and various buffers. For H. halobium cells kept anaerobically in dark, a total pmf consisting of both $\Delta\psi$ and Δ pH components (total 130 to 150 mV, interior negative) was achieved. This pmf increased further by 20-30 mV when the light was on. The pmf seems to be coupled to the active transport of Na^+ out of the vesicles (Lanyi & MacDonald, 1976) which is used as the driving force for the light induced transport of some amino acids (see next section). The development of a Na^+ gradient during illumination seems to play an important role in energy coupling. These and similar results indicate the existence of an electrogenic H^+/Na^+ antiport mechanism ($H^+/Na^+ > 1$) in H. halobium which facilitates the uphill Na^+ eflux. The gradients of Na^+ and H^+ are thus coupled to each other such that ($Na^+_{out} \gg Na^+_{in}$). These gradients seem to be capable of explaining some of the complexities of pmf (Lanyi & MacDonald, 1977). Blocking the ATP synthesing enzyme with the specific reagent dicyclohexyl-carbodiimide (DCCD) increases the pmf value to go on as high as 280 mV in the presence of light (Michel & Oesterhelt, 1976). Thus the electrochemical gradient

appears to be of the right size for its proposed function and can be induced by light in cell envelopes devoid of intracellular function. These measurements made by using cell-envelopes agree with those in which the pm is incorporated in black lipid membranes (Dancshazy & Karvaly, 1976),(Drachev et al, 1976), (Shieh & Packer, 1976). As discussed above, the origin of a pre-existing gradient present in the dark, in anaerobic cells may be concerned with the equilibrium of other ionic species across the cell membrane. The pmf causes phosphorylation of ADP with the ratio of 2.9 protons/ATP. Initial alkalization is explained in terms of pre-existing gredients across the membrane (Bogomolni et al, 1976).

(j) Light induced active transport of amino acids:

The vesicles used in the above study are also shown to accumulate amino acids in the presence of light (MacDonald & Lanyi, 1975). Subsequent studies have revealed a plausible mechanism for the amino acid transport across the membrane in response to light induced electrical and chemical gredients (Hubbard et al, 1976),(MacDonald & Lanyi, 1975). Nineteen out of twenty amino acids have been shown to be actively accumulated by these vesicles in response to illumination or to an artificially created Na^+ gradient. Sodium activated amino acid transport occurs in direct response to the pmf generated. Glutamate is transported only in response to a Na^+ gradient. Experimental evidence suggests that there are symmetrical carriers

that can transport amino acids equally well in both directions across the vesicle membrane depending on the direction of the driving force.

(k) Biogenesis of the purple membrane:

The biosynthesis of pm occurs only in the presence of light and at a low rate of aeration. Pm is a simple system by which one can study membrane biogenesis. It can also be used to investigate the spatial relation between the synthesis and insertion of a protein in the membrane. In the case of bR, the synthesis of retinal and bacterio-opsin are induced separately by a low oxygen tension. Free bacterio-opsin inhibits its own synthesis. Also, bacterio-opsin inhibits retinal biosynthesis by blocking cyclization of lycopene, a precursor of retinal. In short, both bacterio-opsin and retinal biosynthesis is induced separately. However, they can inhibit and control each other's induction (Sumper & Hermann, 1976, a & b). Also, the bacterio-opsin formed in the absence of retinal (due to nicotine inhibition) does not form a lattice structure with addition of retinal after extraction although it can form the lattice structure if the retinal is added to metabolizing cells. This indicates that some modification of bacterio-opsin occurs in living cells after the addition of retinal.

(l) Phototaxis in cell containing purple membrane:

Phototactic responses in H. halobium have been studied by Hildebrand & Dencher (1975). This response can be

divided into two types: (1) response to a reduction in the light intensity which has an action spectrum centered at 565nm and (2) response to increased light intensity which has an action spectrum with several peaks in the ultraviolet to blue region. The function of these responses seems to be to allow the bacteria to go to high intensity of light in 565 nm region but exclude it from areas near dsmaging UV light. The first response is dependent on the presence of pm in the membrane.

For more detailed information, a recent review by Henderson (1977) is recommended. On the other hand, for an introduction to the purple membrane without technical details, an article by Stoeckenius (1976) is sufficient.

CHAPTER 4

METHODS AND MATERIALS

METHODS:

(a) Culture conditions for Halobacterium halobium:

Halobacterium halobium strain R_1 (Mutant) was used for all membrane experiments. This mutant does not form gas vacuoles (see chapter 3, page 29); therefore, contamination due to intracytoplasmic membrane can be avoided. The bacteria were stored on a 1.8% agar + growth medium (see materials) slant at 5°C and transferred every three months. Preparation of a 10 litre culture (normally a 10 litre culture was necessary for a reasonable membrane yield) was started from a single colony. A single colony either from a slant or a perti-dish was transferred to 100 ml medium in a 250 ml De Young flask. The flask was placed on a gyratory shaker by Brunswick at 150 rpm. It was illuminated by two Sylvania 10 W cool white fluorescent lights approximately 30 inches above the flask. The intensity of light at the surface of the flask was approximately 0.5 mW. The cells from the colony were grown at 37°C until they reached a stationary phase. An inoculum for a 10 litre culture was obtained by growing 500 ml culture in each of two 1 litre De Young flasks from the starter 100 ml culture. Every time, 10% inoculum was used, the initial optical density (O. D.) was between 0.05 - 0.06 at 660 nm. The 10 litre culture

was grown at 37°C in a 5 gallon carboy which was placed in an incubation room. The intensity of light, provided by 12 cool white 10 W lights around the carboy, at the center of the carboy was approximately 1-3 mW/cm^2. The culture was aerated by a 4 inch teflon stirrer attached to a glass rod which was, in turn, attached to an overhead motor. The top of the carboy was open to air and the sterility was not maintained after the 10 litre culture was inoculated. However, the absence of any contamination was ensured by the following criteria: (i) the incubation room was periodically sterilized by UV lights. (ii) a sample from the carboy at the bacterium's stationary phase was streaked periodically on a perti-dish; no morphological change in the colonies was observed. (iii) the growth medium was left exposed to air for a long time and streaked to determine airbourne contamination and this also was negative. The initial O. D. of the cells in the carboy was approximately 0.06 and reached 0.3 at 660 nm after 150 hours. The turbidity at 660 nm was used as a measure of cell-growth, which was often verified by counting the cells in a Petrof-Hauser counter. The pm content of the cells was determined by the lysis of the cells with a 1:1 dilution using distilled water and measuring the O. D. at 560 nm. The pm content in our preparations was parallel to the cell growth (Fig. 4.1). However, the length of the H. halobium rods decreased as the cells reached a stationary phase.

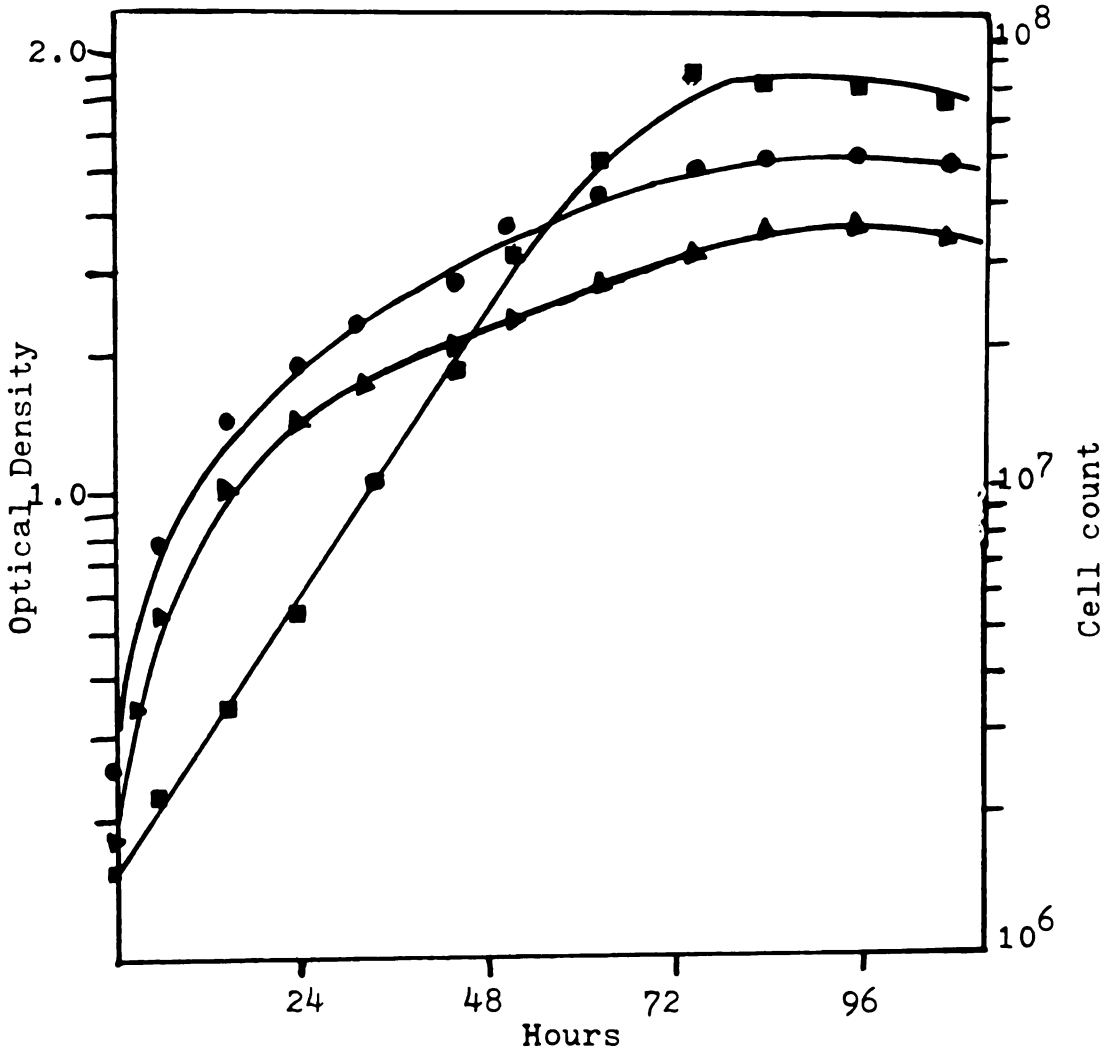

Figure 4.1 Growth curve of H. halobium

Halobacterium halobium were grown in 5 gallon carboy at optimum aeration and light intensity.

a. Optical density of the whole cells at 660 nm —●—●—●—
b. Optical density of the cells ruptured with 1:1 distilled water to measure pm content at 560 nm —▲—▲—▲—
c. Cell count measured using Petrof-Hauser counter and a phase contrast microscope at 300 magnification —■—■—■—

(b) Harvesting:

The bacteria were harvested by centrifugation in a GS-3 rotor at 8,000 rpm for 15 minutes. The pellets from a 10 litre culture were washed twice in salts 1 (see materials) and resuspended in 200 ml of salts 1. For the experiments where the fluidity and the phase transition temperature of cell membrane vesicles (cmv) and pm were comparedusing the spin and fluorescence probes, the harvested cells were divided into three parts; one part was used for isolation of cmv, the remaining two parts were used for the isolation of the pm.

(c) Isolation of H. halobium cell membrane vesicles:

The cells suspended in approximately 70 ml of salts 1 in a plastic bottle were placed in an ice bucket and liquid nitrogen was poured into the bucket such that the bacteria became completely frozen. The ice bucket containing the liquid nitrogen and the plastic bottle was stored overnight in a cold room. After thawing, the suspension became highly viscous due to the leaking of the cytoplasmic content. Two thousand kunitz units of DNAse I were added to the lysed cells and the suspension was stirred for one hour at room temperature. The cells were then dialyzed with 6 litres of salts 2 (see materials) (2 litre container with two changes every 4 hours). The dialysis tubing by Thomas Scientific Apparatus which had diameter of 5/8 inch and a molecular cutoff of 12,000 daltons was soaked in salts 2 for two hours to remove glycerol prior to use. The dialyzed cells

were centrifuged for 5 minutes at 6,000 rpm to remove cellular debris and then for 1 hour at 18,000 rpm in a SS-34 rotor. These two centrifugation steps were repeated until the color of the supernatant changed from deep orange to colorless or a very faint purple. A Thomas teflon tissue grinder Model C was used to resuspend the pellets. This procedure, essentially developed by Oesterhelt and Stoeckenius (1974) reportedly yields cytoplasmic membrane vesicles of H. haolbium without the cell wall. The cmv were stable for at least 3 months according to ESR data. However, they were used within a week for the spectroscopic measurements.

(d) Isolation of purple membrane:

The harvested cells were dialyzed against 15 litres of double distilled water (dd H_2O) in a 5 litre continuous flow dialysis apparatus. These were then treated with 4,000 kunitz units of DNAse I. The pm fraction was centrifuged for 1 hour at 18,000 rpm in a SS-34 rotor. After removal of supernatant, 5 ml of dd H_2O were added to the pellets an and they wer gently shaken so that the cell-debris remained as a pellet and the pm could be decanted. The decanted pm in water was homogenized with a Thomas tissue grinder. This process was repeated until no muddy-colored cell-debris remained and the color of the supernatant changed from deep orange to faint purple. The final pellet was resuspended in 10 ml of dd H_2O for a density gradient centrifugation. A SW Ti 41 rotor and Beckman LB ultracentrifuge

was used for this centrifugation. A continuous 30%-50% gradient was prepared by forming a 1 ml cusion of 60% sucrose and then adding 5 ml of each of 50% and 30% sucrose to a custom made continuous density gradient maker. Two ml of the pm sample were added to the gradient in each of six cellulose nitrate tubes. The gradients were centrifuged to equilibriate for 18 hours at 40,000 rpm yielded a dense, purple band and a diffuse, low concentration red band. The pm band in sucrose was collected with a disposable pipette after discarding the top layers. The pm in sucrose obtained from the density gradient was washed twice in dd H_2O at 18,000 rpm for one hour, stored as pellets and resuspended as necessary. Similar to cmv, pm was stable for at least 3 months by the same criteria. The approximate yield of the pm was 40-60 mg/10 litre carboy.

(e) Criteria for the purity of the purple membrane:

(i) The complex medium, Bacterio-peptone from the same batch was used for all experiments to ensure that no variation in the growth medium could be experienced.

(ii) The equilibrium density gradient centrifugation of continuous sucrose gradient of pm showed a single, sharp band. If the pm were contaminated by other membranes, the band would be diffuse or more than one band would have been observed.

(iii) The absorption spectrum (Fig. 4.2) is identical to that reported in the literature (Oesterhelt & Stoeckenius, 1974). As reported in the literature, the ratio of

Figure 4.2

Absorption spectrum of the purple membrane from the bacteria grown in our laboratory

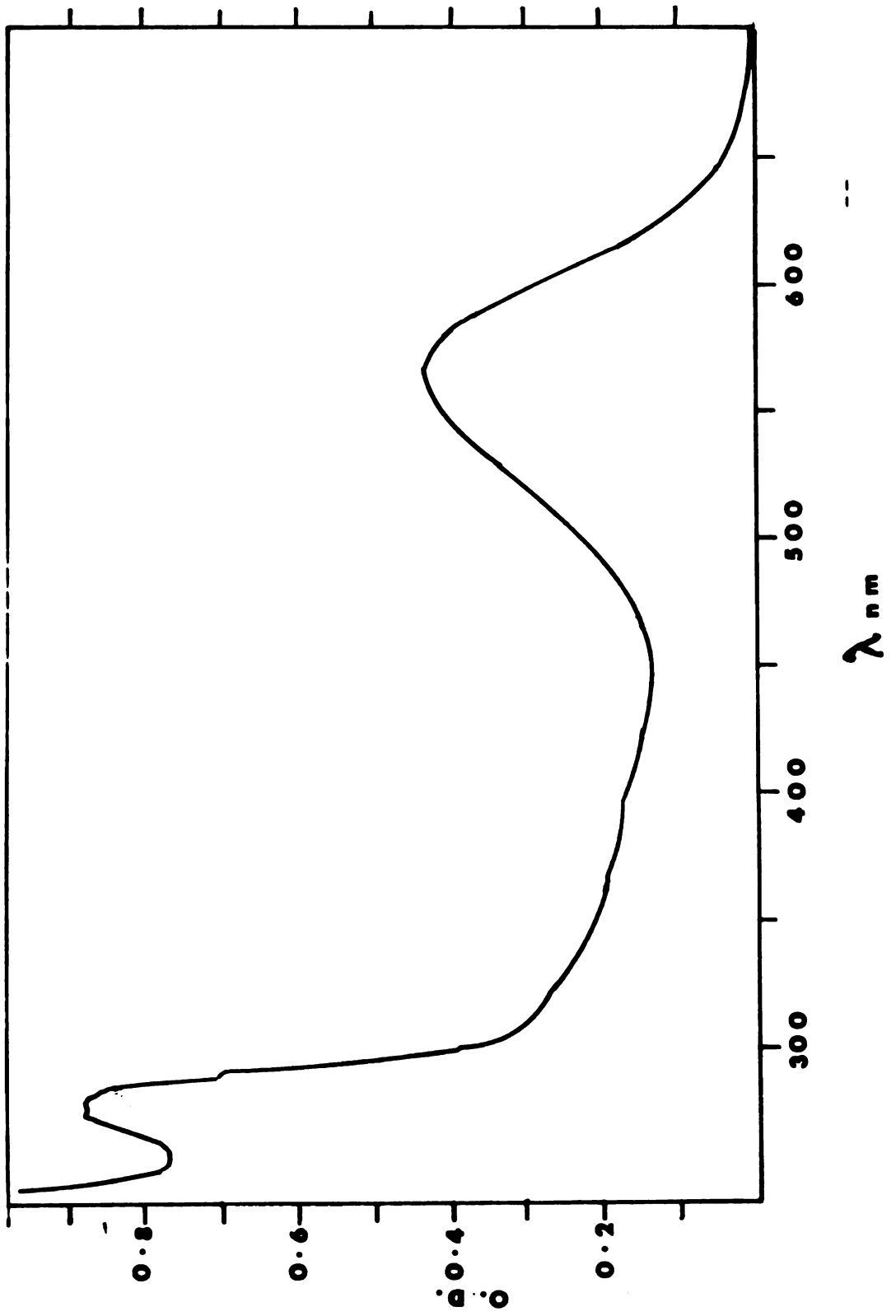
0·8
0·6
0·4
0·2
0·0
300
400
500
600
λ nm

the 280 nm (protein) peak to the 560 nm (purple) peak is 1.9 to 1.0.

(iv) Electrophoresis of the pm band on a SDS (sodium dodecyl sulfate) polyacrylamide gels (PAGE) was another criterion for purity. The stacking gels used were 5% acrylamide, the separating gels were 9% acrylamide. The gels were stained with Coomassie brilliant blue (Laemmi et al, 1970). The purple membrane protein (bR) migrated as a single band. Two gels were overloaded with protein to ckeck for a small contamination; however, no minor bands could be detected which indicated no contamination.

(v) To determine the protein:lipid ratio of pm in our preparation, the dry weight protein analysis of pm was performed. The vacuum drying procedure was used to determine the dry weight of pm and the concentration of protein for that sample was determined by the method of Lowry (Lowry et al, 1951). The protein:non-protein (lipid) ratio for our preparation was 78:22 (5% error) which is in close agreement with the reported value of 75:25 (Oesterhelt & Stoeckenius, 1971).

(vi) The cmv were coated with 1% phosphotungstic acid (PTA), and subjected to electron microscopy which revealed the cmv to be cloed, single wall vesicles.

(f) Preparation of liposomes:

0.1 ml of 10 mg/ml phosphotidyl choline (PC) in chloroform and 10 µl of 10 mM AS in ethanol were added to 10 ml of liposome buffer (see materials) to make a 0.1%

aqueous dispersion. The molar ratio of probe:lipid was 1:50. A Bronson sonifier (Model W 185 D) was used to sonicate the dispersion at power setting 4 (meter setting approximately 60 W) in a Branson sonifier container which could be water cooled and was gas exchangeable. The temperature of circulating water was 12-15°C and the sonication was performed under a flow of nitrogen.

(g) Purple membrane liposomes:

Closed vesicles containing fragments of pm sheets and PC liposomes were obtained by sonicating 300-500 µg of protein (pm) in pm-liposome buffer (see materials) and PC liposomes together for 10 minutes in a water jacketed sonifier container. The power setting for pm-liposomes was 2 (20 W).

(h) Bleaching of purple membrane:

The published methods for bleaching the pm vary considerably in pH and NH_2OH concentration (Oesterhelt et al, 1974),(Becher & Ebery, 1976),(Bauer et al, 1976). The method described below was determined to be optimal. A fresh solution of 0.2 M NH_2OH was prepared prior to bleaching and the pH was adjusted to 7.0 by adding NaOH pellets. A typical sample for bleaching experiments consisted of approximately 0.5 mg of bR in 15 ml of NH_2OH. For illumination, a three cm diameter hole was bored in a 900 W Xenon lamp housing to allow white light. The light was filtered through 8 cm optical path of 1% $CuSO_4$ and a Corning cutoff filter 3-70 to transmit the light between 500 nm and 700

nm. The filtered light was collimated by a lens; the intensity of light at the sample position was 5 mW/cm^2. The sample was stirred while bleaching. A fan was used to maintain the temperature of the sample at room temperature. Typically, about 30-40 hours of light exposure were needed for bleaching 1.5 mg of bR. Alternatively, 1.5 mg of bR in 5 ml of 0.2 M NH_2OH, pH 7.0 was exposed to an Argon 513 nm laser for 10-15 minutes at 3 watts power. Although the temperature of the sample reached 50^oC during bleaching, the degree of reconstitution of Xenon bleached and Argon bleached pm was equal. For stepwise bleaching, the absorbance of pm at 560 nm was monitored as a function of time. One hundred percent bleaching resulted in the loss of the 560 nm peak, which could also be detected visually as the disappearance of the purple color.

Bleaching of pm was also achieved by the addition of a 1:5 ratio of ether:basal salts (salts 1) added to the pm. The ether bleaching is reversible i. e. no additional retinal is needed for the reconstitution. However, the absorption maximum of the native pm is changed due to the addition of ether indicating some changes in bR and/or the membrane, therefore, ether bleaching was considered undesirable.

(i) Reconstitution of purple membrane:

The bleached pm was washed free of NH_2OH before attempting reconstitution. Typically, 10-12 µl of 1 mM retinal was sufficient for 100% reconstitution of 300 µg bR in either

0.01 M Tris, pH 7.0 or dd H_2O. Stepwise reconstitution was achieved by adding 2 ul of 1 mM 13-cis or all-trans retinal to the same concentration of bR each time (see Fig. 4.3 for bleaching and reconstitution).

(j) Solubilization of purple membrane:

Non-ionic detergents, e. g. Triton X-100, dodecyl trimethyl ammonium bromide (DTAB) reduced the scattering of the pm supsension significantly for the spectroscopic measurements, however, they caused a blue shift to 4-10 nm.in the 560 nm peak of the pm indicating less interaction between chromophore and protein and/or conforamtional change in the protein. Therefore, detergents were not used in this study. For reproducing some CD data (Becher & Ebery, 1976), pm was suspended in 0.3% Triton X-100 in 0.01 M Tris buffer, pH 7.0. Under these conditions, the pm became bleached overnight without exposing it to light. DTAB was used for the same purpose and was found satisfactory compared to Triton X-100.

(k) Gel chromoatography:

This technique was used occasionally to remove free probe from the sample. Sephadex G-25 (coarse) gels were swelled in boiling water for two hours. The pm in distilled water adhered to the gel and could be removed by eluting it with 0.01 M Tris, pH 7.0. However, due to the occurance of the dilution of the sample, centrifugation or dialysis was preferred to gel chromatography.

Figure 4.3

Absorption spectra of bacteriorhodopsin under various conditions of bleaching and reconstitution.

a. Absorption of native purple membrane ————————

b. Absorption of purple membrane bleached using 0.2 M NH_2OH, pH 7.0 and visible light for 30 hours —·—·—·—

c. Absorption of bleached purple membrane reconstituted with 12 μl of 1 mM all-trans retinal — — — — —

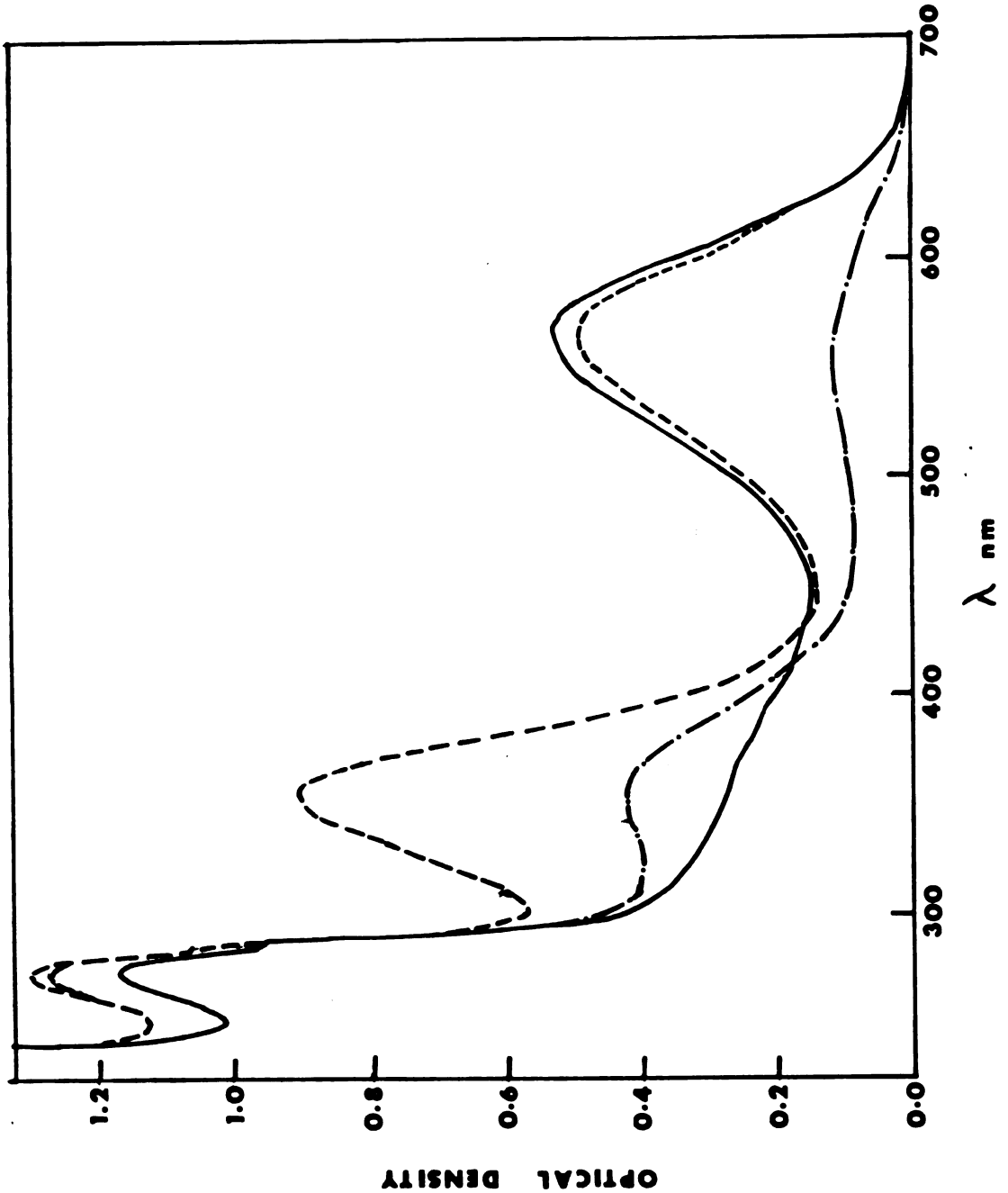
OPTICAL DENSITY
1.2
1.0
0.8
0.6
0.4
0.2
0.0
300
400
500
600
700
λ nm

(l) Labelling of membranes:

Fatty acid fluorescence or spin probes were routinely incorporated in the membrane by mild sonication. For ESR, 8 µl of 10mM probe in ethanol was added to 0.4 ml of 20-30 mg/ml bR sample, vortexed for 1 minute and sonicated for 10 minutes using a Cole-Parmer one quart sonicator. For fluorescence probes, 20 µl of 10 mM AS in ethanol was added to 1-2 mg of bR (probe:lipid ratio of about 1:50) in 5 ml of 0.01 M Tris, pH 7.0 or dd H_2O, vortexed for one minute and sonicated for 10 minutes at 37°C. Different solvents e. g. hexane or chloroform were used to dissolve the probe, however, for fatty acid probes, ethanol was found to be the most desirable solvent.

(m) Temperature variation studies:

(i) A circulating water bath in conjunction with the Aminco waterjacketed cell holder was used for temperature variation between 5°C to 50°C. A mixture of ice and water in a reservoir was gradually heated by using a Bronwell Co. thermomix II, 750 W heater and pumped through the cell-holder. The temperature of the cuvette was monitored by a thermocouple thermometer with an internal reference.

(ii) Bubbling of liquid nitrogen to obtain temperatures between -150°C to room temperature was used for obtaining the contraction factor and DNSA in ethanol data. A quartz dewar with a flat quartz excitation window and a one cm square Suprasil cuvette were used for these studies. The temperature of a sample was controlled by boiling liquid

nitrogen from a reservoir using a (5 watts, 100 ohms) power resistor and allowing the cold nitrogen gas to flow into the sample dewar at different rates. A variable temperature control accessary by Wescan Instruments, Inc. (Model 240, temperature controller) was used to lower and maintain the temperature. The probe of the temperature was inserted in the optical dewar and the power resistor was connected or disconnected to control the boiling of liquid nitrogen according to the setting of the controller, which was previously calibrated with the temperature. A normally closed relay was used to invert the on and off cycle of the power due to the fact that an inverse relation between temperature and heater was needed (Fig. 4.4).

(n) Spectral measurements:

(i) Electron spin resonance (ESR): ESR spectra were recorded using Varian E 112 Century Spectrometer operated at 9.1 GHz. For fatty acid spin probes, the center of the magnetic field was set at 3270 guass. A Varian temperature control accessary was used to change the temperature of the sample, however, the actual temperature of the sample fluctuated by as much as $5^{o}C$ at extreme temperatures as compared with a thermocouple. The temperature of the sample in a flat, quartz microcell was monitored by a thermocouple attached to the microcell using a Bailey thermocouple thermometer. Dry ice was stored in the reservoir and the lowest temperature of the sample (below which the aqueous membrane samples froze) was $-5^{o}C$. A plot of incident

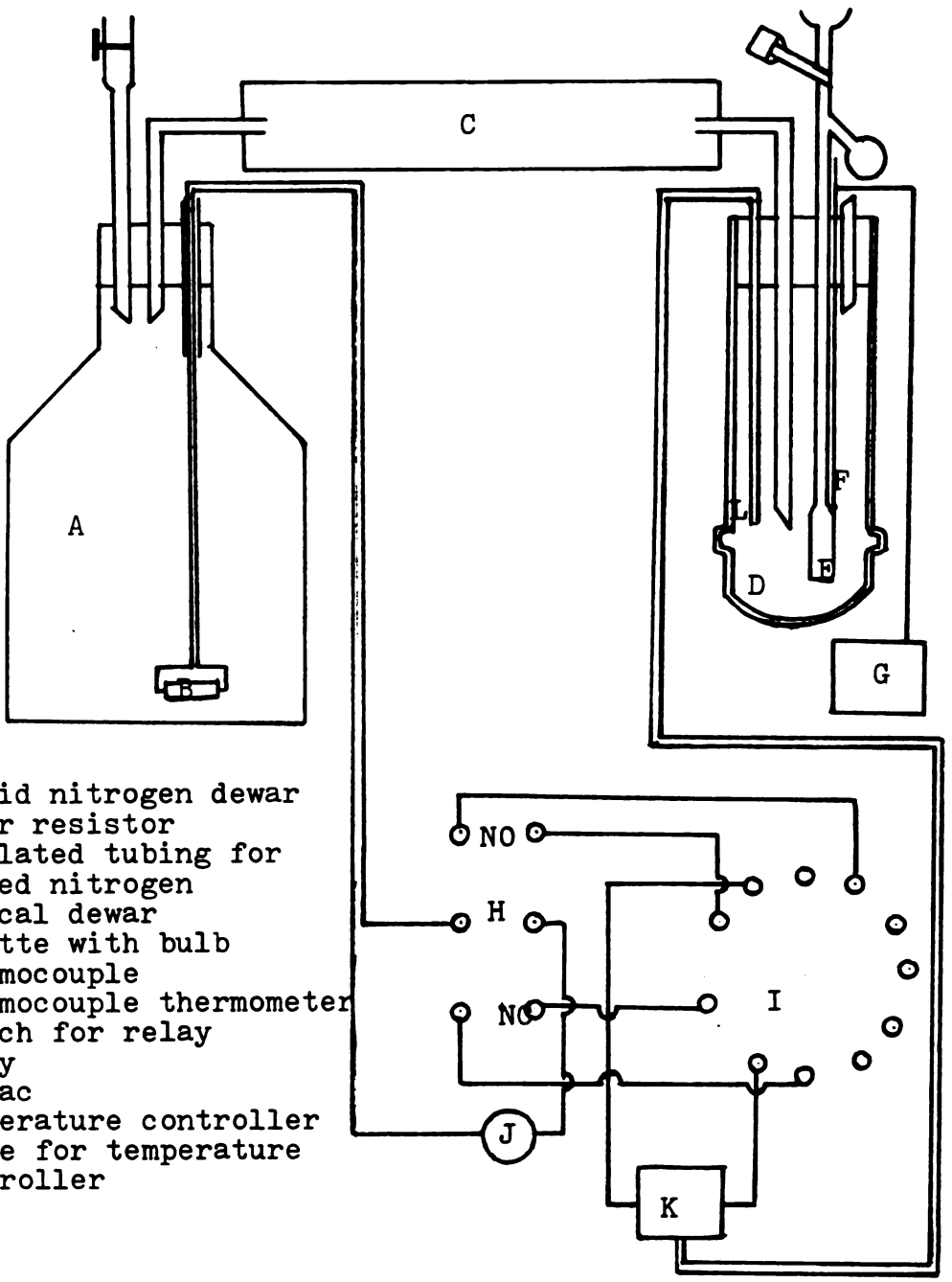

A-liquid nitrogen dewar
B-power resistor
C-insulated tubing for bioled nitrogen
D-optical dewar
E-cuvette with bulb
F-thermocouple
G-thermocouple thermometer
H-switch for relay
I-relay
J-variac
K-temperature controller
L-probe for temperature controller

Figure 4.4 Schematic of the temperature control accessary for the temperature between 100°K and 300°K.

microwave intensity was set at 10 mW. Similarly, an increase in the modulation amplitude increased the gain of the signal. In this case, the fine-structure of the ESR spectrum tended to disappear as a result of the increase in gain. Therefore, the modulation amplitude was set at 3.2 G. The receiver gain was between 2×10^3 to 6×10^3. The time constant was set at 0.25 seconds and the spectra were recorded using either 4 min/scan or 8 min/scan speeds.

(ii) Absorption spectra: These were recorded using a Cary 15 spectrophotometer.

(iii) Circular dichroism spectra (CD): CD spectra were recorded at the Biophysics Department, University of Michigan courtesy of Prof. Zand. A JASCO model ORD/UV-5 with a SPROUL Scientific SS-20 CD modification was used. The pm was suspended in 0.01 M Tris, pH 7.0 in a one cm rectangular cuvette. The concentration of the bR was 200 μg/ml which showed $O.D._{560}=1.0$ on the Cary 15 and $O.D._{560}=0.4$ on the JASCO photomultiplier scale. The CD scale was 2 millidegrees per cm, the time constant was 4 seconds and the speed of the recorder was set at 2 which corresponded to 10 nm per minute.

(iv) Emission spectra: Routine fluorescence spectra were obtained by an Aminco-Keirs spectrofluorimeter modified with an EMI 978 IR phototube. For higher resolution, a component system was used. A 900 W Xenon lamp (powered by a Christie Silicon Rectifier (MHM-900-28) power supply), was used.as an excitation source. The wavelengths of

excitation were selected by a Bausch and Lomb 10 cm grating blazed at 3000 Å in a B & L 500 mm monochromator. A TRW sample holder with collimating lenses were used for aligning the excitation and emission components. The emission monochromator was a 750 mm Czerny-Turner spectrometer (Spex 1711-II) in conjunction with a Princeston Applied Research PAR-lock-in amplifier (model HR-8) and an EMI 9558 QA phototube. The power supply for the phototube was a Fluke 412 B which normally operated as 1100 V. The signal, with a chopper as a reference was connected to a Bristol Dynamaster recorder. The resolution of this system was 2 nm.

(v) Quantum yields: Quantum yields for DNSA in various solvents at room temperature were obtained by utilizing a double beem quantum yield instrument interfaced with a PDP 11 computer (Holland et al, 1973). Quantum yields for DNSA in ethanol at different temperatures and for AS in various solvents were obtained by using an Aminco-Keirs instrument and comparing the measured areas of the sample and the reference. The O. D. of the sample and the reference was kept less than 0.2 for all wavelengths and adjusted to be equal at the excitation wavelength. The method of comparing the areas of the spectra was similarly used to measure the changes in the abosrbance as a function of temperature to obtain the contraction factor. Scattering due to the optical dewar was compensated fro in both cases.

(vi) Nanosecond time resolved fluorescence decay measurements: The nanosecond fluorescence decay curves were obtained with a single photon counting, time resolved spectrophotometer built in our laboratory and described elsewhere (Avouris et al, 1974). This instrument consists of a deuterium nanosecond flash lamp, a 1P28 phototube to start the signal. The sample holder, an emission monochromator (B & L 500 mm, similar to the one described in the emission spectra), a high gain (10^8) and low noise phototube Amperex 56 DUVP which is capable of amplifying a single photon into an electric pulse to stop the signal, a time to amplitude converter Ortec 475, a multichannel analyzer Nuclear data 1100 to collect and store the data; also to transmit the data to the computer, HP 7200 A plotter etc. (Fig. 4.5). Interference or band-pass filters were used for excitation. Various computer programs are used to calculate the life-time of the fluorescence decay. A deconvolution analysis developed by Ware (ware et al, 1973) and tripex analysis (Ware W. R., personal communication) are found satisfactory for multicomponent decay. Details of various computer programs to calculate the life-times corrected for lamp shifts and for photmultiplier response are in preparation (Kennedy & El-Bayoumi, in preparation).

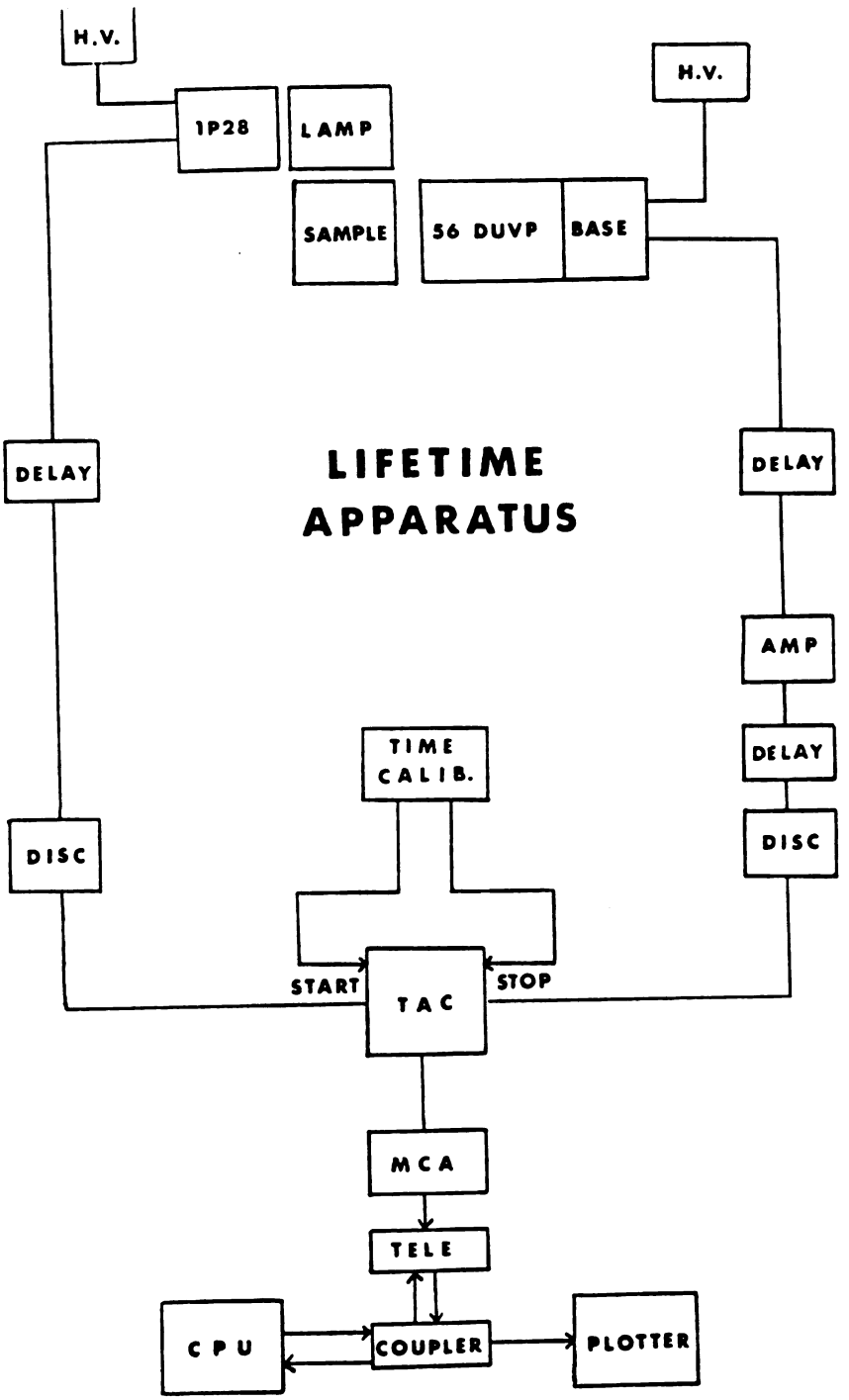

Figure 4.5 Nanosecond Time-resolved Spectrofluorimeter.

MATERIALS:

Chemicals: N-oxyl-4', 4'-dimethyl oxazolidin 5-keto stearic acid (5-NS) and n-oxyl-4',4'-dimethyl oxazolidine 12-keto stearic acid (12-NS) were purchased from Synvar Corp., Palo Alto, California. 12-(9-anthroyl) stearic acid (AS), dansyl sulfanoamide (DNSA), 13-cis retinal, all-trans retinal, DNAase I from bovine pancreas were purchased from Sigma. 1,6 diphenyl 2,4,6-hexatriene (DPH) was purchased from Eastman. Diphenyl anthracene (DPA), anthracene-9-carboxylic acid (ACA), and naphthalene were purchased from Aldrich.

Solvents: Ethanol, n-propanol and diethyl ether were redistilled in our lab. 3-methyl pentane (3-MP) was purified by the method of Potts (1952) modified in our laboratory and reported by Avouris (Avouris, 1974). Spectrograde glycerine was purchased from Aldrich. Spectrograde EPA was purchased from the American Instrument Company. Spectrograde methanol was purchased from Mallincrodt. Spectrograde benzene, cyclohexane, hexane, and 2-methyl butane (isopentane) were purchased from Matheson, Coleman and Bell (MC/B).

Growth medium: For 1000 ml of medium:

NaCl.....	250.0 gm
$MgSO_4.7H_2O$.....	20.0 gm
trisodium citrate.$2H_2O$	3.0 gm
KCl	2.0 gm
$CaCl_2.2H_2O$	0.2 gm

Ten gm Bacto-peptone (Bacteriological-technical by Difco) were mixed separately with 100 ml of dd H_2O and was autoclaved. The salts were dissolved in dd H_2O to make an 850 ml volume and were autoclaved separately. After autoclaving, the peptone was mixed with the salts; the pH was adjusted by adding 5 ml of 0.5 N NaOH to 7.4; then the total volume of the medium was made to 1000 ml with sterile, dd H_2O.

Buffers:

Salts 1: These are 'basal salts'; salts that are listed in the medium without peptone.

Salts 2:

1.0 M NaCl

20 mM $MgSO_4 \cdot 7H_2O$

10 mM Tris-Cl

pH 7.4

Liposome buffer (PCV):

0.1 M NaCl

0.05 M Tris-Cl

pH 8.0

Purple membrane liposome buffer:

0.15 M KCl

0.01 M Tris-Cl

pH 7.0

CHAPTER 5

PHOTOPHYSICS OF A POLARITY PROBE (DANSYL SULFANOAMIDE) AND A PACKING PROBE (ANTHROYL STEARATE)

(a) Introduction:

As discussed in chapter 2, the polarity probes e. g. DNSA, ANS, AS are weakly fluorescent in solvents of high polarity. As the polarity of the medium decreases, the quantum yield of fluorescence of the probe increases and the λ_{max} shifts towards higher energies. These effects are interpreted in terms of the solvent relaxation of the polar solvent around the probe molecule. The degree of the solvent relaxation depends upon the ability of the solvent molecules to reorient themselves around the probe molecule during the life-time of the excited state. Therefore, in a highly viscous, polar medium, even though the dipole moment of the solvent molecules is high, the solvent relaxation does not occur during the life-time of the excited state giving rise to an emission similar to that in a non-polar solvent (solvent which has a lower dipole moment). In this chapter, the medium effects (polarity and rigidity) on the luminiscence properties of two probe molecules, dansyl sulfanoamide (DNSA) and anthroyl stearate (AS) are studied in detail. In order to differentiate between the properties of DNSA in a polar and viscous versus in a non-polar and fluid medium, the effect of temperature on the emission

maximum, fluorescence quantum yield and life-time of DNSA in a polar solvent is studied. This study required the measurement of solvent densities as a function of temperature in order to compensate for absorption changes due to the solution contraction. These contraction factors were also obtained for three other widely used organic solvents. Photophysical studies of probes is divided into three parts:

(b) Contraction factor:

Temperature dependence of the fluorescence quantum yield can be utilized to gain significant information about the electronic transitions as well as the intramolecular interactions in the excited states. However, caution must be exercised while interpreting the change in the quantum yield of a fluorescent molecule upon changes in the temperature. The fluorescence quantum yield $\Phi_f(T)$ as a function of temperature is determined relative to its value of $\Phi^o_f(T)$ at room temperature by the equation (Mantulin & Hubert, 1973) is given by:

$$\Phi_f(T) = \Phi^o_f(T) \frac{\int F(\bar{\nu},T)d\bar{\nu} \quad D \quad n^2(T)}{\int F_o(\bar{\nu},T)d\bar{\nu} \; D(T) \quad n_o^2} \quad .....5.1$$

where F is the corrected fluorescence spectrum

D is the optical density of the solvent

n is the refractive index of the solvent

Therefore, to obtain a true increase in the quantum yield of fluorescence at a lower temperature, the change in the density of a solvent must be compensated for. The ratio of $D_o/D(T)$ in the above equation compensates for the

temperature dependence of (i) the density of the solvent and (ii) the bandwidths, spectral shifts and transition probabilities fo the absorption peaks. The ratio of $D_o/D(T)$, termed as the 'contraction factor' can be obtained by the measurement of the absorption spectrum of a molecule in the same spectral range as the excitation of most aromatic or conjugated linear probe molecules. We studied this contraction factor quantitatively by determining the change in the absorption spectrum of 9-10 diphenyl anthracene (DPA) in different solvents as a function of temperature. The contraction factor was experimentally determined as follows:

$$\text{Contraction factor} = \frac{\text{Absorption spectrum at room temp.}}{\text{Absorption spectrum at lower temp.}}$$

$$= \frac{\text{Area of absorption curve at room temperature}}{\text{Area of absorption curve at a lower temperature}}$$

Assuming that the extinction coefficient of DPA is independent of temperature, the increase in the intensity of absorption by lowering the temperature was solely attributed to the ratio $D_o/D(T)$ for that particular solvent. As stated earlier, the contraction factor was obtained for the following solvents: (i) ethanol (ii) n-propanol (iii) 3-methyl pentane (3-MP) and (iv) methyl cyclohexane (MCH): isopentane (IP) in the ratio 3:1. Also, two probe molecules, DPA and naphthalene were used to obtain the contraction factor for ethanol to show that the

contraction factor is independent of the properties of a solute (Fig. 5.1).

It can be seen from the equation 5.1 that the correction in the refractive index is also necessary to obtain the total correction factor $\mathcal{F}(T)$. The $\mathcal{F}(T)$ is given by

$$\mathcal{F}(T) = \frac{D_o}{D(T)} \cdot \frac{n^2(T)}{n_o^2} \quad \ldots\ldots\ldots\ldots\ldots\ldots 5.2$$

We have obtained $D_o/D(T)$ (contraction factor) by the experimental procedure, that factor can be used ot determine the refractive index at various temperatures by using one of the two equations given below:

$$\text{(i)} \quad \frac{n - 1}{d} = \text{constant} \quad \ldots\ldots\ldots\ldots\ldots\ldots 5.3$$

$$\text{(ii)} \quad \frac{n^2(T) - 1}{b - n(T) + 0.4} = (T) \quad \ldots\ldots\ldots\ldots\ldots\ldots 5.4$$

The plots from these two equations showed that the equation 5.4 was more satisfactory as the deviation in the linearity of the experimental points was lower. The constant in the equation 5.4 was obtained by using known values of the refractive index obtained by the above equation for ethanol, n-propanol and 3-MP at various temperatures is shown in Fig. 5.2.

As mentioned earlier, by combining the contraction factor obtained from the absorption spectra and the refractive index obtained by the equation 5.4, the total

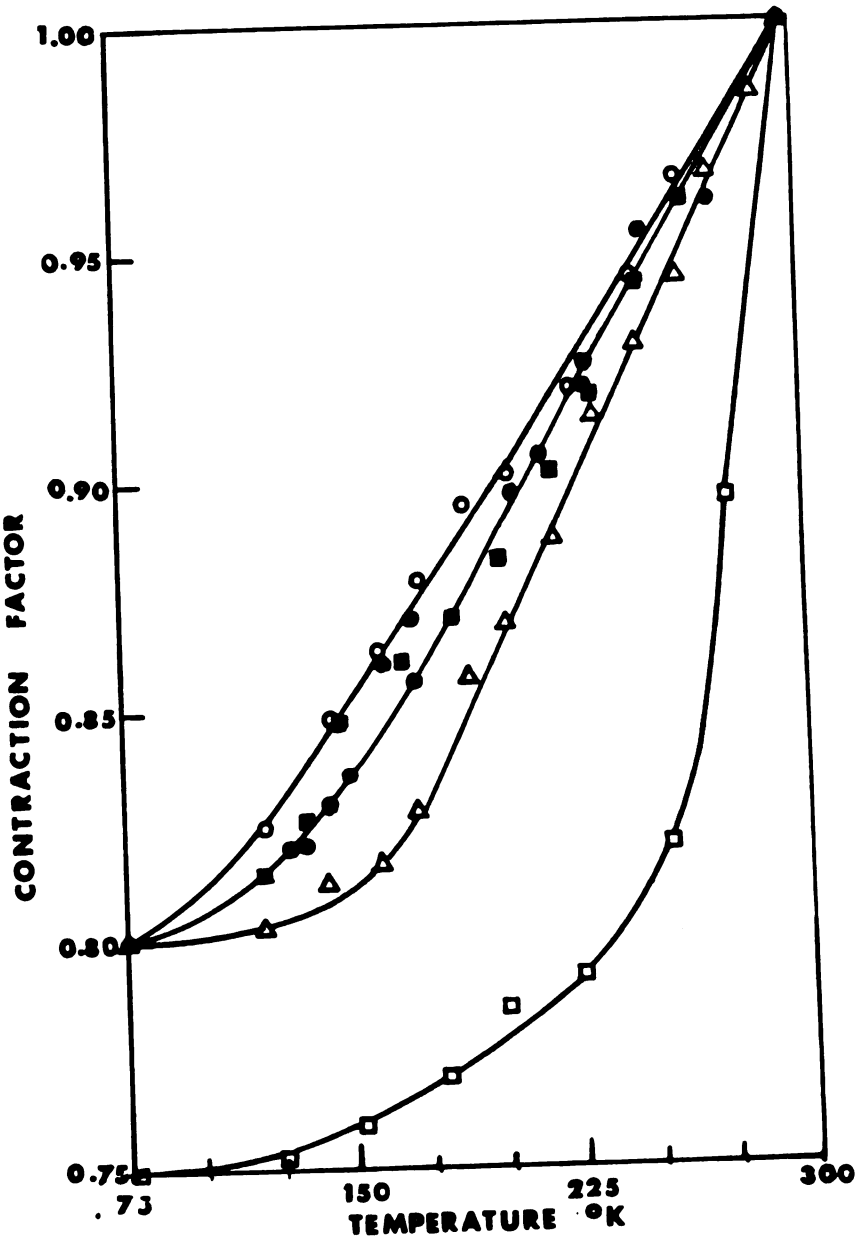

Figure 5.1 Contraction factor

Contraction factor for different solvents as a function of temperature. Solute used for all solvents, diphenyl anthrecene (DPA), for ethanol, another solute, naphthalene was used.
a. propanol—o—o— b. 3-methyl pentane —△—△—
c. methyl cyclohexane:isopentane (3:1) —□—□—
d. ethanol-DPA—●—●—, ethanol-naphthalene—■—■—

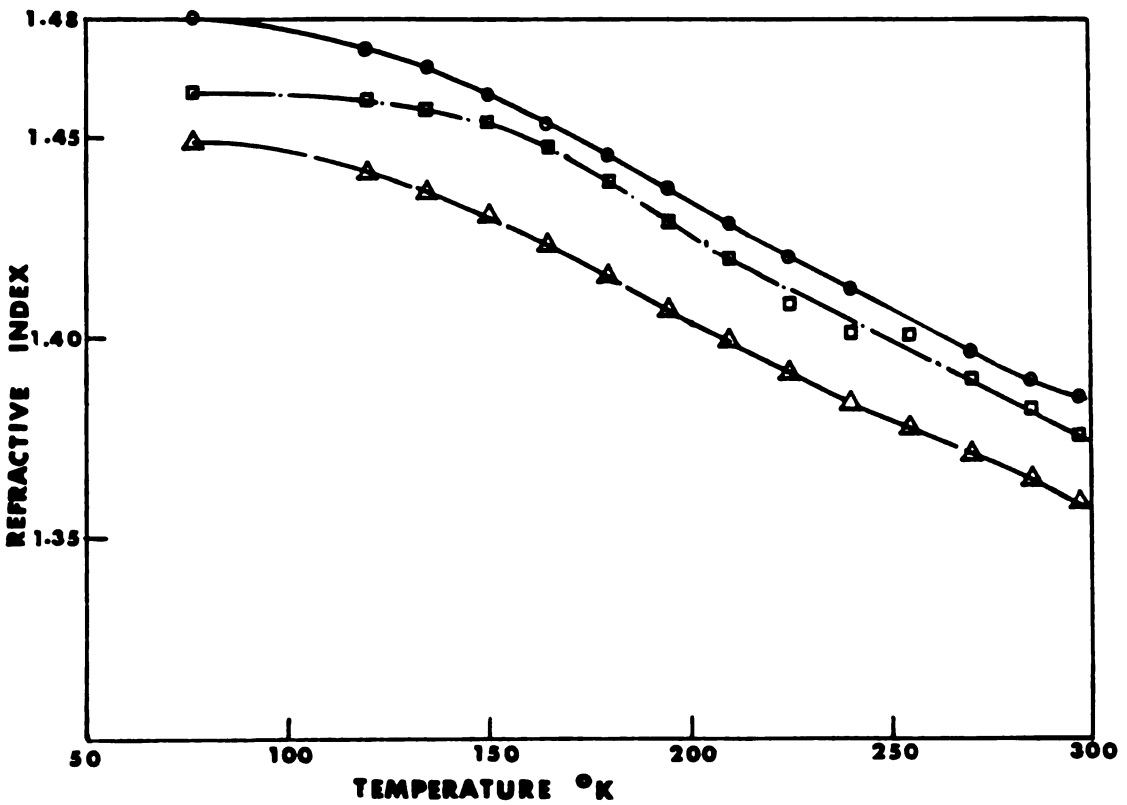

Figure 5.2 Refractive index of various solvents

Refractive index of the solvents
a. ethanol —□—□— b. propanol—○—○—
c. 3-methyl pentane —△—△—
Equation used: (n-1)/d = constant

correction factor $\mathcal{F}(T)$, to be applied to tbe corrected fluorescence is given by the known values of the equation 5.2. The $\mathcal{F}(T)$ is made available for the following solvent solvents: (i) ethanol (ii) n-propanol and (iii) 3-MP (Fig. 5.3). The results of this study are applied to correct the quantum yield of DNSA in ethanol at different temperatures. The contraction factor should prove valuable in studying emission and absorption properties of molecules as a function of temperature in these solvents.

(c) Dansyl sulfanoamide:

Dansyl (2-2 dimethylamino-naphthalene-6-)sulfanoamide (DNSA) is a "polarity probe" which is widely used to determine the nature of its binding site and changes in its fluorescence parameters due to conformational changes in biological macromolecules and membranes. It has been shown that DNSA forms a highly fluorescent complex with bovine carbonic anhydrase at its active site and upon binding, its fluorescence properties enhance dramatically (Chen & Kearnhan, 1967). DNSA and other dansyl probes which have a fluorescent 2-amino-naphthalene-6-sulfonate group attached to a functional group such as an amide, chloride, amino acid, cadaverine etc are used in the biological systems according to the specificity of their functional groups. However, the fluorescence properties of these molecules should be studied in the simple solvents in greater detail to derive more information about biological systems. The fluorescence properties of some dansyl derivatives have

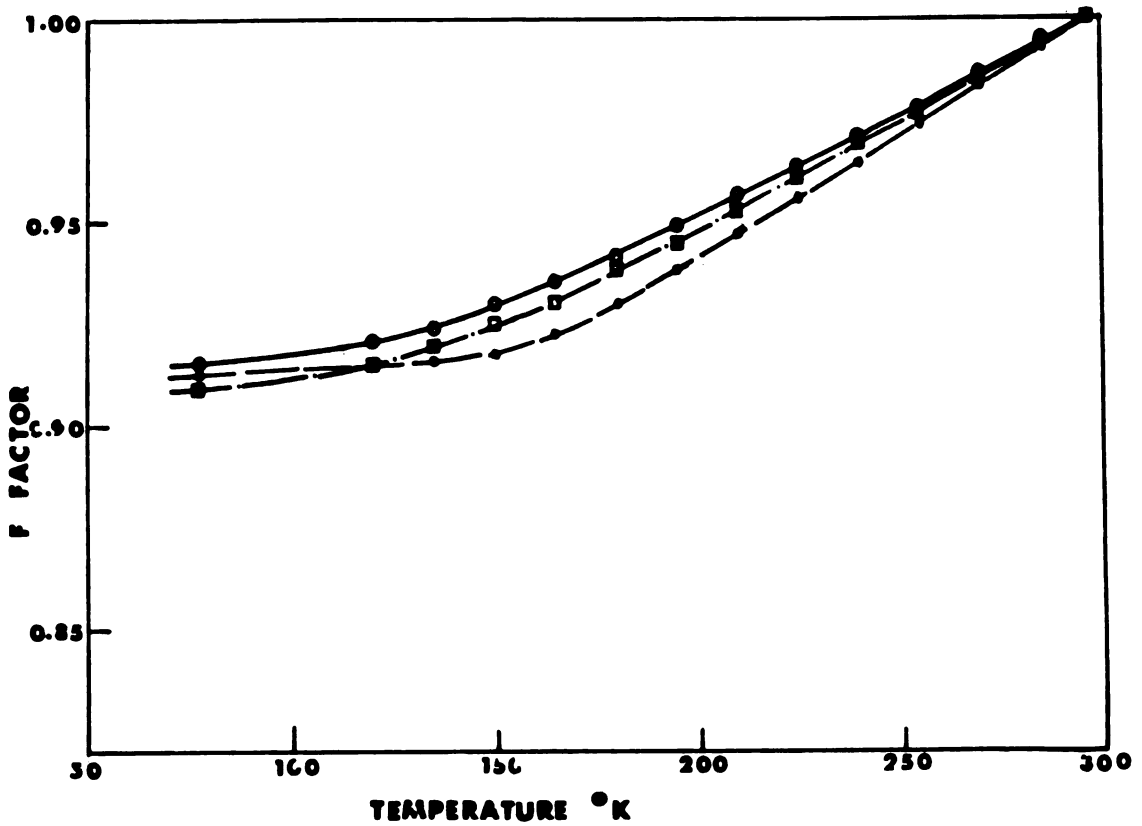

Figure 5.3 $\mathcal{J}$ factor for various solvents

$\mathcal{J}$ factor for various solvents were determined by combining the contraction factor and the refractive index at individual temperatures
a. ethanol —□—□— b. propanol —○—○—
c. 3-methyl pentane —●—●—

been measured in mixed solvents, one polar and other non-polar (Li et al, 1975),(Seliskar & Brand, 1971).

The dipole moment of this molecule increases upon excitation, thus the relaxation of the solvent cage leads to different emission maxima depending on the polarity of the solvent as shown in Fig. 5.4. We have studied the fluorescence properties, e. g. an emission maximum, fluorescence quantum yield and life-time of fluorescence decay of DNSA in solvents of varying polarity. The results are shown in Table 5.1. One may observe that as the 'polarity' of the medium increases, the quantum yield (ϕ_f) and life-time (τ_f) decreases and the wave-length maximum (λ_{max}) increases. Degassing by bubbling dry nitrogen leads to an increase in the value of ϕ_f, and τ_f, without a change in λ_{max}. This is interpreted in terms of oxygen quenching of fluorescence via intersystem crossing enhancement mechanism. That is, oxygen enhances the spin-orbit coupling hence increasing the rate constant of intersystem crossing to triplet state leading to an observed fluorescence quenching. The effect of oxygen quenching is particularly significant in benzene medium. It can be seen that the τ_f of DNSA was 19.1 nsec in n-propanol but decreased gradually to 16.0 nsec in methanol and then dramatically to 2.2 nsec in water. Similarly, the emission wavelength maximum of DNSA changed from 495 nm in propanol to 505 nm in methanol and to 550 nm in water. Interaction of water with DNSA leads to the large observed

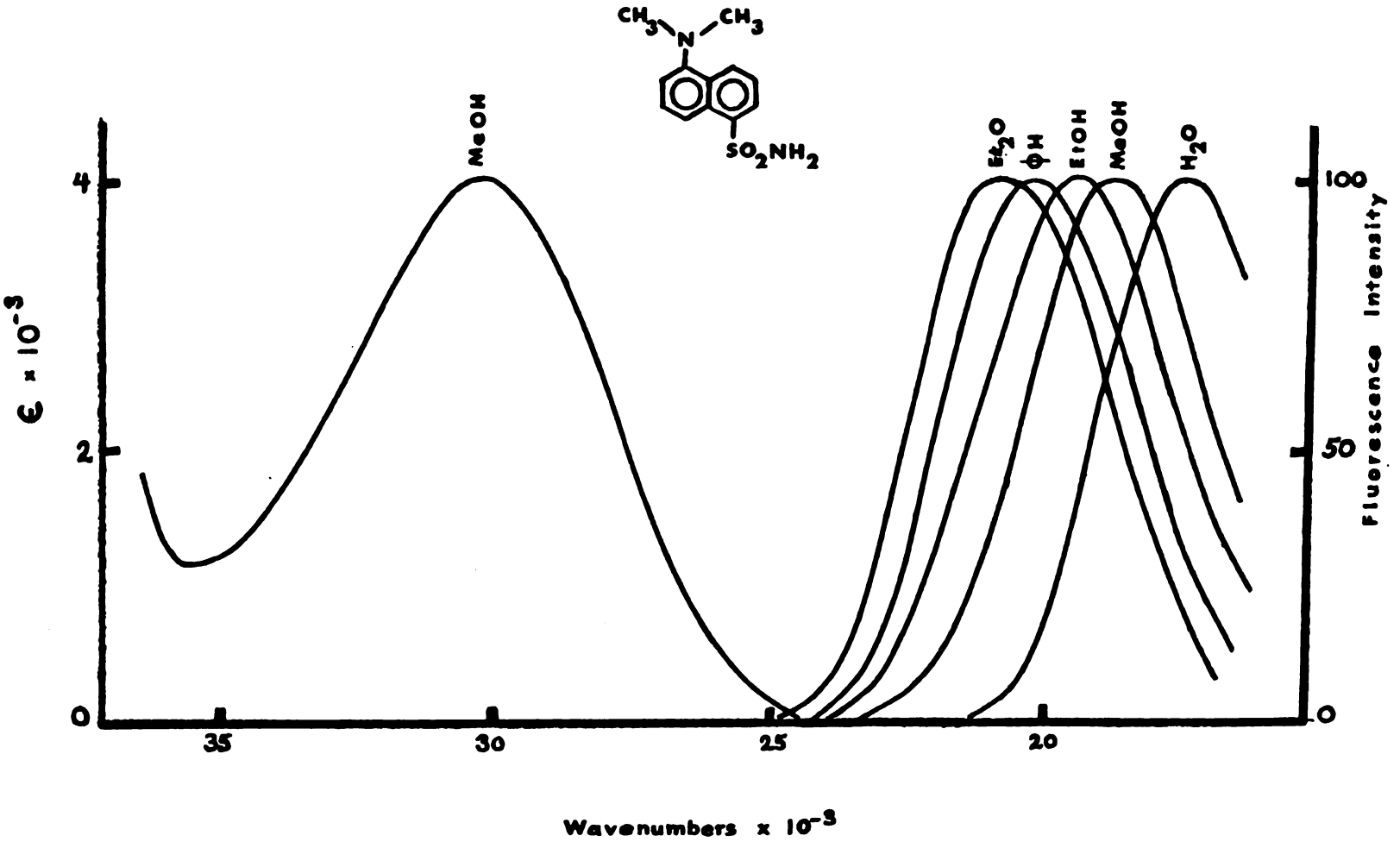

Figure 5.4 Emission maxima of DNSA in various solvents

Emission properties of 10^{-5} M DNSA in various solvents (Reproduced from El-Bayoumi, 1976). Spectra are recorded at room temperature

Solvent		Ether	Benzene	Propanol	Ethanol	Methanol	D_2O	H_2O
Solvent Properties		4.36	2.275	20.33	24.55	32.70	-	78.54
		1.15	0	3.09	1.66	2.87	-	1.84
	n	1.3526	1.5011	1.3850	1.3611	1.3288	1.3388	1.3333
τ_f nsec		11.1	11.3	13.4	12.2	10.9	6.2	2.1
τ_f nsec (degassed)		14.5	16.1	19.1	18.3	16.0	-	2.2
ϕ_f		0.5361	0.447	0.4911	0.41	0.3563	0.11	0.055
ϕ_f (degassed)		0.7516	0.8069	0.7467	0.5786	0.5082	-	0.055
τ_m° nsec (degassed)		19.3	24.5	25.6	31.6	31.5	-	38.3
τ_c° nsec		38	39	48	53	56	57	59
λ_{max}	nm	470	475	495	500	505	540	550

Table 5.1 Emission properties of DNSA in various solvents

Emission properties (τ_f, ϕ_f, λ_{max}) of 10^{-5} M DNSA in various solvents at room temperature measured before and after degassing. $_{ex}$ = 330 nm.

shift of the emission maximum and life-time is due to an expected enhancement of radiationless transition via the triplet state ($S_1 \rightsquigarrow T$) and/or directly to the ground state ($S_1 \rightsquigarrow S_o$). The fluorescence life-time (τ_f= 6.2 nsec) and the quantum yield (ϕ_f= 0.11) of DNSA in D_2O is more than double that in H_2O. This is interpreted in terms of a deuterium isotope solvent effect which limits radiationless transitions. It is interesting to note that in benzene, the emission maximum occurs at 475 nm which is at a longer wave wavelength than ether (470)nm . Benzene has a lower dielectric constant than ether and is non-polar. This may imply specific interactions of DNSA with benzene. Natural fluorescence life-time of DNSA for all solvents is calculated from the experimental ϕ_f and τ_f such that

$$\tau_m^o = \frac{\tau_f}{\phi_f} \qquad \text{.....5.5}$$

The τ_c^o is given by Strickler-Berg equation as follows:

$$\frac{1}{\tau_o} = \frac{8\pi \times 2303\, n_f 3}{c^2\, N\, n_a} \left\langle \bar{\nu}_f^{-3} \right\rangle_{Av}^{-1} \int \frac{\epsilon\, d\nu}{\nu} \qquad \text{.....5.6}$$

which is modified to

$$\frac{1}{\tau_o} = 2.88 \times 10^{-9}\, n^2 \left\langle \nu_f^{-3} \right\rangle_{Av}^{-1} \int \frac{\epsilon\, d\nu}{\nu} \qquad \text{..... 5.7}$$

where n is the refractive index of the solvent and $\left\langle \nu_f^{-3} \right\rangle_{Av}$ is the reciprocal of the mean value of the frequency over the fluorescence spectrum. The quantity $-\frac{1}{\tau_c^o}$ is calcualted as the radiative transition probability from the lowest excited electronic state to the ground state. The trend of $-\frac{1}{\tau_m^o}$ is similar to $-\frac{1}{\tau_c^o}$ which means that the changes in the fluorescence energies and refractive indices of the solvents accounts for the observed radiations.

The emission parameters of DNSA obtained in ethanol at different temperatures (300°K to 77°K) are shown in Fig. 5.5. As the viscosity of ethanol increased upon lowering the temperature, τ_f decreased and λ_{max} also decreased in a more or less parallel fashion. Thus, in ethanol at room temperature (fluid medium), τ_f = 18.6 nsec, λ_{max} = 500 nm, while at 77°K, (rigid medium), τ_f = 13.5 nsec and λ_{max} = 450 nm. It is difficult to distinguish between a polar-rigid medium and a non-polar fluid medium on the basis of τ_f and λ_{max} measurements alone. To distinguish between these two situations, one requires the measurement of nanosecond depolarization decay of the probe molecule. Longer relaxation times are expected in the rigid media.

(d) Anthroyl stearate:

Anthroyl stearate (AS) is a fluorescence probe designed to investigate the hydrocarbon lipid region of an artificial or a biological membrane. The fluorescence moiety 9-anthroic carboxylic acid is covalently linked to

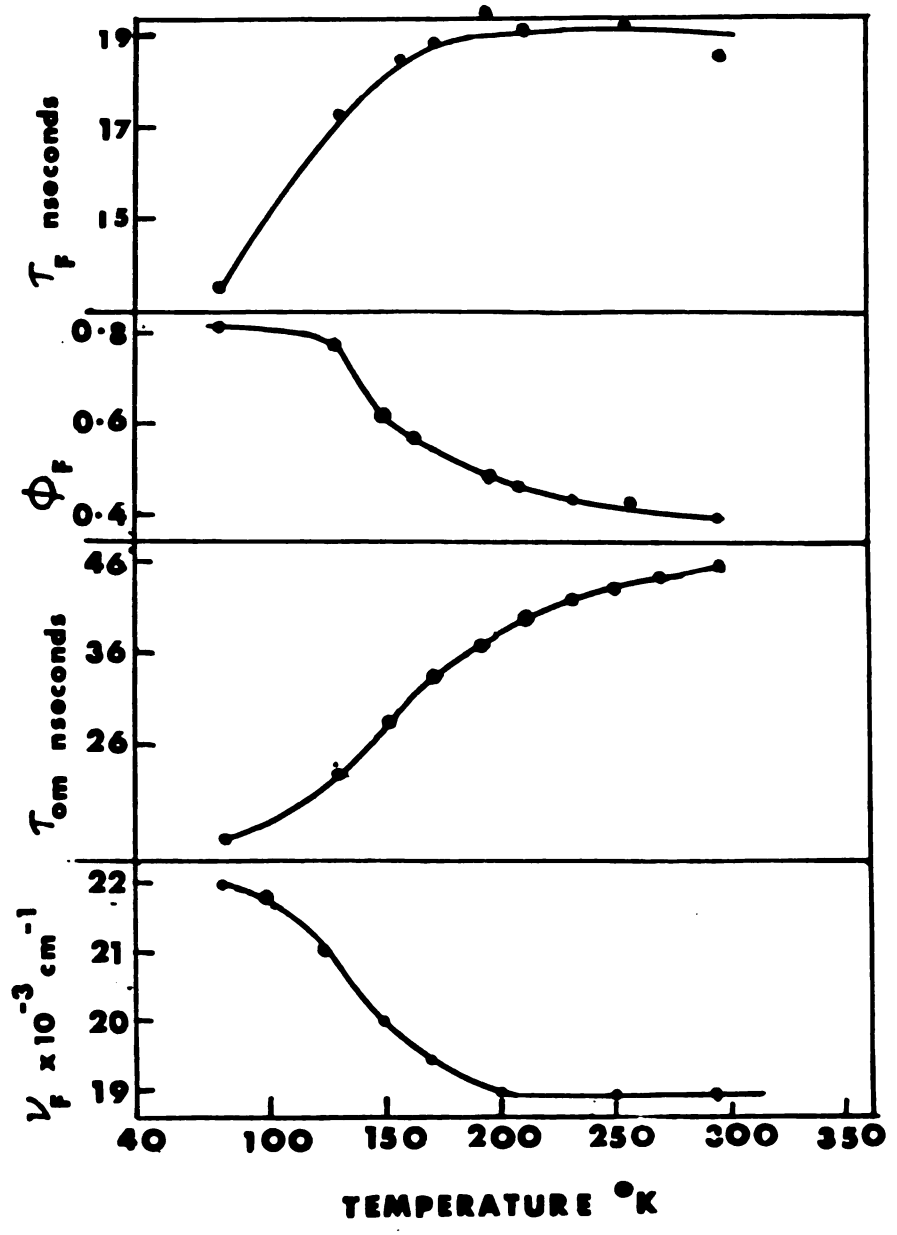

Figure 5.5 Emission properties (τ_f, ϕ_f, τ^o_m and ν_f) of DNSA in ethanol at various temperatures.

stearic acid at the twelfth carbon position to anchor the probe in the membrane. Since the report of its synthesis in 1970, (Waggoner & Stryer, 1970), AS has been widely used for the determination of (i) the orientation in the model membrane (Yguerbide & Stryer, 1971), (Badley, 1973) (ii) the effect of cholesterol on erythrocytes (Vanderkooi et al, 1974) (iii) the state of energization of the chloroplast membranes (Vandermeulen & Govindjee, 1974) and many other biological membranes. In our study, we are focusing our attention on an excited state intramolecular processes of AS that explain its emission properties. This probe undergoes a geometric relaxation in the excited state such that the plane of the carboxyl group becomes planar with respect to the anthracene moiety; the extent of such relaxation depends on the viscosity of the medium. In addition, the dipole moment of AS molecules increases upon excitation leading to solvent cage relaxation depending upon the solvent polarity.

The emission spectra of AS in different solvents were obtained (Table 5.2). Our results showed slightly larger shifts in the emission maximum than previously reported (Waggoner & Stryer, 1970). The shift of the fluorescence maximum from 450 nm in 3-MP to 475 nm in methanol, both at room temperature, is due to the relaxation of polar methanol molecules around excited state AS molecules. The emission maximum of AS in ethanol at room temperature is 468 nm.

Solvent	3-MP	Methanol	Ethanol	Hexane	Glycerine
τ_f nsec	6.8	1.8	3.1	6.5	8.5
ϕ_f	0.31	0.061	0.18	0.37	-
λ_{max} nm	450	475	468	450	453

Table 5.2 Emission properties of AS in various solvents at room temperaaure. λ_{ex}= 365 nm.

In order to understand the effect of the increase in the viscosity of a polar medium, AS was dissolved in glycerine. Although glycerine is more polar than ethanol (dielectric constant of glycerine is 42.5 compared with that of ethanol is 24.55), the emission maximum of AS in glycerine was at higher energies (453 nm) than in ethanol (468 nm). Also, the life-time of AS was higher in glycerine (τ_f = 8.5 nsec) compared with that in ethanol (τ_f = 3.1 nsec). These results are interpreted in terms of the higher viscosity of glycerine (1.490 cp) compared with ethanol (1.2 cp). In order to further investigate the effect of the viscosity of the solvent on the AS emission, the fluorescence spectra of AS in 3-MP was obtained at room temperature and at 77°K. The emission maximum of AS in 3-MP at room temperature was at 450 nm, that at 77°K was at 427 nm (Fig. 5.6). This shift to higher energy is due to the increase in the viscosity of the solvent indicated an excited state intra-molecular geometric relaxation which occurs in the fluid medium.

Experiments were performed to investigate the emission properties of AS in a polar medium (ethanol) both at room temperature and at 77°K. The emission maximum of AS in ethanol at room temperature, as stated earlier, was at 468 nm, that at 77°K was at 407 nm (Fig. 5.7). Emission at such a short wavelength (407 nm) in rigid ethanol cannot be solely due to the prevention of the solvent molecule relaxation in the excited state. Our

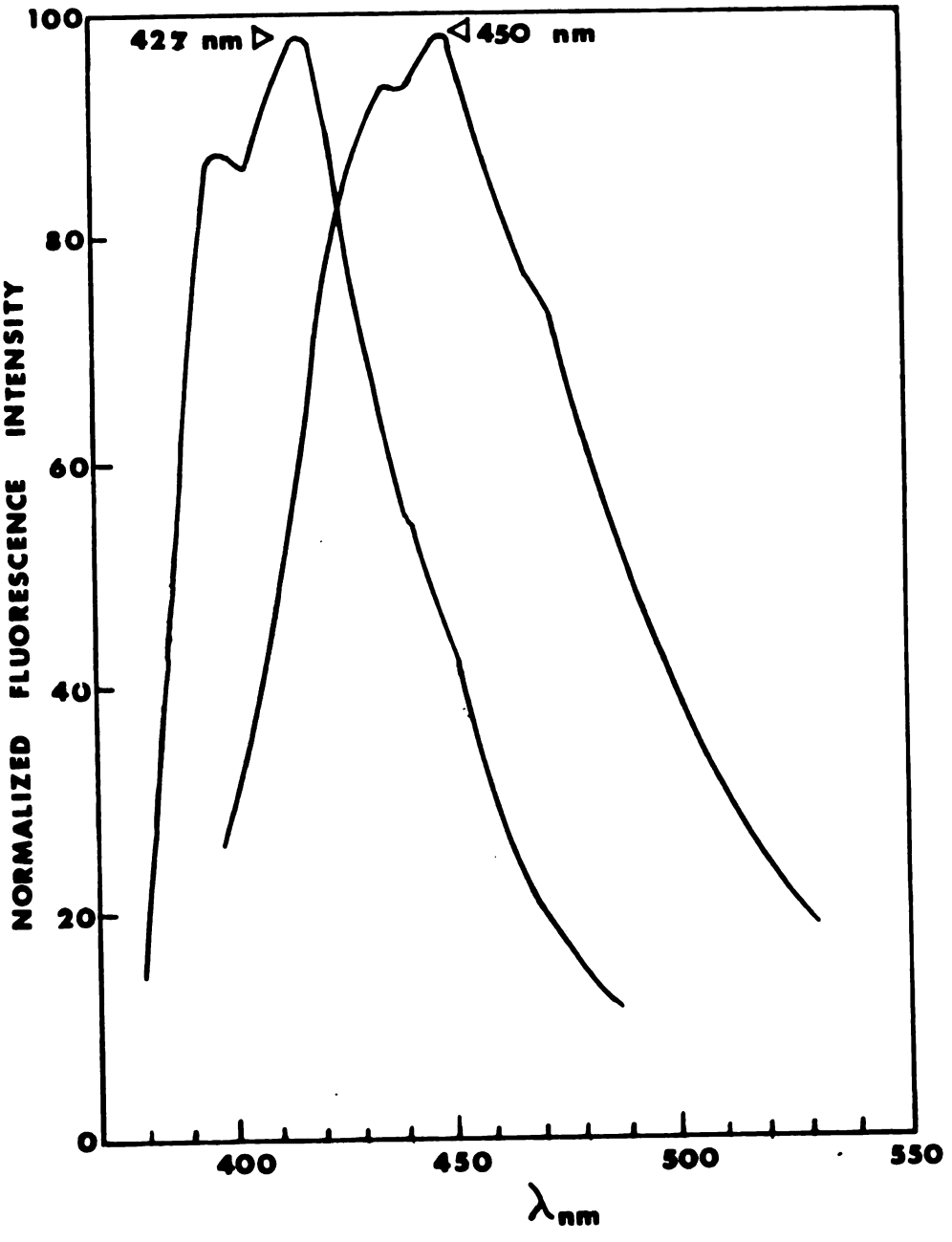

Figure 5.6 Emission spectra of 10^{-5} M AS in 3-methyl pentane (i) room temperature and (ii) 77°K. λ_{ex}= 365 nm.

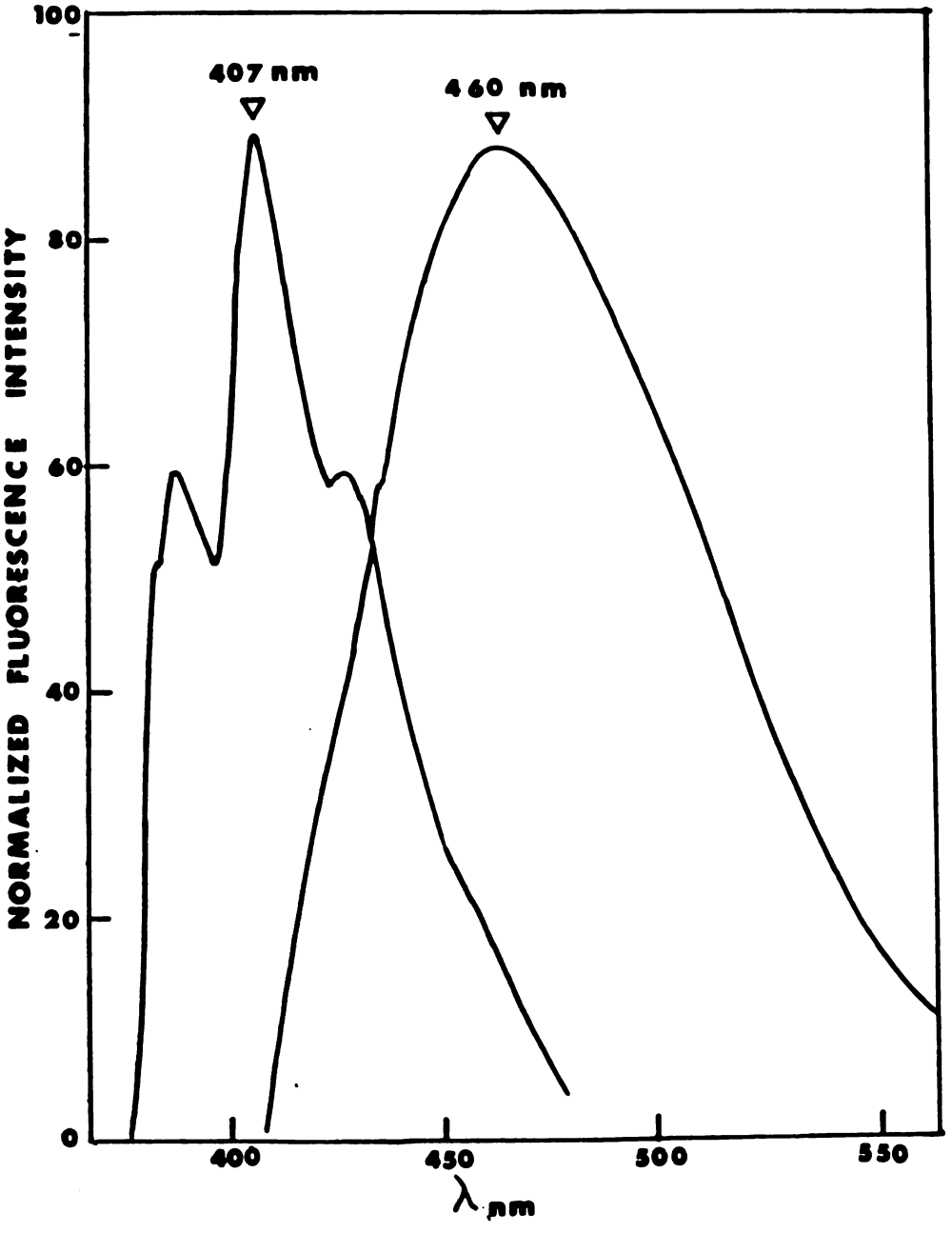

Figure 5.7 Emission spectra of AS in ethanol at (i) room temperature and (ii) 77°K. λ_{ex}=365 nm.

interpretation of these results is in terms of a ground state configuration of AS in which the anthracene ring is more out of plane with the carboxylic group in ethanol compared with 3-MP. Hydrogen bonding of ethanol with the carboxylic group constrained by the fatty acid chain faces such configuration. Thus, in rigid ethanol, the emitting species is essentially anthracene, hence more structured blue fluorescence (407 nm) is observed. In order to investigate the effect of fatty acid chain on the emission properties of anthracene carboxylic acid, ACA (without fatty acid chain), were measured. Fluorescence life-time of AS and ACA was equal (3.2 nsec) at room temperature, at 77^{o}K, life-time of AS was 11.2 nsec, that of ACA was 12.1 nsec. The emission maximum of ACA was at 465 nm at room temperature, that in rigid ethanol occured at 422 nm (Fig. 5.8). In this case, the constraining effect of the fatty acid chain is absent and a relatively more planar configuration is possible.

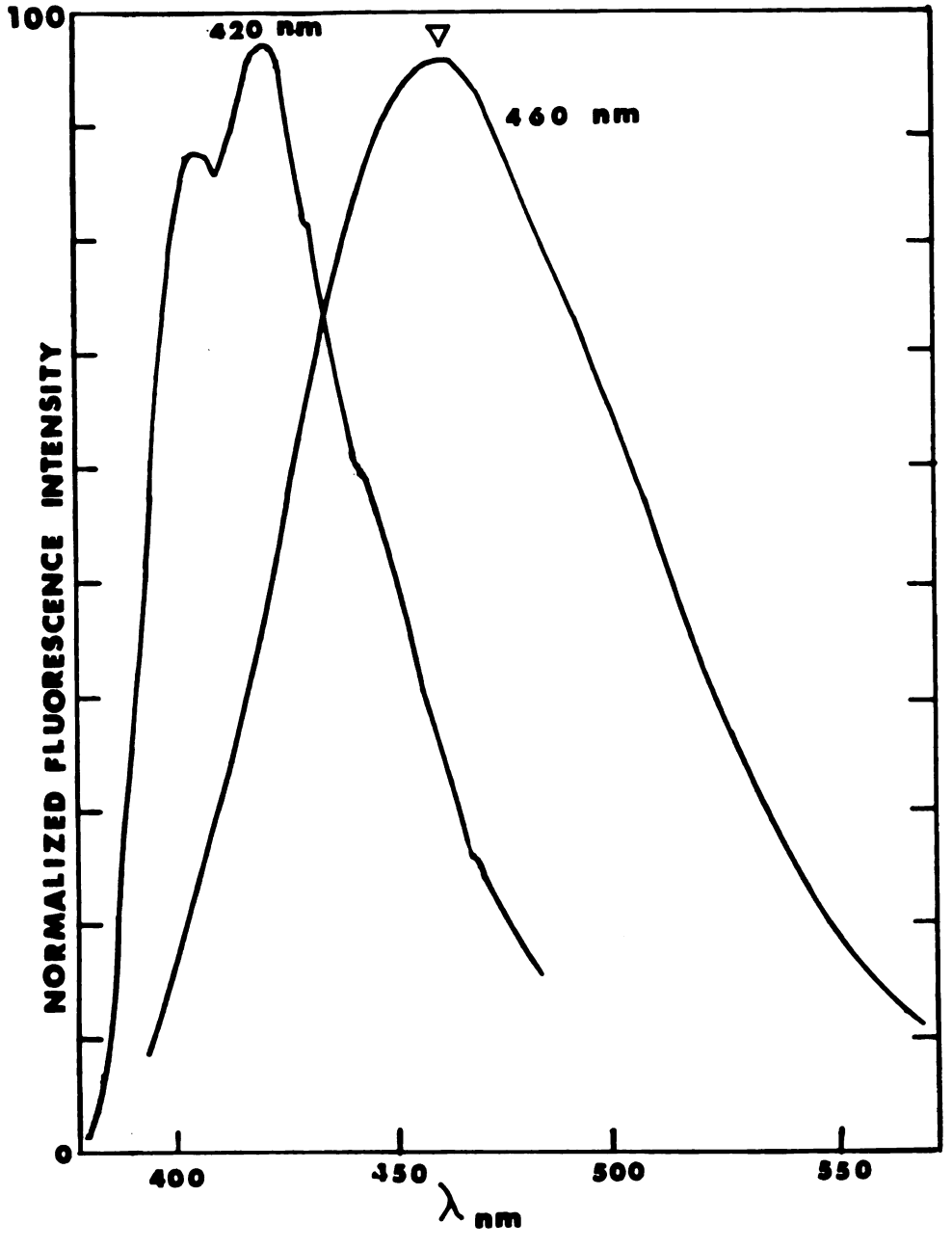

Figure 5.8 Emission spectra of 10^{-5} M ACA in ethanol at (i) room temperature and (ii) 77°K λ_{ex}=365 nm

CHAPTER 6

FLUIDITY STUDIES IN PURPLE MEMBRANE AND CELL MEMBRANE VESICLES USING ELECTRON SPIN RESONANCE (ESR) AND FLUORESCENCE PROBES

(a) Introduction:

In this chapter we have combined spin and fluorescence probe techniques to make a comparative study of the fluidity of pm and cell membrane vesicles (cmv). Fatty acids labelled either with a spin probe or a fluorescence probe are incorporated in pm and cmv to investigate the microviscosity, phase transition temperature and lipid-protein interaction in these membranes. Our studies show that the phase transition temperature of pm is higher than that of cmv and does not depend upon the presence of Na^+. The change in the fluidity of pm above the phase transition is small compared with the case of cmv. Energy transfer experiments suggest that the rigidity of pm is due to the fact that most of the lipid molecules interacting with bacteriorhodopsin (bR). The probes used are shown in Fig. 6.1

(b) Fluidity and phase transition temperatures of purple membrane and cell membrane vesicles using spin probes:

A typical ESR first derivative spectrum of pm at room temperature labelled with 5-NS is shown in Fig. 6.2. The hyperfine splitting ($2T_{//}$) of 5-NS in pm is 62.6 G at room

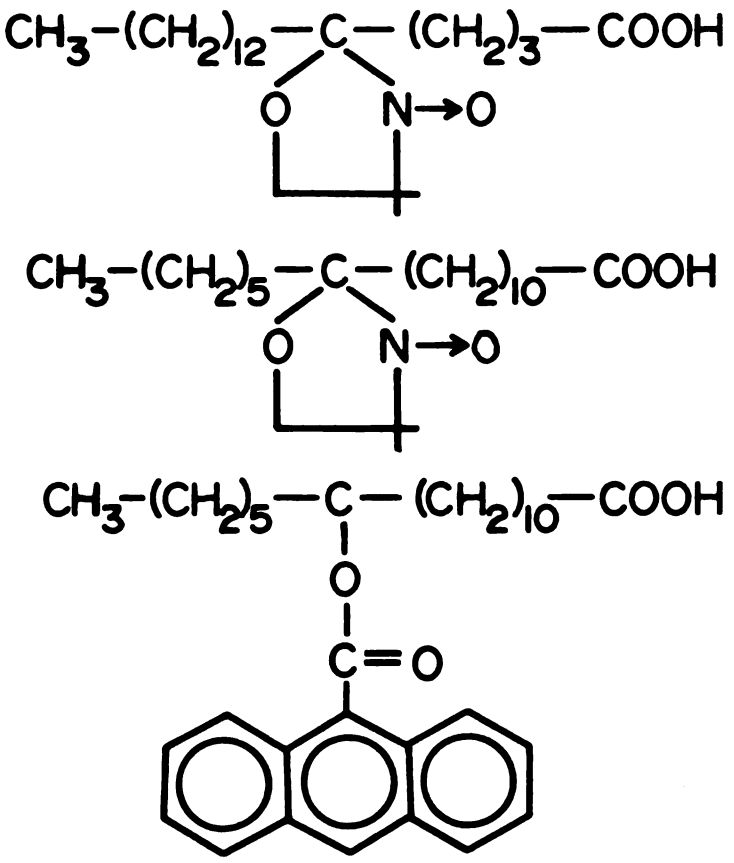

Figure 6.1 Structure of electron spin resonance and fluorescence probes for the fluidity studies

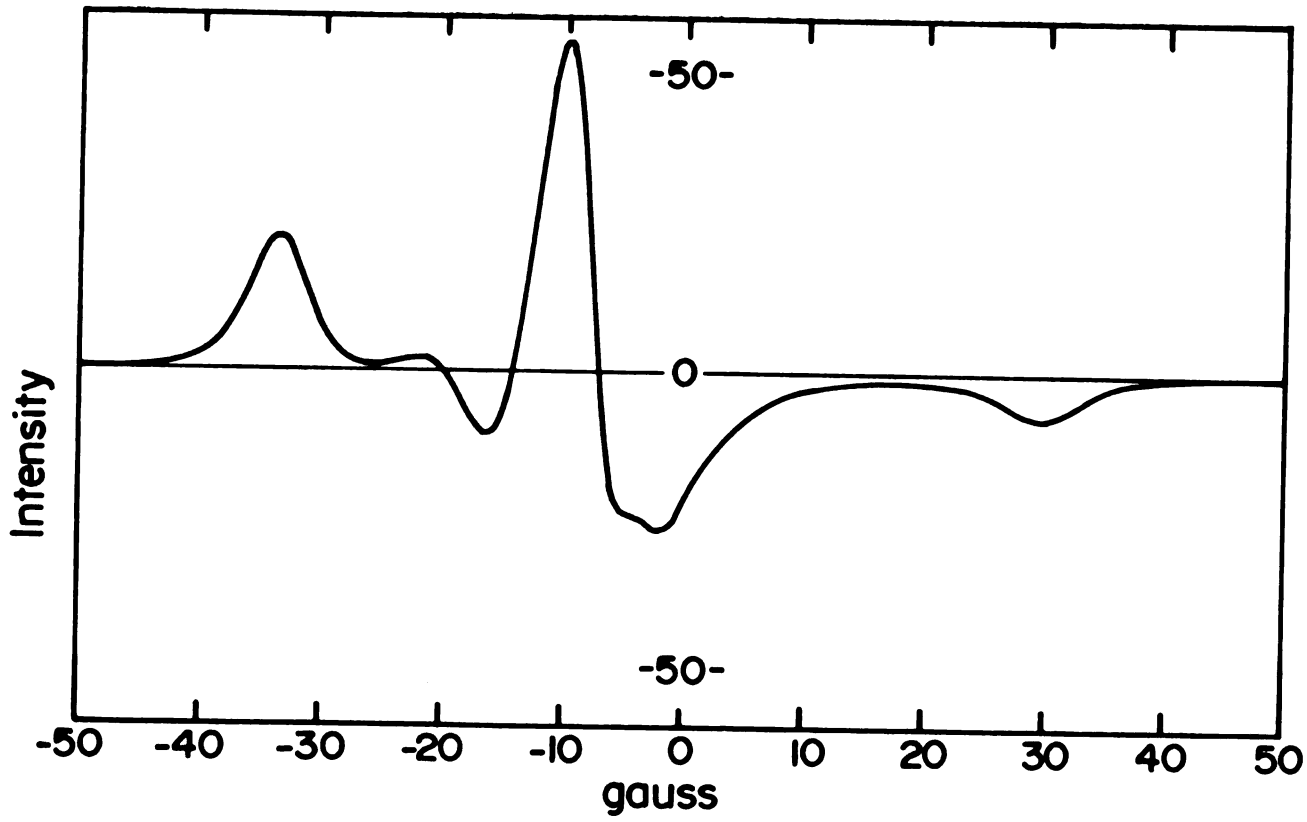

Figure 6.2 A typical ESR spectrum of 5-NS in pm

A typical ESR first derivative spectrum of the purple membrane labelled with 5-ns. 10 ul of 10 mM 5-NS were added to 0.4 ml of 20 mg/ml pm protein in salts 2. Microwave frequency was set at 9.1 GH_z, field set at 3270 G.

temperature. This value of $2T_{//}$ is one of the highest for biological membranes (Chignell & Chignell, 1975) which shows extreme immobilization of the spin probe. The $2T_{//}$ of the cmv, although smaller than that of pm, is also large, 61.2 G, reflecting a high viscosity of cmv. The plots of $2T_{//}$ of 5-NS in pm and cmv against temperature are shown in Fig. 6.3. The thermotropic phase transition of 5-NS occurs at about 31°C for pm and at about 22°C for cmv. The phase transition temperature of pm, 31°C, is slightly higher than the published value (Chignell & Chignell, 1975). Although the $2T_{//}$ of 5-NS is higher than that of cmv at all temperatures, the change in the slope of the $2T_{//}$ with the temperature (above the phase transition temperature of pm) in cmv is much larger than in the case of pm. The phase transition temperatures reported here probably represent a transition from gel + liquid crystalline to liquid crystalline lipid regions (Lee, 1975),(Oldfield et al, 1972),((Shimshick & McConnell, 1973). The small change in the slope of the $2T_{//}$ of the pm below and above the phase transition reflects the restricted mobility of the pm lipids in the liquid crystalline phase. The pm suspended in deionized distilled water gives the same phase transition temperature as that suspended in salts. A sample of pm was dialyzed with 10 mM EDTA, redialyzed with distilled water, then it was washed and resuspended in either 1 mM or 100 mM Mg^{2+}. The $2T_{//}$ of 5-NS in the pm at 37°C remained unchanged for all three (0, 1 mM, 100 mM) concentrations

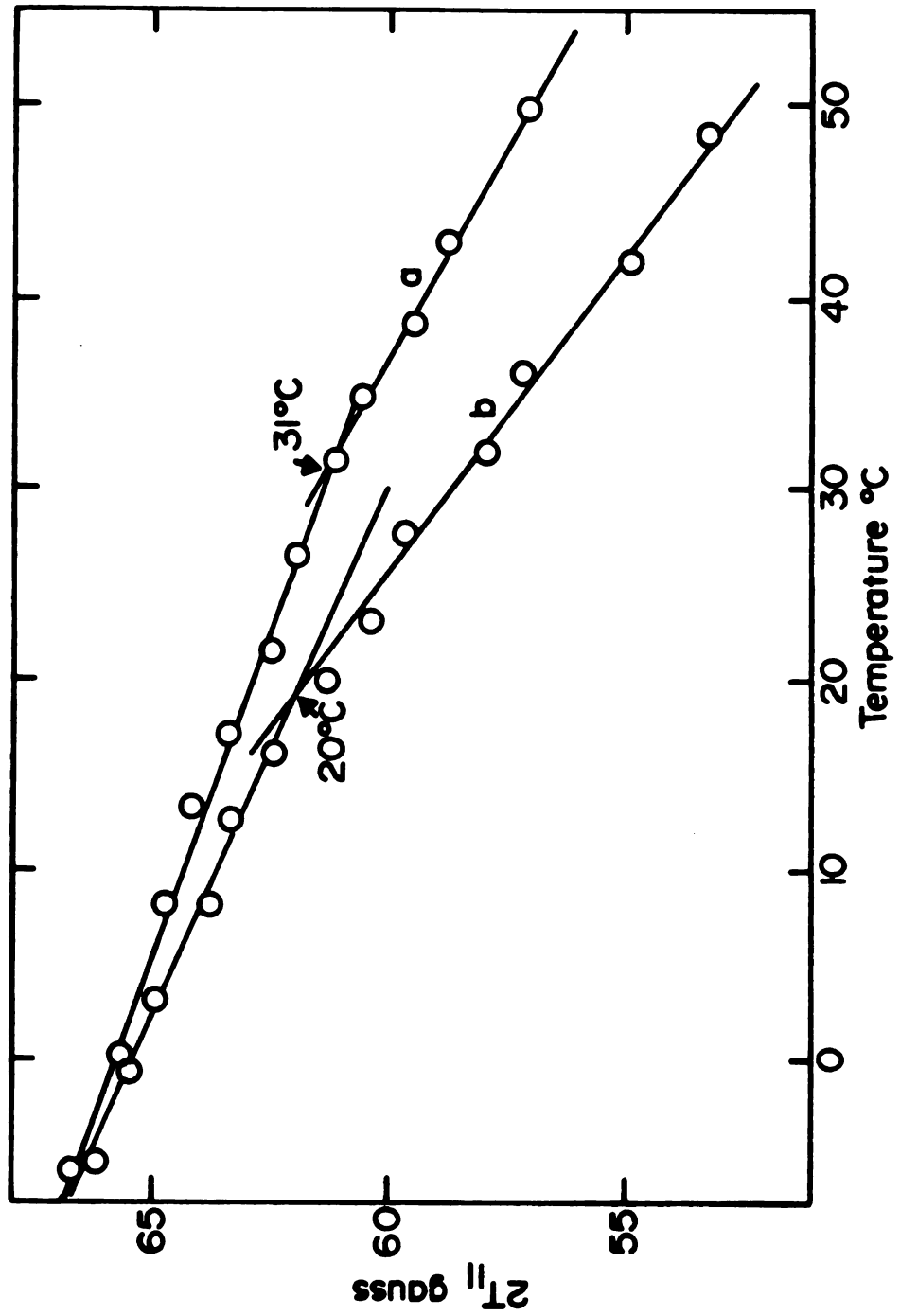

Figure 6.3 Plot of $2T_{//}$ of 5-NS in (i) pm and (ii) cmv as a function of temperature

of Mg^{2+} for one set of experiments. Our data indicate that the monovalent cation Na^{+} and possibly divelent cation Mg^{2+} do not change the value of $2T_{//}$ of 5-NS in the pm at 37°C. It appears that these cations do not influence the organization of the lipids in the pm at growth temperature. It has been shown that in case of T. acidophila, the addition of divalent cation Ca^{2+} raises the temperature of the gel to gel + liquid crystalline transition (Weller & Haug, 1977). For pm, that transition may occur at a low temperature and thus could not be detected. The comparatively low value (22°C) of the phase transition temperature in cmv indicates that the spin probe is incorporated predominantly in regions other than pm patches which are more fluid than pm, particularly above the phase transition (Oldfield et al, 1972).

The cmv for the above experiments were isolated from cells grown at the optimum conditions for the biosynthesis of pm. The extent of pm was approximately 40% w/w with slight variation depending on the preparation. To determine whether the presence of pm changes the phase transition temperature or not, the cells were grown at a low light intensity and a high rate of aeration to inhibit pm biosynthesis. These cells were lysed and assayed spectrophotometrically. They did not contain the characteristic pm band at 560-570 nm. The thermotropic phase transition of the vesicles isolated from these cells occured at about 19°C compared to 22°C for the cmv containing the pm.

In order to investigate the rigidity of the hydrocarbon region of the cmv towards the center of the bilayer, they were labelled using 12-NS. The thermotropic phase transition of 12-NS incorporated in the cmv occurs at about 18°C compared with 22°C for 5-NS as shown in Fig. 6.4. The relatively small change in the phase transition temperature using 5-NS and 12-NS indicates that the rigidity of the hydrocarbon region of the cmv extends at least upto 12 th carbon position.

It is well established that H. halobium polar lipids are mainly diphytanyl ether analogs of phospholipids and glycolipids (Kates, 1972),(Marshall & Brown, 1968),(Plachy et al, 1974). These phytanyl ethers contain a methyl group at carbons 15, 11, 7 and 3 from the ether linkage. Model studies indicate that the branching methyl can pack rather well in all-trans configuration if the lipid chains are tilted to about 20° from the normal or if the lipid molecules are staggered (Plachy et al, 1974). The resulting closer packing extends the rigidity further down the hydrocarbon chain compared with the saturated, unbranched situation. The closeness of the phase transition temperature of 12-NS (18°C) and 5-NS (22°C) in cmv may indicate regions of similar rigidity between the 5 th and 12 th carbon due to closer packing. On the other hand, as proposed by Plachy et al (1974), the nitroxyl radical of the 12-NS molecule may be in the glycerol region at low temperature and in hydrocarbon region at high temperatures. If this is the

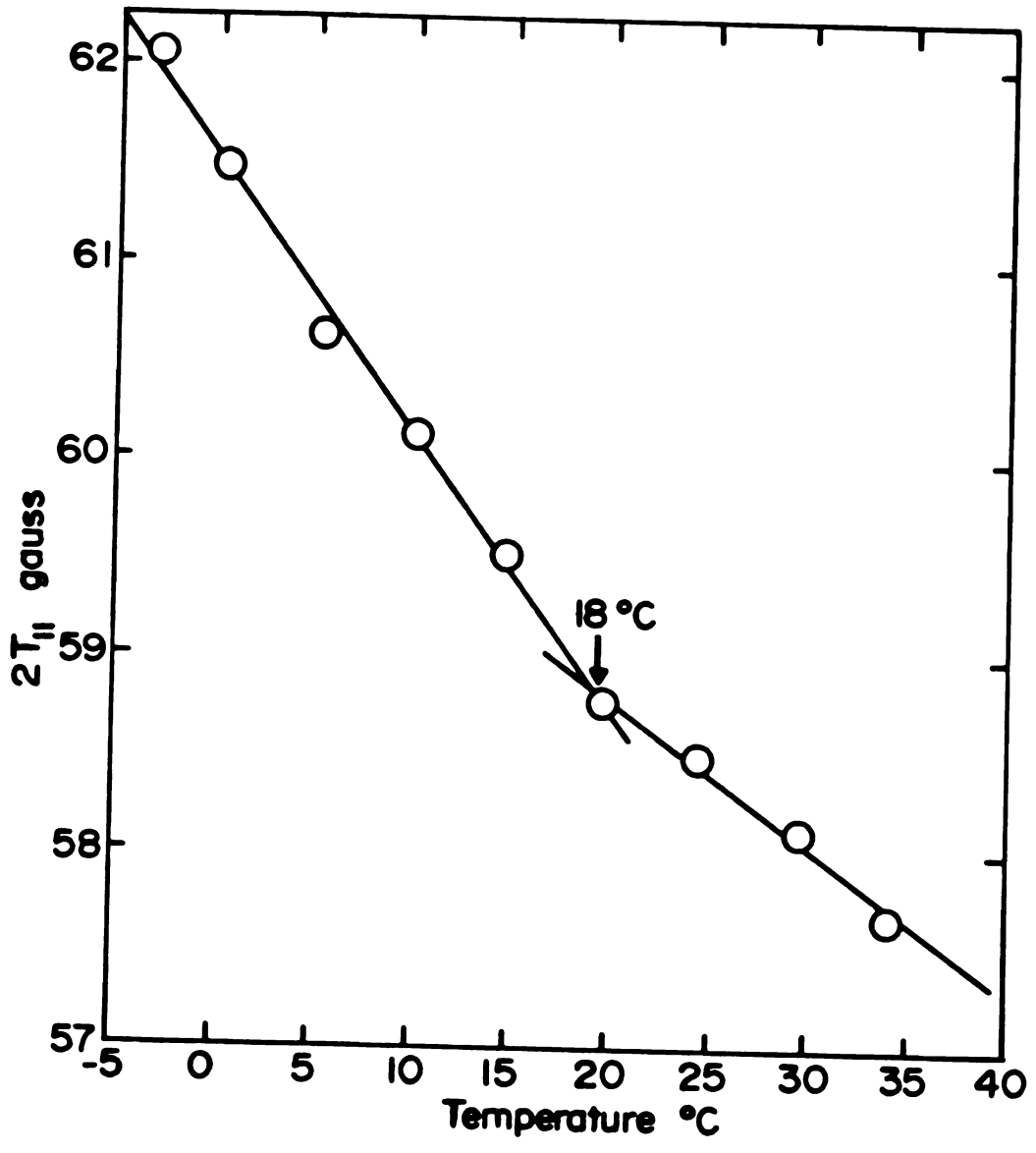

Figure 6.4 Plot of $2T_{//}$ of 12-NS in cmv as a function of temperature.

case, the 12-NS results may not mean extended rigidity upto the twelfth carbon. Although this point cannot be resolved conclusively, our fluorescence studies make us feel that the rigidity extends upto the twelfth carbon.

(c) Fluidity and packing of purple membrane and cell membrane vesicles using a fluorescence probe, anthroyl stearate:

The pm, cmv and, as a control, phosphatidyl choline vesicles (pcv) were labelled with AS in pcv suspended in liposome buffer. The emission maximum of AS in pcv occurs at 446 nm. The emission maximum of AS in cmv occurs at 437 nm and has a slight shoulder at 417 nm. Finally, the emission maximum of AS in pm occurs at 435 nm and has another peak at 417 nm (Fig. 6.5).

The life-time of decay of fluorescence of AS in pcv is 12.6 nsec (Vander kooi et al, 1974),(Waggoner & Stryer, 1970). The decay of fluorescence of AS in pcv can be fitted by a single exponential. On the other hand, there are three components of the fluorescence decay of AS in the cmv and in pm. The shortest one is attributed to the scattering due to the size of the membranes. In order to keep the probe:lipid ratio below 1:100, the concentration of the membrane is usually 20-30 μg/ml, which causes some scattering. The other two components are τ_1 = 3.6 nsec and τ_2 = 10.0 nsec for the cmv. They are τ_1 = 3.2 nsce and τ_2 = 9.1 nsec for the pm. The τ_1 component of the decay is attributed to the AS probe molecules that undergo

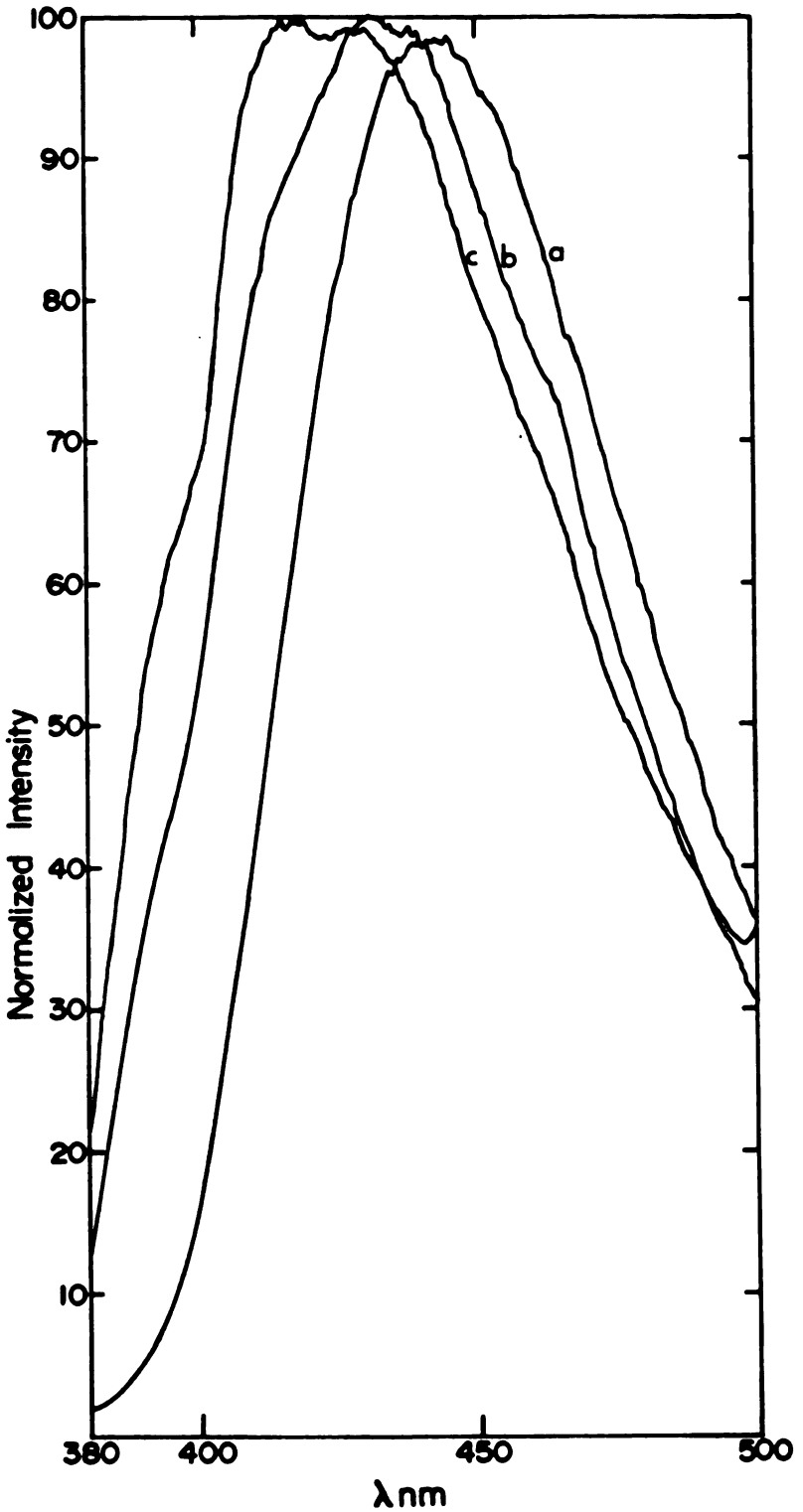

Figure 6.5 Emission spectra of 10^{-5} M AS in (a) pcv in liposome buffer, (b) cmv in salts 2, and (c) pm in distilled water.

energy transfer by Förster mechanism (Förster, 1951) to the chromophore of the bR or to the carotenoid pigments in the cmv. Such energy transfer is possible due to the spectral overlap between AS emission and the absorption of bR or carotenoid pigments. To verify that the origin of the τ_1 component in the pm as being due to fluorescence decay of AS involved in the energy transfer, the pm labelled with AS was bleached. The spectral overlap between the emission of AS and the absorption of the bleached pm (oxime absorbs at 355 nm) is much less than with the absorption of bR in the native pm and hence the energy transfer is expected to be less efficient in the bleached pm. Upon bleaching AS labelled pm, the emission maximum of AS remained at 435 nm, however, the fluorescence intensity increased almost 100% and the long component τ_2 of the fluorescence decay became more dominent compared with the case of native pm. These results are interpretted in terms of an efficient energy transfer from AS to bR. The decay of AS fluorescence in E. coli outer membrane vesicles (ecomv), which is another rigid membrane (the rigidity of ecomv is similar to that of cmv as measured by $2T_{//}$ of 5-NS, Gupte & McGroarty, unpublished results), but where no energy transfer is expected, has been measured. As expected, the contribution of the long component τ_2 to the fluorescence decay of ecomv is much larger than in the native or bleached pm (Fig. 6.6).

The study of the fluorescence properties of AS in the

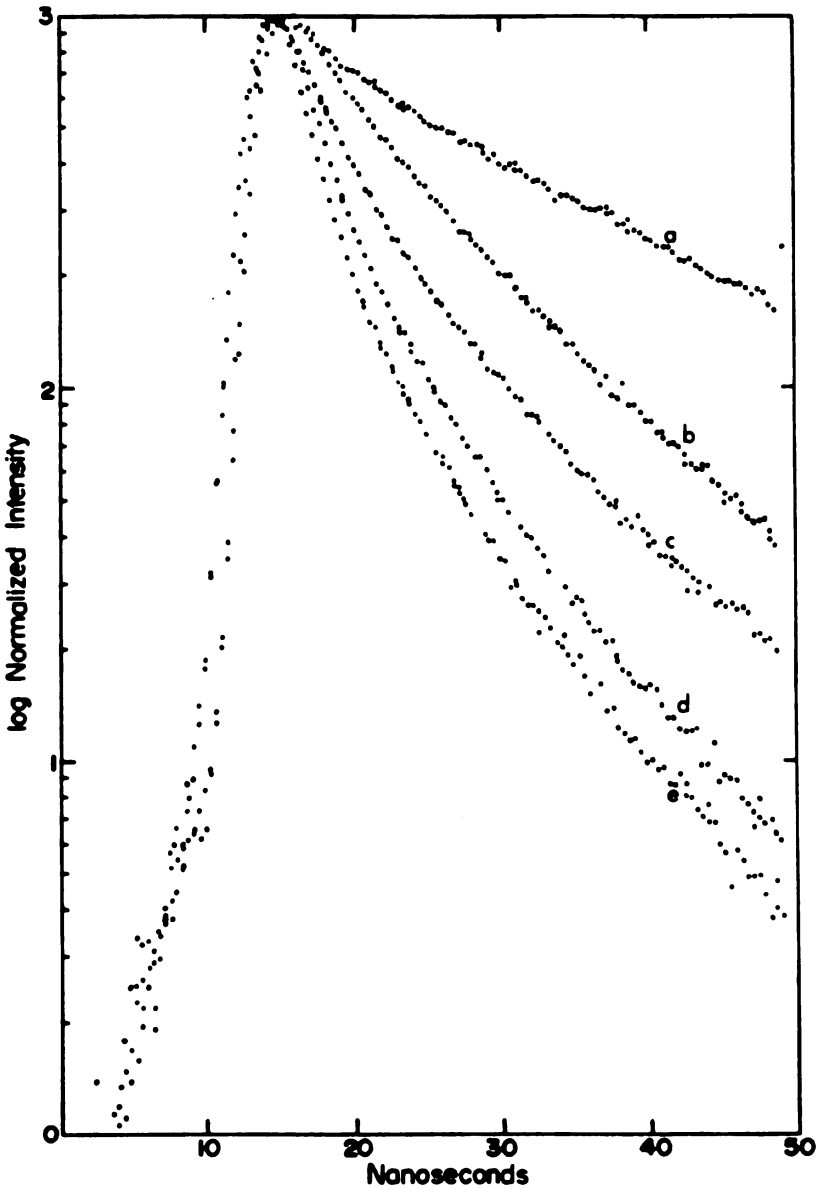

Figure 6.6 Decay of AS fluorescence in various membranes

Decay of AS fluorescence in various membranes was obtained by nanosecond time-resolved spectroscopy. A 365 nm interference filter was used for excitation and decay was monitored at the individual emission maxima. The decay was observed in the following membranes: (a) pcv, (b) ecomv, (c) bleached pm, (d) cmv, and (e) pm.

pm and cmv and coupling these results with those obtained using spin probes 5-NS and 12-NS strengthens our previous arguments and adds to our understanding regarding the structure of these membranes. As discussed in Chpater 5, the AS probe undergoes a geometrical relaxation in the excited state such that the plane of the carboxyl group becomes more planar with respect to the anthracene moiety; the extent of such relaxation depends on the viscosity of the medium. The emission maximum of AS in fluid hydrocarbon medium occurs at 450 nm, whereas in rigid hydrocarbon medium ($77^{o}K$) the maximum shifts dramatically to 427 nm. In addition, the dipole moment of AS molecules increases upon excitation leading to solvent cage relaxation dependent on solvent polarity. The fluorescence wavelength maximum of AS shifts to lower energies and the fluorescence life-time decreases as the polarity of the medium is increased. The fluorescence maximum of AS in pcv shows that the probe is in hydrocarbon environment (Waggoner & Stryer, 1970). It has been shown that the emission maximum shifts to higher energies as the temperature is lowered (Vanderkooi, 1972). This indicates that the increased rigidity of lipid environment at lower temperature shifts the emission maximum of AS to higher energies. In our experiments, the AS emission shifted from 446 nm in the pcv to 437 nm in cmv to 435 nm in pm indicating that the environment of the hydrocarbon region of the lipids of H. halobium is more rigid than pcv and the pm lipids are

more restricted than the cmv lipids. AS in the pm had another peak at 417 nm. This emission maximum occurs at higher energies than the emission maximum of AS in rigid hydrocarbon medium (427 nm). The 417 nm emission probably originates from tightly packed AS molecules where the carboxyl group is further twisted out of plane of the anthracene ring due to the packing restrictions in the membrane such that the emission is more like anthracene than anthracene carboxylic acid in rigid hydrocarbon medium.

The fluorescence wavelength maximum of the AS probe incorporated in the pm and cmv changed with temperature as shown in Fig. 6.7. To interpret such changes, one must point out that the fluorescence maximum of AS depends on the extent of excited state relaxation of the fluorescence moiety which in turn depends on the microscopic "viscosity" in the immediate vicinity of the fluorescence moiety. In other words, it depends on the free volume available for the motion of the anthracene ring. It is not surprising, therefore, to see that a phase transition temperature obtained from these measurements will not reflect the macroscopic viscosity of the membrane as measured by 5-NS or 12-NS ESR probes, but may correspond to a rotational degree of freedom in the fatty acid molecule; which may be probably the same in the pm and cmv. The tighter packing of the lipid molecules in pm due to the bR protein molecules will, however, limit the relaxation of the AS probe, compared to its relaxation in cmv giving rise to a smaller

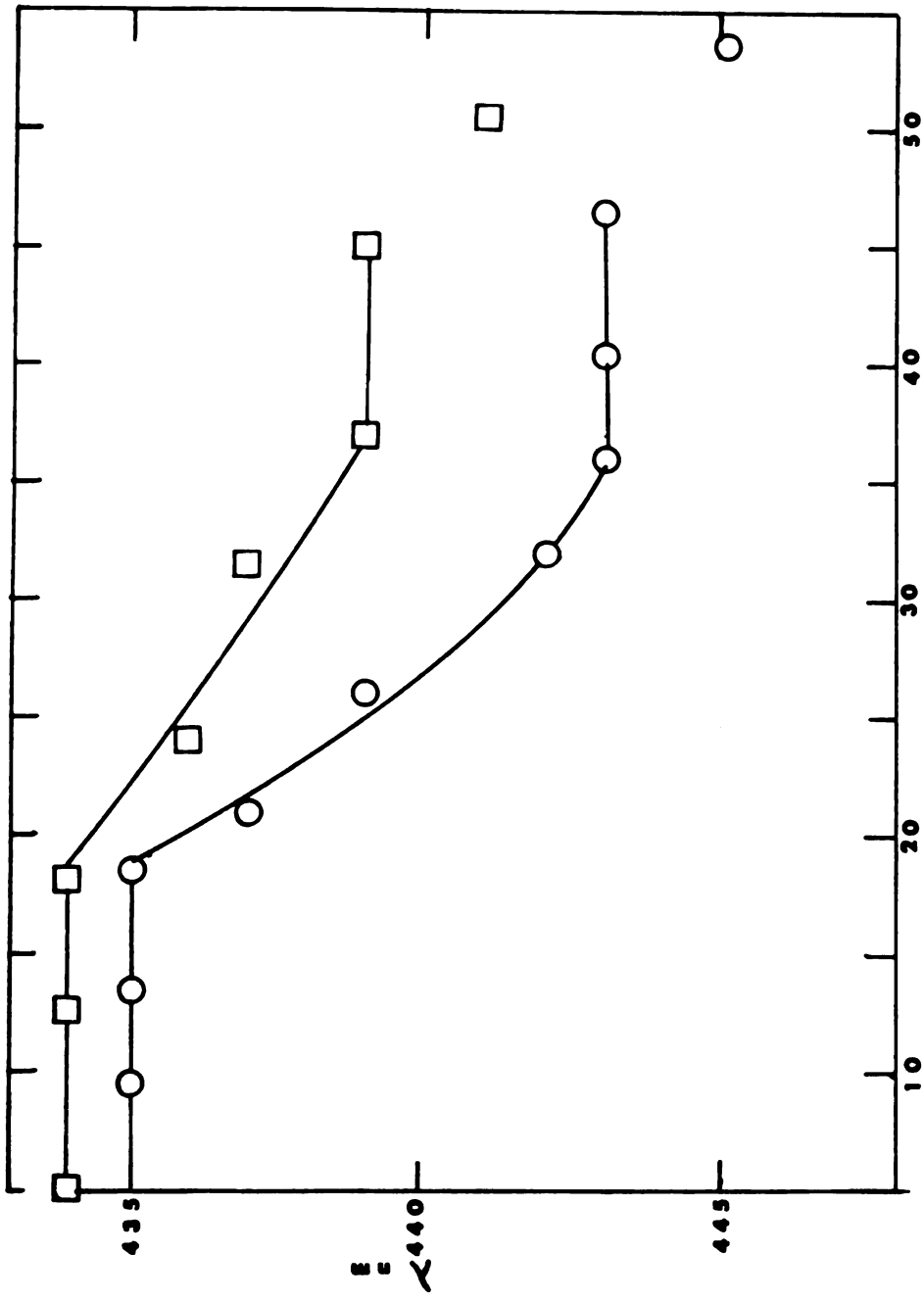

Figure 6.7 The temperature dependence of the emission maxima of AS in (i) pm and (ii) cmv.

change in the emission maximum of pm compared to cmv. Thus one should look for the value and the change (434 nm for pm at low temperature compared to 435 nm for cmv, also 439 nm for pm at high temperature compared to 443 nm for cmv) in the emission wavelength maximum of the AS probe molecules to compare membrane fluidity. It is clear from the figure 6.7 that the fluidity of the pm and cmv is similar at low temperature (below 20°C) but above 35°C, the cmv is such less rigid compared with pm. Such observation is consistent with ESR data previously discussed. It is interesting to note that the pm labelled at room temperature showed a smaller decrease in the intensity of fluorescence as a function of temperature compared with the pm labelled at 37°C. Highly ordered domain of the bulk lipids below the phase transition may have limited the insertion of the probe in that domain compared with its insertion at the boundary lipids or at the hydrophobic sites within the protein. The fluidity of the boundary lipids is known not to change significantly as a result of phase transition (Wunderlich et al, 1975), accounting for a smaller decrease in the intensity of fluorescence of AS in the pm labelled a at room temperature. No such difference was observed for 5-NS which may be explained in terms of the bulkier and more hydrophobic AS probe.

(d) Review of the structure and composition differences in lipids and proteins of purple membrane versus cell membrane vesicles:

The evidence presented so far clearly indicates that the pm is more rigid than cmv. The structural differences in pm and cmv are discussed here to explain the possible cause of such a difference. The ratio of protein:non-protein (lipid) in our preparation was 78:22 (5% error) compared with published value of 75:25.

(i) Lipids: In general the halophilic lipids are very acidic. The composition of the red and purple membrane lipids of H. cutirubrum (Kushwaha et al, 1975) and the similarities in the pm of H. cutirubrum and H. halobium (Kushwaha et al, 1976) have led us to believe that these two bacteria are structurally very similar. Therefore, the lipids of H. cutirubrum in the red and purple membrane are compared:

(a) Lipid composition: About 34% lipids of pm are different from those of the red membrane. The pm contains 19.3% triglycosyl diether, 10.3% glycolipid sulfate and 4.8% phosphotidyl glycerosulfate. The glycolipids of the red membrane are not identified, however, are different. These different lipids in the pm are mainly sulfated lipids. The influence of a sulfate polar group instead of a phosphate polar group on the ionic interaction of the membrane is not known but may be important for the cation interaction and consequently the solubilization of cmv in distilled water.

(b) Percentage of lipids: Also, the red membrane(cmv) contains more lipids. About 37-38% lipids are present in cmv compared to about 25% of pm.

(ii) Proteins: The halobacteria proteins are, in general, more acidic (Larsen, 1967). In case of H. halobium, the degree of acidity is very different for cmv and pm (Lanyi, 1974). Mole percent excess acidic residues in cmv is 17.5, in pm 6.2. Another factor is the ratio of volume for polar and non-polar residues: it is 1.124 for cmv, 0.610 for pm. Also, the hydrophobicity index (in Kcal/ residue) for cmv is 0.934, for pm it is 1.261. All these factors indicate the difference in the nature of the proteins in these two membranes. Lanyi (1974) states that above 0.5 M NaCl concentration, hydrophobic interaction is a major factor in the salt relation of halophilic proteins. There is a body of indirect evidence (Brown, 1976) that in halophiles, the hydrophobic bonds are intrinsically weaker than non-halophiles and that they require the "salting out" effect of high concentrations of NaCl to bring them upto the "normal"strength. If the higher degree of hydrophobicity in the bR can be used to consider pm as a "non-halophile" membrane and if mole percent excess of acidic and polar residues of cmv over pm is taken into account, the difference in the requirement of NaCl may, at least partially, be explained. Also, the trimeric unit of pm (Henderson & Unwin, 1975) may be formed by a hydrophobic interaction between the neighbouring proteins

without involving lipids for added stability.

The X-ray diffraction and electron microscopy data (Blaurock, 1975),(Henderson & Unwin, 1975) raise some interesting questions about the location of lipid domains in the pm. The molecular weight of a glycolipid sulfate is 1241.6 daltons (Kates, 1972), therefore, the minimum number of lipids:protein based on 25:75 weight ratio is 7. For a trimeric unit, there are 20-25 lipids according to this calculation. To fill the space between a trimeric unit according to Henderson-Unwin model (1975), 10 lipid molecules of 60 Å are needed (Blaurock, 1975) if a lipid bilayer is considered. This calculation leaves only 10-15 molecules per unit cell of proteins for a "lipid domain". The rigidity of pm above the phase transition can be explained by considering the influence of the proteins restricting the hydrocarbon chain. Therefore, the lipid-protein interaction seems to be a very important factor in the maintainance of rigidity in the pm.

(e) Summary:

In summary, our study of the fluidity of pm and cmv employing ESR and fluorescence probe techniqueshas shown that the cmv is a rigid membrane, although less rigid than pm. In cmv, the rigidity extends at least to the 12 th carbon atom of the acyl chain reflecting a tight packing. The presence of Na^+ or possibly Mg^{2+} does not affect the fluidity of pm at growth temperature. The rigidity of cmv lacking pm is smaller than cmv containing pm. Relative

fluidities of pm and cmv can be measured using the magnitude and change in the fluorescence wavelength maxima of AS probes. There are essentially two populations of AS molecules in pm, one near the protein molecules that undergoes an efficient energy transfer to bR, the other population in the bulk lipid phase of pm. AS molecules in the lipid region of cmv outside pm patches exhibit some energy transfer to carotenoid pigments. In addition of being a fluidity probe, the As molecule is also a "packing" probe reflecting the packing restrictions on the ground state configuration of the anthracene carboxylic acid chromophore. The rigidity of pm seems to be due to high protein:lipid ratio and interdigitation of protein in the membrane.

CHAPTER 7

CHROMOPHORE INTERACTIONS OF BACTERIORHODOPSIN OF THE PURPLE MEMBRANE

(a) Background:

As stated earlier, the retinal in bR is covalently bound to an ε-amino group of a lysine of the opsin moiety via a Schiff base, similar to rhodopsin. The chromophore of bR kept in dark (dark adapted) has an absorption peak at about 560 nm. If bR is exposed to visible light between 500 and 700 nm, the absorption maximum of the 'purple' peak shifts from 560 to 568 nm (Becher & Cassim, 1976). The chromophore of this light adapted bR is shown to be all-trans retinal (Jan 1975),(Pettei et al, 1977) while in the dark adapted bR, it is a mixture (1:1) of all-trans and 13-cis retinal. In contrast to other rhodopsins, the chromophore of bR, all-trans retinal, stays covalently bound to the protein after the absorption of a photon.

The unprotonated retinal-Schiff base (e. g. retinal tertiary butyl amine) absorbs around 380 nm, depending upon the particular isomer. The absorption shifts to much longer wavelengths, the extent of which depends on the particular species from which rhodopsins are obtained. For bovine rhodopsin, this absorption maximum is at 500 nm, in case of bacterial rhodopsin (bR), it shifts to 568 nm. For some invertebrate species, the absorption maximum shifts

further to 620 nm. Various models and theories have been proposed to account for the observed red shift in rhodopsins from the from the studies performed on the model compounds. Most recent studies of the retinal-Schiff bases are summarized as follows:

(b) Some theoretical considerations for the absorption of the retinal-Schiff base:

(1) Retinal: The retinal molecule can be divided into three parts to understand the nature of its interaction. (i) linear polyene (conjugated chain) (ii) β-ionone ring and (iii) aldehyde moiety. The conjugated polyene structure is primarily important for the absorption of retinal. The observed absorption bands of the linear polyene corresponds to $\pi \rightarrow \pi^*$ transition (Honig et al, 1975). In case of the simplest polyene, butadiene, four π-electrons correspond to the molecular excited state levels whereas for octatetraene, which is the backbone of retinal, there are eight such levels. The 1^1Bu state is strongly allowed and corresponds to the intense lowest energy band normally observed in the polyenes. The β-ionone ring is twisted at bond 6-7 due to the interaction of 7-H, 8-H and 5-CH_3 causing steric hindrance. Additional twisting is exerted due to cis-isomerization. In addition, the $n \rightarrow \pi^*$ transition of aldehyde moiety is important to introduce the red shift. The cis isomers of retinals in various rhodopsins are twisted in addition to the bend (Hubbard, 1976). The 11-cis retinal is the most crowded of all isomers due to the hindrence

between 11-H and 13-CH_3. The quantum yield for the photo-induced isomerization of various cis-isomers to all-trans retinal, (which has lowest energy) ranges upto 0.5 (Land, 1975). These studies indicate that larger the steric hendrance of an isomer, more important is the protein environment to accomodate the twisted molecule.

(2) Retinal-Schiff base: The effect of the environment on the retinal and on Schiff-base linkage may also be responsible for the bathochromic (red) shift mentioned earlier. Several researchers have suggested that the red shift in rhodopsins can be explained by some sort of solvent effect due to protein, e. g. various interactions due to amino acid residues in the immediate vicinity, on the chromophore. Therefore, the environmental effects on the retinal-Schiff base spectra in various solutions as a model system have been studied for understanding the effect of the protein environment on the chromophore of rhodopsins. Conclusions of these studies range from charge-transfer complexes (Mendelsohn, 1973) to a combination of anion separation and rotation about the 6-7 single bond of the chromophore, induced by the binding to the protein. Some experiments are designed to understand the mechanisms of the solvent effects using the solvents to mimic various amino acids, coupled with the calculations of protonated Schiff-base spectra charge distribution. These types of experiments indicate that highly polarizable amino acid side chains and electrostatic interactions involving

ionized amino acid carboxylates are capable of providing a microenvironment which can explain red shifts of the protonated retinal-Schiff bases upto 620 nm (Kliger et al, 1977),(Milder & Kliger, 1977). This microenvironment (cavity) may also be isolated from the external solvent effects and may be specific to facilitate close interactions with various parts of retinal-Schiff base.

(c) Review of the optical activity of bacteriorhodopsin

On the structural basis, the interaction of retinal with the protein can be investigated by the optical activity of rhodopsins. Although no circular dichroism (CD) is observed for retinal in solution, all rhodopsins exhibit strong optical activity induced by asymmetry from the proteins. In contrast to bovine rhodopsin (and similar rhodopsins in a fluid membrane), which has two positive bands, one at about 481 nm and the other at about 335 nm (Honig & Ebery, 1974), bR has a positive band at 500 nm, a negative band at 620 nm and a crossover at the absorption maximum. If the trimeric units (see chapter 4) of bRs in the pm are solubilized with detergent, the negative band disappears (Heyn et al, 1975),(Ebery & Becher, 1976). Therefore, it seems that the occurence of the negative band is not due to chromophore-protein interaction. The optical activity of pm, therefore, can be divided into (i) positive band due to chromophore-protein interaction and (ii) positive and negative band due to chromophore-chromophore (exciton) interaction between the

neighbouring proteins. Upon solubilization, the functional trimeric unit may become uncoupled, abolsihing the exciton interaction. Other rhodopsins are known not to exist in a polymeric form. As a result, only positive CD spectra due to protein-chromophore interaction is observed. Two hypotheses have been proposed to explain the nature of the optical activity of chromophore-protein interaction. One model suggests that the chromophore transition is coupled to an asymmetric center in the protein, while the second model suggests that protein binding induced the chromophore to adapt a unique asymmetric conformation that is optically active. Calculations indicate that both models are capable of accounting for the observed magnitude of the optical activity (Honig et al, 1975).

The difference in the nature of the CD spectra between bovine rhodopsin and bR is probably due to exciton interaction (Heyn et al, 1976),(Kriebel & Albrecht, 1976). The extent of exciton interaction can be predicted by taking into consideration the transition dipole moments, rotational strengths and symmetry rules. Therefore, a brief discussion of the exciton coupling is in order.

(d) Theory of exciton interaction:

An exciton is described as a wavepacket travelling through a crystal lattice. It represents a neutral particle which is associated with the wavepacket in the same way a particle or 'photon' is associated with a light wave packet (El-Bayoumi, 1961). As discussed in chapter 2, the

integrated intensity of an absorption band may be directly proportional to the square of the electric dipole moment for the transition. The transition dipole moment has a fixed direction within a molecular group. Just as the observed absorption may arise from its dipole strength, CD arises from the rotatory strength R which can be measured by the area of the CD band. The measurement of the optical activity can detect only the relative orientations of the transition dipole moments in its constituent groups, not the positions and orientations of atoms and bonds. The symmetry rules, which are discussed below, provide predictions of the sign and order of magnitude of the optical activity from the molecular conformations. These symmetry rules are based on (i) one electron mechanism for $n \rightarrow \pi^*$ transitions, (ii) dipole coupleing mechanisms for strong transitions and (iii) electric-magnetic coupling (Schellman, 1968). Out of these three rules, the dipole coupling mechanism is the most significant for the exciton interaction. The magnitude of the shift caused by the exciton interaction is a function of the oscillator strength of the transition of the free molecules under study and to a great extent depends on the distance between the interacting molecules and their geometric orientation.

For two identical coupled transitions, the exciton predicts a splitting of the absorption band and a couplet type CD spectrum. The wavelengths of the absorption maxima of the split band is given by:

$$|\lambda_+ - \lambda_-| = \frac{2|V_{12}|}{hc}(\lambda_{max})^2 \quad \ldots\ldots\ldots 7.1$$

where $|V_{12}|$ is the coupling energy and is proportional to the monomer absorption (λ_{max}). The CD spectrum of a dimer is given by

$$\Delta\epsilon(\lambda) = (\Delta\epsilon_{max}) \; e^{-((\lambda-\lambda_-)/\Delta)^2} - e^{((\lambda-\lambda_+)/\Delta)^2} \quad \ldots\ldots\ldots 7.2$$

where Δ is the bandwidth of the absorption band and is the wavelength of the monomer absorption maximum. λ_+ and λ_- are the wavelengths of the absorption maxima of the split bands (Heyn, 1975). The absorption frequencies, dipole strengths and rotational strengths for various orientations of the exciton dimers have been calculated (Tinoco, 1963). This dimer model can be extended to trimers and infinite polymers. An excellent theoretical discussion about the excitonic interaction in a trimeric unit is given by Kriebel and Albrecht (1976).

(e) Experimental absorption and circular dichroism data of bleached and stepwise reconstituted purple membrane:

We have obtained the absorption and CD spectra of bleached and stepwise reconstituted pm to investigate the nature of chromophore interactions of bRs in the pm. As stated earlier, the color of pm is actually intense purple, similar to bright red color of dark adapted rhodopsin. In

the presence of visible light, the red color of rhodopsin changes to glossy yellow. This disappearance of the color of rhodopsin is referred to as "bleaching". BR cannot be bleached by mere exposure to visible light, it bleaches only with a harsh chemical treatment coupled with visible light. It can be reversibly bleached either by organic solvents such as ether, dimethyl sulfoxide (Hess & Oesterhelt, 1973) or by NH_2OH, pH 7.0 (Oesterhelt et al, 1974).

We achieved the stepwise bleaching of pm by suspending it in 0.2 M NH_2OH, pH 7.0, and exposing it to visible light between 500 and 700 nm, and monitoring the decrease in the absorbance at 560 nm with time (Fig. 7.1). The retinal Schiff base bond is broken by its reaction with NH_2OH in the presence of light, forming a retinal oxime. Once this covalent bond is broken, the interaction of retinal Schiff base with protein which is responsible for its absorbance diminishes, and there is an equivalent increase in the retinal oxime peak at 355 nm. Reconstitution was achieved by stepwise addition of 2 µl of 1 mM 13-cis or all-trans retinal to 3 ml of 10^{-5} M bR of washed, bleached pm. The purple color returned as a result of the reconstitution. After adding 13-cis retinal, the bleached pm was incubated in dark for ten minutes (dark adapted). At low concentrations of retinal, only a small percent of the bRs were reconstituted, thus, most of the trimeric units had only one reconstituted bR (i. e. monomer). When the

Figure 7.1 Absorption spectra of stepwise bleaching of pm.

Absorption spectra of stepwise bleaching of pm (3 ml of 10^{-5} M) bR in 0.2 M NH_2OH, pH 7.0 observed with time. (a) native pm ——— (b) through(e) partially bleached pm (f) fully bleached pm..... . The intensity of 570 nm peak + 355 nm is constant.

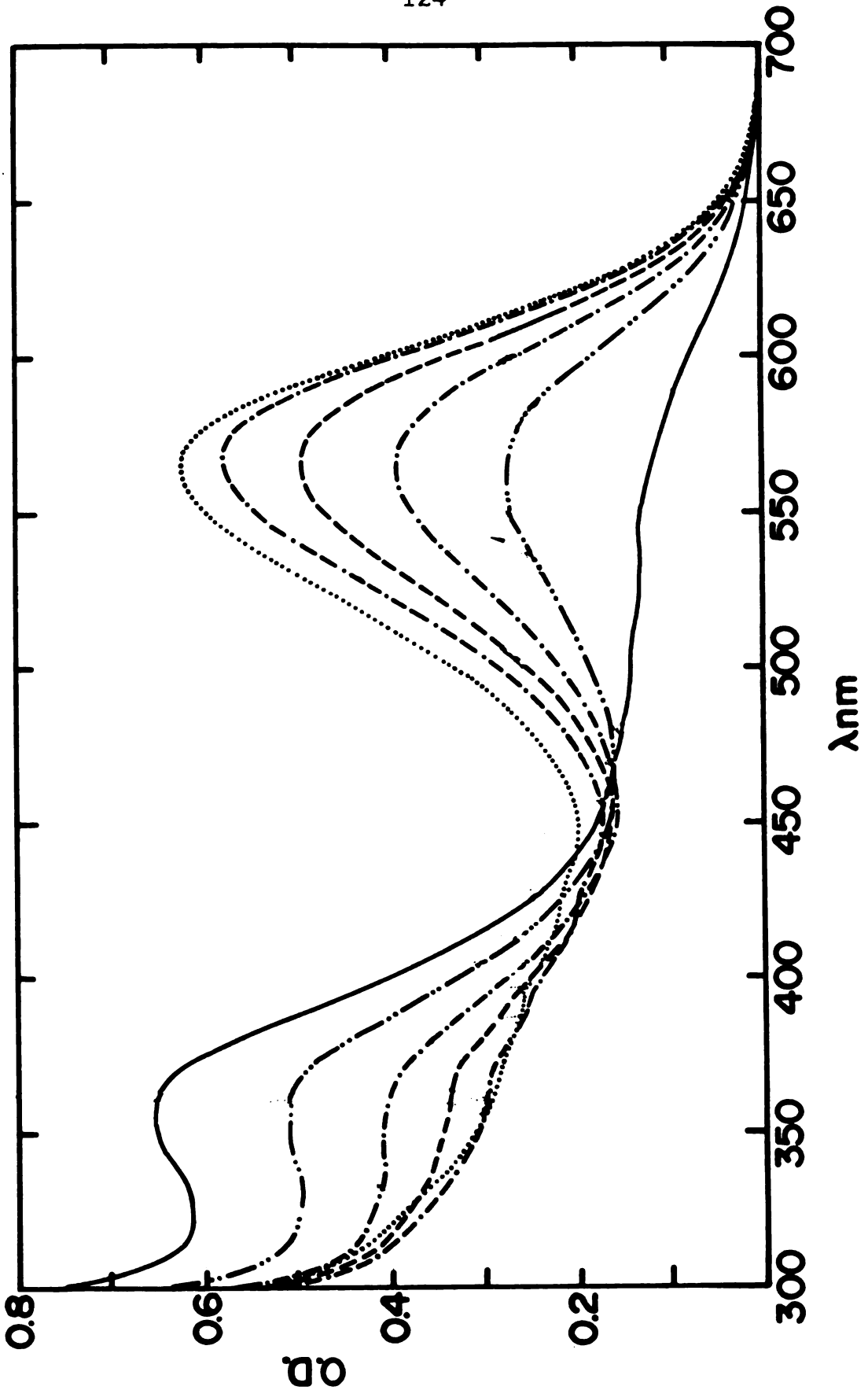
0.8
0.6
0.4
0.2
O.D.
300
350
400
450
500
550
600
650
700
λnm

concentration of retinal was increased such that the retinal to bR ratio was 1.2:1, most of the trimeric units were fully reconstituted (i. e. trimers) (Becher & Ebery, 1976). The absorption maximum of the dark adapted monomer is at 544 nm, that of the trimer is at 560 nm (Fig. 7.2). The retinal in organic solvents absorbs at 360 nm. If retinal would have been incorporated non-specifically in the membrane rather than in the specific binding site (cavity), it would have absorbed at 355-360 nm instead of absorbing at 560 nm. During the reconstitution experiments, the intensity of absorption of retinal oxime peak remained unchanged until all the bRs were reconstituted. This observation indicates that no retinals were non-specifically attached to the other (lipid) regions in pm unless all the binding sites in the bR were filled. In other words, the affinity of retinal towards the 'cavity' in the protein must be larger than towards the membrane lipids due to its amphipathic nature. The absorption spectra of the light adapted monomers and trimers were similarly obtained by adding various concentrations of all-trans retinal and exposing the sample to visible light between 500 and 700 nm for ten minutes after each addition. The absorption maximum of light adapted monomer occured at 551 nm, that of trimer occured at 568 nm, similar to that shown in Fig. 7.2. The shift of the absorption to lower energies (approximately 500 wavenumbers) compared with monomer absorption for the trimer absorption in both cases resulted from the

Figure 7.2 Absorption spectra of stepwise reconstitution of bR with all-trans retinal.

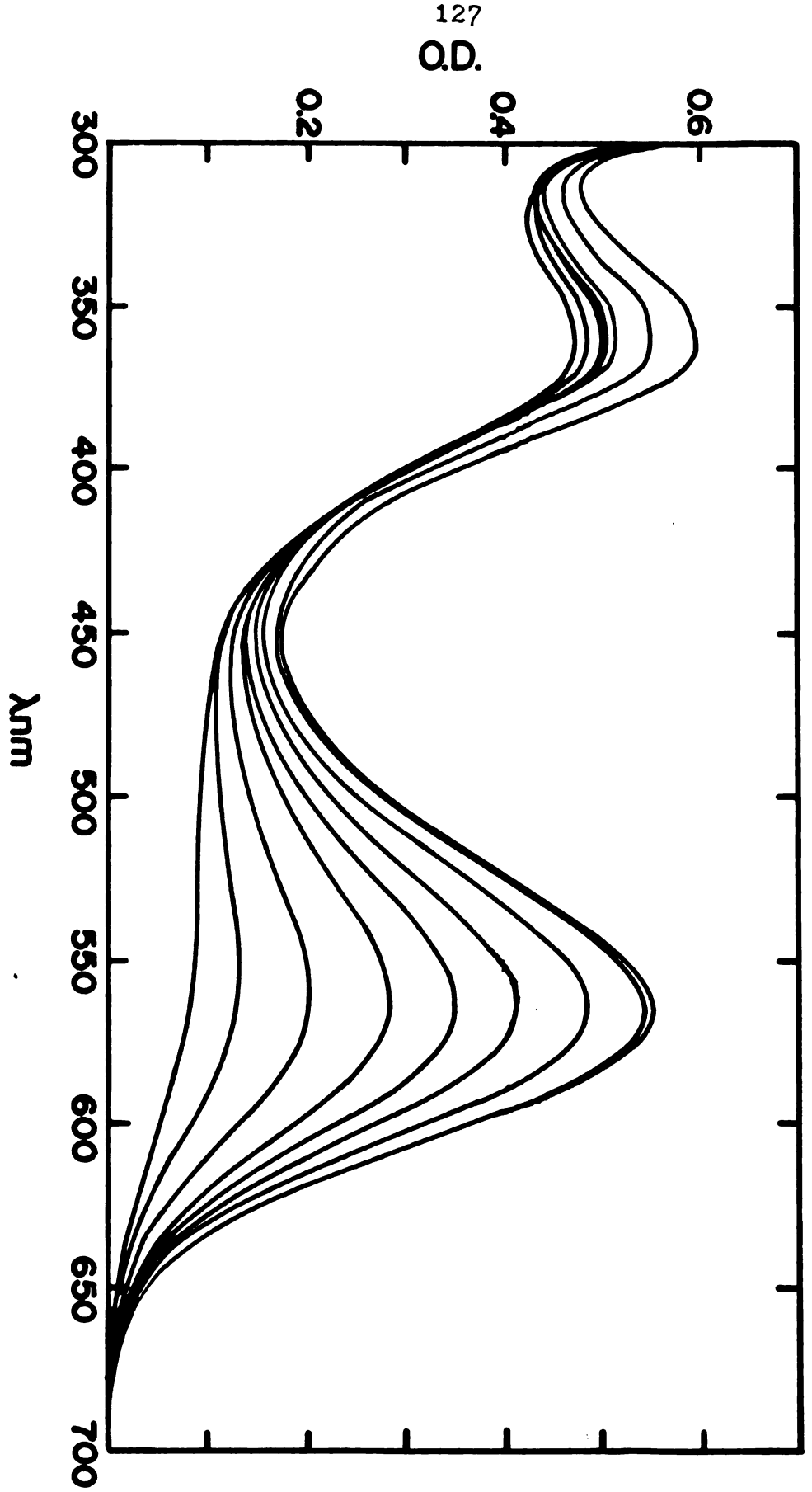
O.D.
0.2
0.4
0.6
300
350
400
450
500
550
600
650
700
λnm

exciton interaction. As discussed in chapter 4, three molecules of bR form a trimeric unit leading to P3 symmetry (each of the three molecules makes a side of an equilateral triangle).From the electron microscopy data, it seems that the retinal Schiff base situated in each of the three bR molecules also must be symmetrical around the P3 symmetry axis. However, the functional unit of symmetry of a trimeric unit may be different than the structural unit (Kriebel & Albrecht, 1976). In the case of a monomer, the majority of the trimeric units contain only one bR molecule with a chromophore. Therefore, no exciton interaction is expected. The extent of exciton interaction for pm was shown to depend on the degree of reconstitution as shown in Fig. 7.2 as the increase in the red shift upon stepwise rec reconstitution. The head-to-tail packing of the chromophores leads to a red shift in the absorption maximum. The magnitude of the red shift depends upon (i) the angle between the plane of the membrane and the plane of the chromophore (ii) the dipole moment of the chromophore in the ground state and (iii) the distance between the chromophores. The distance between the retinal-Schiff base chromophores which have P3 symmetry can be calculated by the following equations:

(i) For a degenerate transition $\Delta_{2,3}=1.75\ B\ (\theta,\phi)$...7.3

(ii) For atotally symmetric state $\Delta_1=8.5\ B\ (\theta,\phi)$ 7.4

where $B\ (\theta,\phi)$ is a function of transition dipole moments. From the experimental red shifts, $B\ (\theta,\phi)$ can be

calculated. Further,

$$R^3 = \mu_g^2 \quad |f(\theta, \phi)| \; / \; |B(\theta, \phi)| \quad \ldots\ldots 7.5$$

where μ_g is the ground state dipole moment of the chromophore, $f(\theta, \phi)$ is the dipole-dipole interaction which depends on the orientation of a chromophore in a local co-ordinate system (Kriebel & Albrecht, 1976). From these calculations, an equilateral head to tail packing of three molecules of retinal-Schiff base at an angle of about 20^{o} to the plane of the membrane can account for the CD data and would explain the observed absorption red shift.

Our CD spectra of stepwise reconstitution agreed with the absorption data (Fig. 7.3). The documented red shift in the CD spectra of the positive lobe and the increase in the intensity of both, especially the negative lobe, as a function of the degree of reconstitution was confirmed (Heyn et al, 1975),(Becher & Ebery, 1976),(Bauer et al, 1976),(Ebery, 1977). Furthermore, although the CD spectra showed a positive peak at 355 nm (Fig. 7.3), no interpretation has yet been given. Our experiments show that the magnitude of this 355 nm peak is inversely proportional to the degree of reconstitution. At 100% reconstitution, the 355 nm peak had approximately 10% intensity compared with the peak of the bleached pm. On the other hand, the 355 nm peak of the absorption spectra of the stepwise reconstitution remained unchanged upto 100% reconstitution. As

Figure 7.3 Circular dichroism spectra of stepwise reconstitution of pm with retinal.

Circular dichroism spectra of stepwise reconstitution of pm with appropriate concentration of all-trans retinal. A JASCO model ORD/UV-5 with a SPROUL Scientific SS-20 CD modification was used. The pm was suspended in0.01 M Tris pH 7.0 in a one cm. rectangular cuvette. The concentration of the bR was 200 ug/ml. The CD scale was 2 millidegrees per cm, thetime constant was 4 seconds, speed was 10 nm /minute.

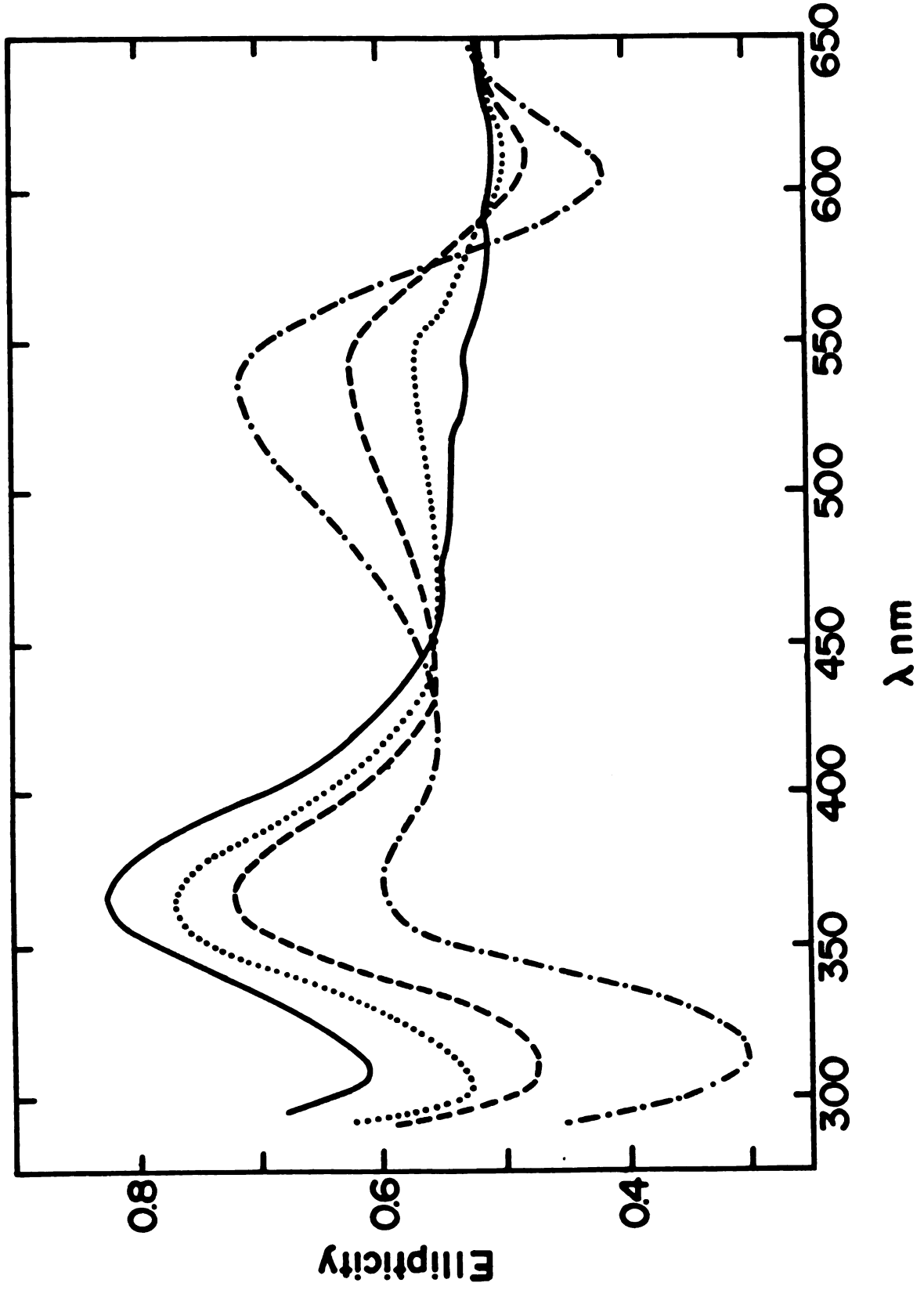
Ellipticity
0.8
0.6
0.4
300
350
400
450
500
550
600
650
λ nm

discussed earlier, the CD activity depends on the asymmetrical conformation and free retinal in solution is not optically active. Therefore, the asymmetry responsible for the 355 nm CD peak has been introduced due to the interaction of retinal with other components of the pm. Our interpretation of the 355 nm peak in the CD spectra is that it corresponds to the retinal oxime which still occupies the 'cavity', i. e. the site for the covalently bound retinal via the Schiff base linkage to bacterio-opsin even after the covalent bond is broken by NH_2OH. Only during the reconstitution of bR is that the oxime is replaced into the cavity with either 13-cis or all-trans retinal, thereby reducing the 355 nm peak. The replaced retinal oxime stays in the lipid matrix of the pm as neither dialysis, nor centrifugation with change of buffer changes the absorption at 355 nm, however, retinal oxime in the lipid bilayer is not expected to exhibit CD activity in the pm.

(f) Fluorescence of retinal oxime:

The retinal oxime fluoresced weakly in bleached pm and had an emission maximum at 490 nm. The oxime fluorescence intensity decreased as a result of the reconstitution of bacterio-opsin by retinal due to energy transfer to bR. Also, the fluorescence spectrum of the reconstituted bR became more structured (Fig. 7.4), indicating a more rigid environment for the retinal oxime in the lipids than in the cavity. This result is supported by steady state fluorescence polarization measurements.

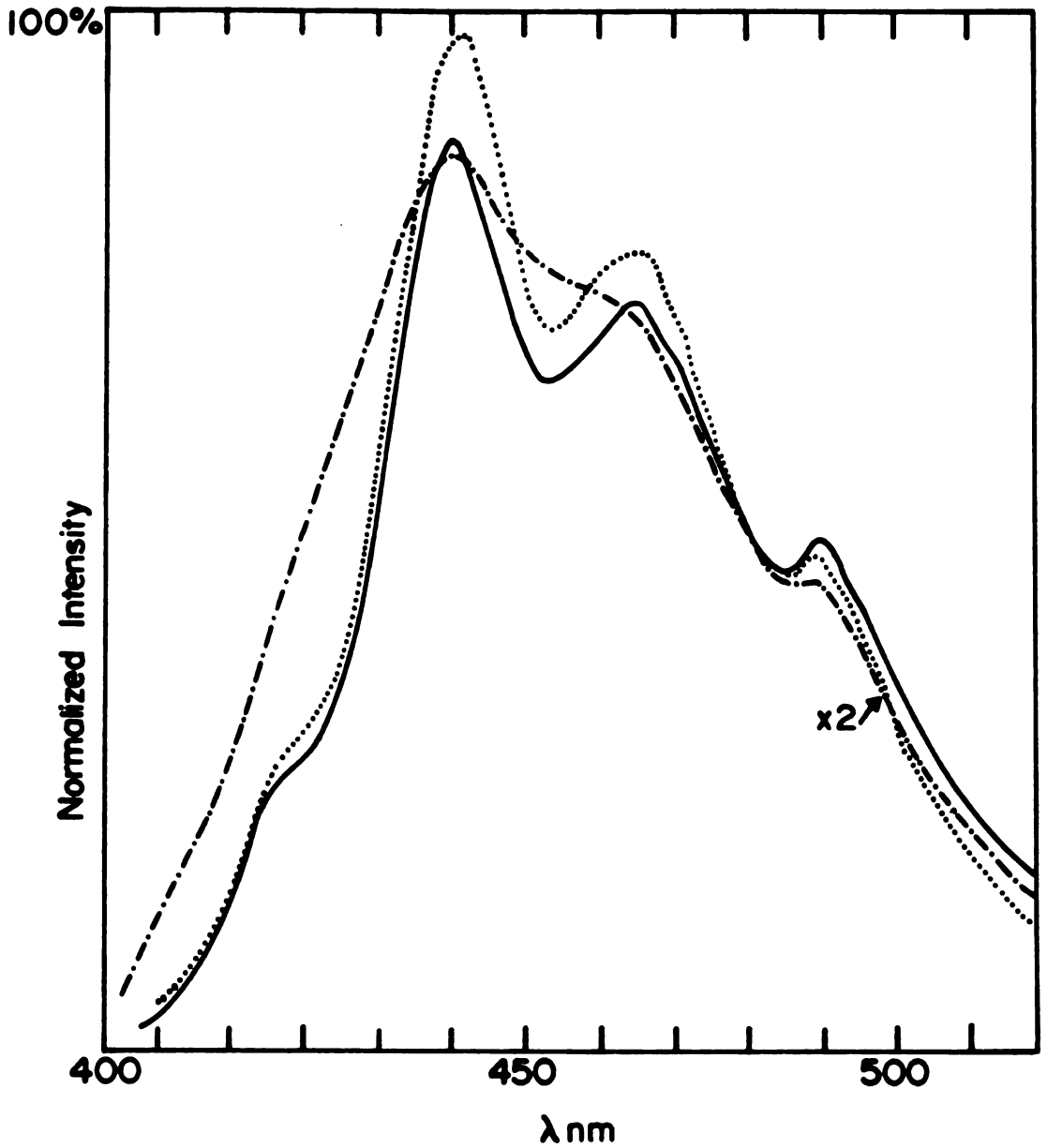

Figure 7.4 Fluorescence spectra of retinal in (i) bleached pm —.—.—.— (ii) reconstituted pm ..... and (iii) native pm ———

(g) Absorption, circular dichroism and fluorescence of fluorescence analog of bacteriorhodopsin:

The fluorescence of native pm is very weak, the lifetime reported for bR is in the picosecond range (Kaufmann et al, 1976). It is thought that a substitution of the chromophore (retinal Schiff base) with a fluorescent analog can be useful in studying chromophore-chromophore interaction, in designing energy transfer experiments and in studying the environment in the cavity. Such analog must be structurally similar to retinal, however, the formation of a Schiff base bond may not be necessary for its incorporation. We found these criteria accurate when we tried to incorporate a non-conjugated, branched linear polyene aldehyde, citral, in bleached pm. Citral can form a Schiff base linkage as that of retinal. From the absorption studies of bleached pm and citral and dialyzed bleached pm, we concluded that citral does not bind to the protein covalently because dialysis removes it. Citral is not fully conjugated and hence its structure is not rigid and probably does not assume a retinal-like configuration necessary for covalent linkage to the protein. Therefore, we decided to use a linear conjugated fluorescent polyene, the dimensions of which are similar to retinal. We have been successful in preparing a diphenyl hexatriene (DPH)-bR analog. The structure of DPH, similar linear polyenes and all-trans retinal is shown in Fig. 7.5. In the course of our study, other authors have prepared other bR-analogs

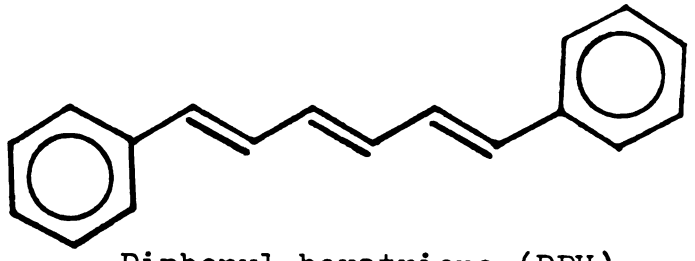

Diphenyl hexatriene (DPH)

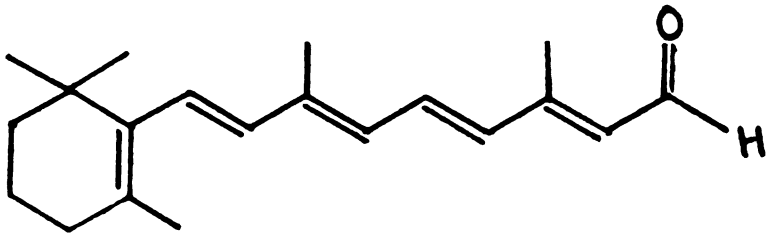

all-trans retinal

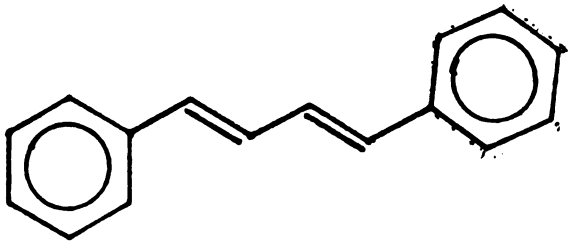

Diphenyl butadiene (DPB)

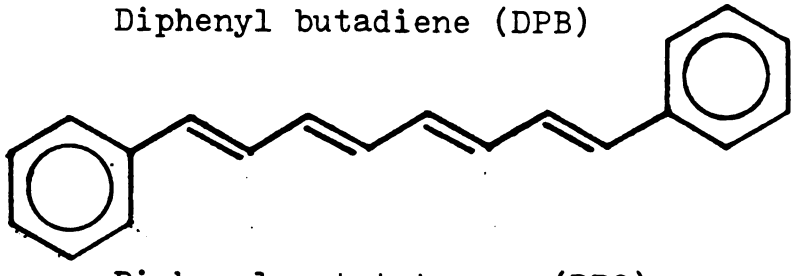

Diphenyl octatetraene (DPO)

Figure 7.5 Structure of some polyenes which may occupy the retinal cavity.

using retinal-analogs e. g. 2-dehydroretinal etc. To our knowledge, DPH-bR is the first fluorescnet analog.

The DPH-bR was obtained by adding 10 μl of 10 mM DPH in tetrahydrofuran (THF) to the bleached pm, incubating at 37°C for one hour and dialyzing the suspension at room temperature with deionized, distilled water to remove unbound probe. This preparation was then reconstituted with retinal. Control bleached pm was mixed and incubated with the same amount of THF, dialyzed then similarly reconstituted. In order to prove that DPH was incorporated in the cavity, the retinal was added to the sample and the increase in the 560 nm peak was measured. Our samples showed that 50% of the sites were occupied by DPH (Fig. 7.6). This observation was taken as an indication that DPH occupies the cavity by replacing retinal oxime and has a larger binding constant that retinal, pointing to the importance of dispersion forces for the binding of the chromophore in the protein cavity.

In order to further investigate the binding site of DPH in bR, CD spectra of bleached pm and bleached pm + DPH were obtained (Fig. 7.7).using 3 ml. of 10^{-5} M bR, 5×10^{-6} M DPH. CD measurements of DPH-bR analog show that the characteristic 355 nm oxime peak decreased in intensity as a result of DPH incorporation in the cavity. This observation indicates that DPH molecules have indeed been incorporated into the cavity, replacing the retinal oxime. Therefore, the DPH-bR analog can be used for the studies

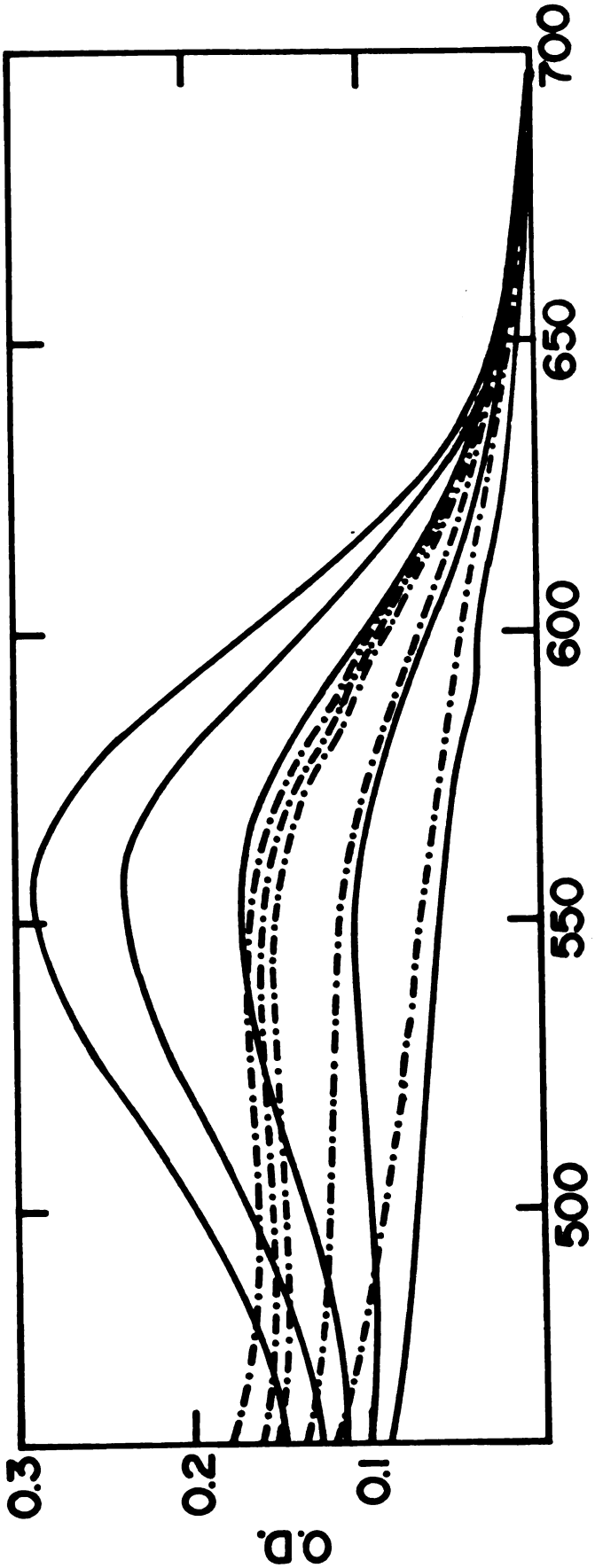

Figure 7.6 Absorption spectra of DPH-bR analog-·-·- and control bleached pm ——— with equimolar retinal.

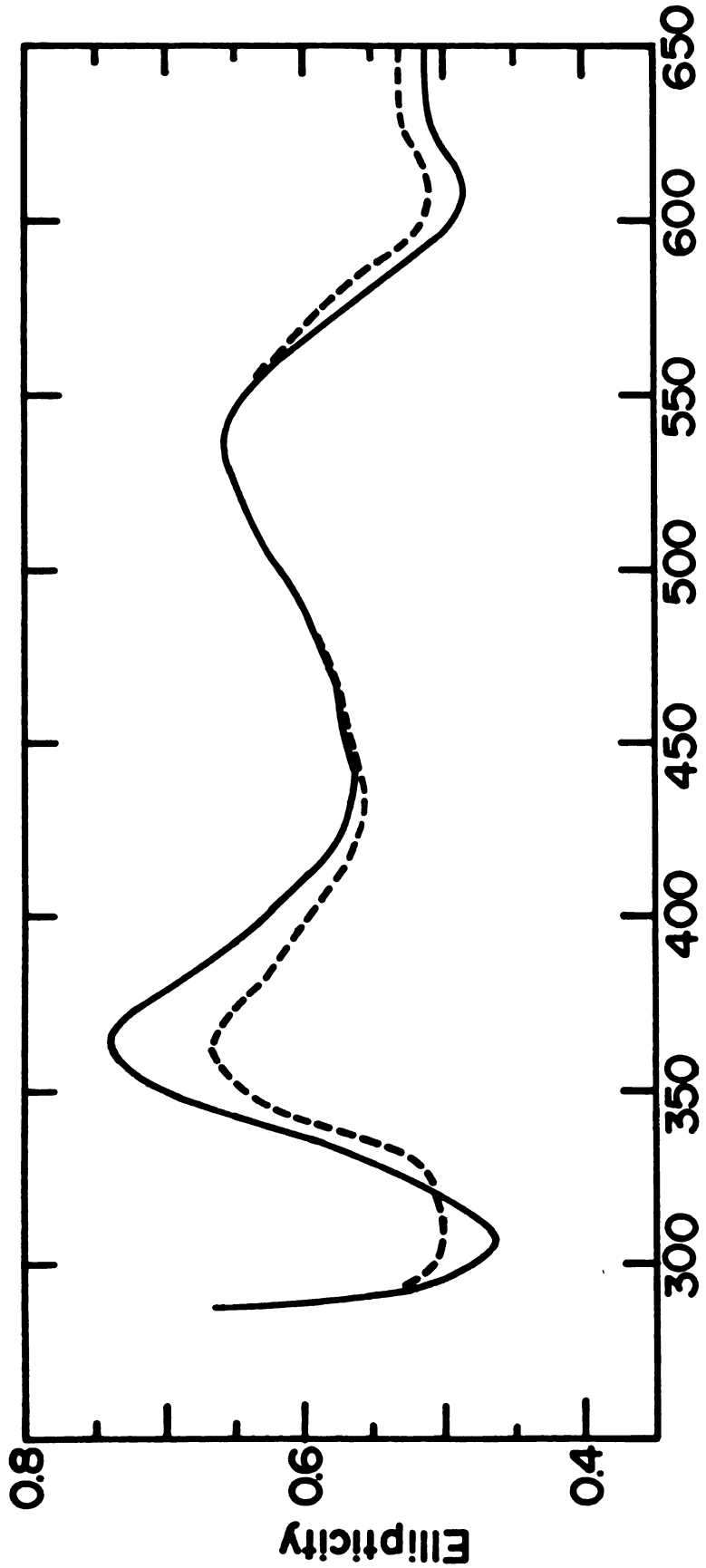

Figure 7.7 Circular dichroism spectra of DPH-bR_ _ _ _ _ and control pm ——— under conditions described in Figure 7.3.

mentioned earlier.

Fluorescence spectra of (i) bleached DPH-bR (ii) reconstituted DPH-bR and (iii) native pm + DPH were obtained (Fig. 7.8). It can be seen that the fluorescence spectra of reconstituted DPH-bR and native pm + DPH were more structured compared to the bleached DPH-bR. This result is in agreement with the fluorescence spectra of retinal oxime in the control bleached pm and reconstituted pm (Fig. 7.5) indicating a more rigid environment for the probes in the lipid matrix compared to the cavity. Steady state fluorescence polarization showed that DPH in the cavity of bR is indeed less rigidly fixed. This observation compared with other experimental evidence whcih show that the cavity can accomodate other retinal isomers. such as 11-cis in addition to 13-cis providing that their geometries are not very different from all-trans retinal (9-cis retinal cannot be incorporated)(Oesterhelt, 1974). The results described in this section indicate that DPH-bR can be successfully used to investigate the nature of the cavity.

(h) Summary:

In summary, chromophore-chromophore exciton interaction of the neighbouring retinals was confirmed with the absorption spectroscopy. The orientation of retinals seemed to be head-to-tail at about 20^{o} from the plane of the membrane. The retinal oxime occupied the cavity even after bleaching, however, it could be removed from the cavity

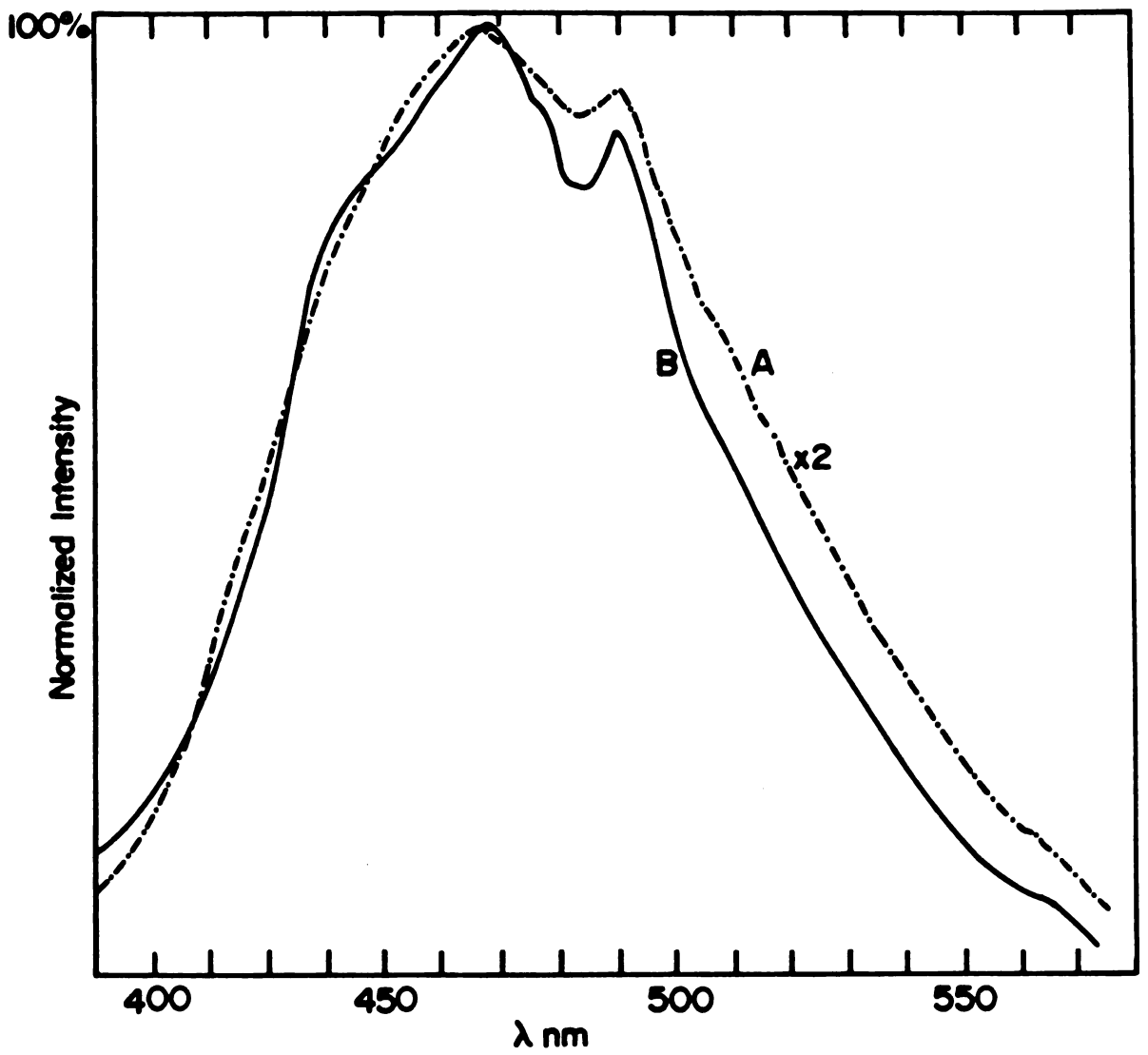

Figure 7.8 Fluorescence spectra of DPH-bR in (i) bleached pm _._._._. and (ii) in reconstituted pm ——— .

during reconstitution. A fluorescence analog of bR, DPH-bR was obtained. The absorption and the CD spectra of this analog showed that DPH occupies the cavity and, therefore, can be a useful tool to further investigate the nature of the cavity. The environment in the cavity appears to be less rigid compared to that of the lipid matrix of the pm. The results of Chapter 6 are in agreement that the rigidity of the pm lipids is indeed very high.

CHAPTER 8

FUTURE WORK

Future work for the continuation of these studies and in other areas can be divided into the following categories:

(a) Effect of environment on the growth and membrane structure/composition:

The fact that H. halobium grows in high salt concentrations makes them favourable for environmental studies. The environmental parameters that may be varied are: metabolite composition, salt concentration, temperature, light intensity, pH etc. One may examine the membrane fluidity using a variety of spin and fluorescence probes. The chemical composition of the membrane would be studied in order to relate it to the membrane fluidity.

(i) Synthetic medium: H. halobium have been shown to grow in synthetic medium instead of peptone (Onishi et al, 1972). In that case, by varying metabolite composition e. g. lowering glycerol concentration, affects carotenoid contents, information about influence of these factors on the rigidity, structure and stability of pm and cmv can be investigated. It is known that only pm lipids are sulfated (Kushwaha et al, 1975). Therefore, the pm biosynthesis may be inhibited giving rise to change in the lattice structure if inorganic sulfates are removed from the growth medium. Secondly, radioactive sulfates in pulses may be used to

monitor the biosynthesis of pm lipids and their insertation in the membrane.

(ii) Effect of salts: It has been shown that Na^+ or Mg^{2+} does not seem to change the rigidity of pm at growth temperature. It would be interesting to change the ratio of monovalent:divalent cations e. g. instead of 4 M NaCl and 20 mM $MgSO_4$, 3 M NaCl and 1 M $MgSO_4$ and to observe the effects of this salt composition on rigidity and the phase transition temperature of pm and cmv. In addition, the effect of lowering of NaCl concentration of the growth medium should be investigated.

(iii) Effect of different growth temperatures on the fluidity: H. halobium can grow upto 59°C (Oesterhelt & Stoeckenius, 1974); the cells may be grown at different temperatures and their membrane fluidity may be compared.

(iv) Effect of different light intensities on the growth: Actinic light and variation in the light intensities may be used to investigate relation between the presence of light and the formation of bR. Radioactive amino acids may be used simultaneously with light at stationary phase of bacteria to investigate the site of pm biosynthesis.

(b) Nature of the retinal binding cavity:

Diphenyl hexatriene (DPH) has been successfully incorporated in the retinal binding site (cavity) of bleached pm (chapter 7). Absorption and steady state fluorescence polarization of DPH show that it is indeed in the cavity.

This fluorescence analog of bR can be used for various experiments to investigate the nature of the cavity. Also, our data show that the retinal oxime stays in the cavity after bleaching with NH_2OH. Quantum yield and life-time of DPH is larger than that of retinal oxime making DPH more desirable for fluorescence studies. These two molecules can be used to gain information about (i) the nature of the cavity (ii) the distance of the cavity from the surface of the membrane (iii) the distance between the chromophores of the neighbouring proteins etc.

(i) Nature of the cavity: Life-time or rotational relaxation time of DPH or retinal oxime may be determined in the cavity and as a control in native pm. The energy transfer from the tryptophans of bR to DPH can also be measured to determine the proximity of tryphophans. If one incorporates DPH-aldehyde, one may expect a fluorescent Schiff base. It has been argued in the literature that the red shift in the absorption of retinal-Schiff,base in pm is due to the polarizability of residues and the presence of ions in or near the cavity. Therefore, the effect of pH or different ionic strength of suspending medium on the chromophore (DPH) aldehyde may be investigated by determining the changes in the emission properties of DPH aldehyde due to these factors. Control experiments should be done by incorporating DPH aldehyde in lipid vesicles and changing the pH or ionic strength of the bathing solution. Other control experiments would be to

incorporate DPH in native pm and to observe the changes in the emission properties. Also, efforts to incorporate DPO or DPB (see chapter 7) may provide informaion about the size of the cavity. If DPO gets incorporated to the same extent as DPH, the cavity may be longer than length of DPH. Or, if more DPB gets incorporated then DPH, the cavity may be barely large enough for dimensions of DPH.

(ii) Distance from the surface of the membrane; Measurement of the distance from the cavity to the surface of the membrane is important in terms of the solvent effects on the retinal-Schiff base. If a fluorescence probe like rubrene is added to the aqueous phase and the fluorescence energy transfer can be measured either from DPH in the cavity to rubrene or from rubrene to the chromophore of bR.

More precise experiments may be designed if, instead of adding the probe to the suspension, it can be specifically bound at a site in bR. Two approaches are possible. (a) Dansyl cadaverene (DC) is known to bind rhodopsin at a specific site using a transglutaminase. If it can be bound to bR at a specific site, it can be used as an energy transfer in this case can pinpoint the distance. Also, bR can be labelled using a covalent spin probe e. g. nitroxide maleimide or nitroxide iodoacetamide. It is known that a spin probe can quench the fluorescence of a probe by spin-orbital coupling if the distance between the two probes is less than 25 Å (Wallach et al 1975). A covalent spin probe and the DPH in the cavity may be able to interact with

each other and hence provide information about the distance between the two probes. (b) Quenching of DPH fluorescence can also be facilitated by adding ionic quenchers to the medium. If the distance between the cavity and the ion is less than the radius of collision quenching, a decrease in DPH fluorescence may be observed. By using ionic quenchers of various sizes, one may be able to obtain indicaion regarding a "pore" or a "channel" in the bR. If a specific labelling using C is achieved, it can be utilized to determine the distance of the cavity from "outside" of the cell. DC added to bind whole cells or closed vesicles containing pm, it will bind only to the outer surface of the membrane. Subsequently isolated pm will be labelled only on the outer surface. Energy transfer in this case will be less ambiguous compared with DC bound to both surfaces of the pm patches.

(iii) Distances in the trimeric unit: By making either DPH or retinal oxime as a donor and chromophore of bR in the neighbouring pretein as an acceptor, the distance between the two chromophores in a trimeric unit may be obtained. These experiments will be more meaningful in the solubilized pm where interactions between different trimeric units are not expected to occur.

(c) Conformaional changes in bR due to a photon absorption;

Fluorescence or ESR probes covalently bound to the protein at a unique site (as described in the previous

section)may provide information about the conformational changes in bR due to a photon absorption. The environment of fluorescence or spin moiety may change significantly as a result of any conformational change such as "pore opening" or any other mechanism responsible for proton dislocation. Flash spectroscopy using a very intense light is needed for these experiments.

(d) Protein-protein and protein-lipid interactions:

Protein-protein interaction seems to extend beyond the trimeric unit (Fisher & Stoeckenius, 1977). Experiments can be designed to study the protein-protein and protein-lipid interaction. Cross-linking of proteins may be performed using bifunctional reagents of known length. Thus the cross-linking of bR in the native pm and in solubilized pm can be attempted to determine the effect of solubilization on the protein-protein interaction. Photosensitive cross-linking of lipids with the lipids and proteins may be used to investigate the quantitative amount of lipids that are boundary lipids. These cross-linking lipids may be meaningful to determine number of necessary lipids for the stability of bR. The α-helical content as measured by CD and the absorbance of the chromophore can be the two criteria for the integrity of the pm in the detergents. Site-specific covalently bound spin probes may also be used to investigate the extent of multimeric unit utilizing spin-spin coupling.

(e) Relation between exciton interaction and function of bacteriorhodpsin:

The chromophore-chromophore exciton interaction raises some important questions about its function in bR. It will be interesting to investigate whether this interaction is only a by-product of the structure or whether it functions as a co-operative effect to increase the efficiency of the photon absorption. If the absorption of a photon by one molecule of bR causes conformational changes in other two molecules of the trimeric unit via exciton interaction leading to deprotonation and reprotonation of the retinal-Schiff base, the efficiency of the system will be tripled. The fact that 2.9 protons are needed to photophosphorylate one molecule of ADP (Henderson, 1977) is suggestive of this interaction. Measurement of pH using pH sensitive fluorescence cyanine dyes under various conditions of light intensity in the cell envelope vesicles and in reconstituted, pm containing vesicles (lipsomes) may prove useful.

BIBLIOGRAPHY

BIBLIOGRAPHY

Alfano, R. R., Yu, W., Govindjee, R., Becher, B., & Ebery, T. G., (1976). Picosecond kinetics of the fluorescence from the chromophore of the purple membrane protein of H. halobium. Biophysical J. 16, 541-545.

Avouris, P., Kordas, J & El-Bayoumi, M. A., (1974). Time-resolved fluorescence study of intramolecular excimer interaction in dinaphthylpropane. Chem. Phys. Letters 26, 373-378.

Azzi, A. (1975). Application of fluorescence probes of membrane studies. Quart. Rev. Biophysics, 8, 1-53.

Badley, R. A., Martin, W. G & Schneider, H., (1973). Dynami Dynamic behaviour of fluorescence probes in lipid bilayer. Biochem. 12, 268-275.

Bauer, P., Dencher, N A. & Heyn, M. P., (1976). Evidence for chromophore-chromophore interaction in the purple membrane from reconstitution experiments of the chromophore free membrane. Biophys. of Structure & Mech. 2, 79-92.

Becher, B. & Cassim, J., (1976). Effect of light adaption in the purple membrane structure of H. halobium. Biophysical J. 16, 1183-1200.

Becher, B. & Ebery, T. G,, (1976). Evidence for chromophore-chromophore (exciton) interaction in the purple membrane of H. halobium. BBRC, 69, 1-6.

Birks, J. B., (1970). Photophysics ofaromatic molecules. Ch. 3, Wiley Interscience.

Blaurock, A. & Stoeckenius, W., (1971). Structure of purple membrane. Nature New Biol. 233, 152-155.

Blaurock, A., (1975). Bacteriorhodopsin: A transmembrane pump containing α-helix. J. Mol. Biol. 93, 139-158.

Blaurock, A., Stoeckenius, W., Oesterhelt, D. & Scherphof, C., (1976). Structure of the cell envelope of H. halobium. J. of Cell Biol. 71, 1-22.

Bogomolni, R. A., Baker, R. A., Lozier, R. H. & Stoeckenius, W., (1976). Light driven proton translocation in H. halobium. BBA, 440, 68-88.

Bogomolni, R. A., (1977). Light energy conservation processes in H. halobium cells. Fed. Proc. 36, 1835-1839.

Breton, J., Viret, J. & Leteirier, F.,(1977). Calcium and chloropromazine interactions in rat synaptic plasma membranes: A spin-label and fluorescence probe study. Arch. Biochem. Biophys. 178, 625-633.

Bretscher, M. S., (1976). Directed lipid flow in cell membrane. Nature 260, 21-23.

Bridgen, J. & Walker, I. D., (1976). Photoreceptor protein from the purple membrane of H. halobium. Molecular weight and retinal binding site. Biochem. 15, 792-298.

Brown, A., (1976). Microbial water stress. Bact. Rev., 40, 803-846.

Campion, A., El-Sayed, M. A., & Terner, J., (1977). Resonsnce Raman kinetic spectroscopy of bacteriorhodopsin on microsecond scale. Biophysical J. 20, 369-375.

Capaldi, R.,(1974). A dynamic model of cell membrane. Scientific American, April 1974, 28-34.

Chance, B., Porte, M., Hess, B. & Oesterhelt, D., (1975). Low temperature kinetics of H^+ changes of bacterial rhodopsin, Biophysical J. 15, 913-917.

Chen, R. F. & Kernohan, J. C., (1967). Combination of bovine carbonic anhydrase with a fluorescent sulfanoamide. J. Biol. Chem. 242, 5813-5823.

Chignell, C. & Chignell, D., (1975). A spin label study of purple membrane from H. halobium. BBRC, 62, 136-143.

Cone, R. A., (1972). Rotational diffusion of rhodopsin in the visual receptor membrane. Nature New Biol. 236, 39-43.

Dancshazy, Z. & Karvaly, B., (1976). Incorporation of bacteriorhodopsin into a bilayer lipid membrane: A photoelectric-spectroscopy spectroscopic study. FEBS Letters 72,1 136-138.

Danon, A. & Stoeckenius, W., (1974). Photophosphorylation' in H. halobium. PNAS 71, 1234-1238.

Drachev, L. A., Frolov, V. N., Kaulen, A. D., Liberman, G. A., Ostroymov, S. A., Plakunove, V. G., Semenov, A. Y. & Skulachev, V. P., (1976). Reconstitution of biological molecular generator of electric current: Bacteriorhodopsin. J. Biol. Chem. 251, 7059-7065.

Edelman, G. M., (1976). Surface modulation in cell recognition and cell grwoth. Science 192, 218-226.

Ebery, T. G., Becher, B., Mao, B., Kilbrid, P. & Honig, B., (1977). Exciton interactions and chromophore orientation in the purple membrane. J. Mol. Biol. in press.

El-Bayoumi, M. A., (1961). Exciton theory: Application to H-bonded complexes. Dissertation, Florida State University.

Englander, J. J. & Englander, S. W., (1977). Comparison of bacterial and animal rhodopsins by hydrogen exchange studies. Nature 261, 658-650.

Esser, A. P. & Lanyi- J. K., (1973). Structure of the lipid phase in cell envelope vesicles from H. cutirubrum. Biochem 12, 1933-1939.

Farias, R. N., Bernabe, B., Morero, R. D., Sineriz, F. & Trucco, R. E., (1975). Regulation of allosteric membrane bound enzymes through changes in membrane lipid composition. BBA 415, 231-251.

Fisher, K. A. & Stoeckenius, W., (2977). Freeze-fractures purple membrane particles: protein content. Science 197, 72-74.

Forster, Th., (1951). Fluoreszenz organischer verbin dung P. 85. Gottengen: Vandehoeck & Ruprecht.

Freifelder, D., (1976). Physical biochemistry: Application to biochemistry and molecular biology. Freeman & Company.

Frye, C. D. & Edidin, M., (1970). The rapid intermixing of cell surface antigens after formation of mouse human heterokarions. J. Cell Sci. 7, 319-335.

Gochner, M. B., Kushwaha, S. C., Kates, M. & Kushner, D. J. (1972). Nutritional control of pigment and isoprenoid compound formation in extremely halophilic bacteria. Arch. Microb. 84, 339-349.

Goldschmidt, C. R., Ottolenghi, M & Korenstein, R., (1976). On the primary quantum yields in the bacteriorhodopsin photocycle. Biophysical J. 16, 839-843.

Goodenough, D. A. & Stoeckenius, W., (1972). Isolation of mouse hepatocyte gap junctions-preliminary chemical classification and X-ray diffraction. J. Cell Biol. 54, 646-650.

Gordesky, S. E., (1976). Phospholipid asymmetry in the huma human erythrocyte membrane. TIBS 1, 208-211.

Gray V.L. & Pitt, P. S., (1976). An improved synthetic growth medium for H. cutirubrum. Can. J. Micro. 22, 440-442.

Hauser, H., Levine, B. A. & Williams, R. J. P., (1976). Interactions of ions with membranes. TIBS 1, 278-281.

Henderson, R., (1977). The purple membrane from H. halobium. Ann. Rev. Biophys., Bioeng. 6, 87-109.

Henderson, R., (1975). The structure of purple membrane from H. halobium: analysis of X-ray diffraction pattern. J. Mol. Biol. 93, 123-138.

Henderson, R. & Unwin, P. N. T., (1975). Three dimensional model of purple membrane obtained by electron microscopy. Nature 257, 28-32.

Henning, U., (1975). Determination of cell shape in bacteria. Ann. Rev. Micro. 29, 45-60.

Hess, B. & Oesterhelt, D., (1974). Reversible photolysis of the purple complex from H. halobium as a basis for the function of the purple membrane. 13 th Congress of BBA, PP. 257-267.

Heyn, M. P., (1975). Dependence of exciton circular dichrosm on oscillator strength. J. of Phys. Chem. 79, 2424-2426.

Heyn, M. P., Bauer, J. J. & Dencher, N. A., (1976). A natural CD label to probe the structure of the purple membrane from H. halobium by means of exciton coupling effects. BBRC, 67, 897-903.

Hildebrand, E. & Dencher, N., (1975). Two photosystems controlling behavioural responses of H. halobium. Nature 257, 46-48.

Holland, J. Teets, R. E. & Timnick, A., (1973). Unique computer centered instrument for simultaneous absorbance and fluorescence measurements. Anal. Chem. 45, 145-153.

Honig, B. & Ebery, T. G., (1974). The structure and spectra of the chromophore of the visual pigments. Ann. Rev. Biophys. Bioeng. 3, 151-177.

Honig, B., Greenberg, A. D., Dinur E. & Ebery, T. G., (1976). Visual-pigment spectra: Implication of the protonation of the retinal Schiff base. Biochem. 15, 4598-4600.

Honig, B., Warshel, A. & Karplus, M., (1975). Theoretical studies of the visual chromophore. Accounts of Chem. Res. 8, 92-100.

Hubbard, J. S., Rinehart, C. A. & Baker, R. A., (1976). Energy coupling in the active transport of amino acids by bacteriorhodopsin-containing cells of H. halobium. J. Bact. 125, 181-190.

Hubbard, R., (1976). 100 years of rhodopsin. TIBS 1, 154-158.

Jan. L. Y., (1975). The isomeric configuration of the bacteriorhodopsin chromophore. Vision Res. 15, 1081-1086.

Kagawa Y., Ohno, K., Yoshida, M. F., Takeuchi, Y. & Sone, N., (1977). Proton translocation by ATPase and bacteriorhodopsin. Fed. Proc. 36, 1815-1818.

Kates. M., (1972). In Snyder (eds) Ether linked lipids, Chemistry and Biology. Academic Press, pp. 351-398.

Kaufman, K. J., Rentzepis, P. M., Stoeckenius, W. & Lewis, A., (1976). Primary photochemical processes in bacteriorhodopsin. BBRC 68, 1109-1115.

Keefer, L. M. & Bradshaw,,R. A., (1977). Structural studies on the H. halobium bacteriorhodopsin. Fed. Proc. 36, 1799-1 1799-1804.

Keith, A. D., Sharnoff, M. & Cohn, G. E., (1973). A summary and evaluation of spin labels as probes for biological membrane structure. BBA 300, 379-423.

Kim, E. K. & Fitt, P. S., (1977). Partial purification and properties of H. cutirubrum L. alanine dehydrogenase. Biochem J. 161, 313-320.

King, G. I., Bogomolni, R. A., Hwang, S. B. & Stoeckenius, W., (1977). Spatial location and orientation of the chromophore of bacteriorhodopsin. Biophysical J. 17, 97 .

Kliger, D. S., Milder, S. J. & Dratz, E. A., (1977). Solvent effects on the spectra of retinal Schiff bases-I. models for the bathochromic shift of the chromophore spectrum in visual pigments. Photochem. Photobiol. 25, 277-286.

Koehler, J. K., (1973). (eds) Advanced techniques in biological electron microscopy. Springler-Verlog.

Konishi
states

Kriebel
action.
purple
4583.

Kung,
Photol
907-91

Kushwa
tion a
membr

Kushw
son c
BBA 4

Land
Phot

Lany
fro

Lar
ele
hal

La
pr
ce

L
p
A

Konishi, R. & Packer, L., (1976). Light-dark conformational states in bacteriorhodopsin. BBRC 72, 1437-1442.

Kriebel, A. N. & Albrecht, A. C., (1976). Excitonic interactions among three chromphores: An application to the purple membrane of H. halobium. J. Chem. Phys. 65, 4575-4583.

Kung, M. C., Devaut, D., Hess. B. & Oesterhelt, D., (1975). Photolysis of bacterial rhodopsin. Biophysical J. 15, 907-911.

Kushwaha, S., Kates, M. & Martin, W., (1975). Characterization and composition of the purple membrane and the red membrane from H. cutirubrum. Can. J. Biochem. 53, 286-292.

Kushwaha, S., Kates, M. & Stoeckenius, W., (1976). Comparison of purple membrane from H. cutirubrum and H. halobium. BBA 426, 703-710.

Land, E. J., (1975). Photochemistry of polyenes. Photochem. Photobiol. 22, 286-288.

Lanyi, J., (1974). Salt dependent properties of proteins from extremely halophilic bacteria. Bact. Rev. 38, 272-290.

Lanyi, J.,K. & MacDonald, R. E., (1976). Existance of electrogenic hydrogen ion/sodium ion antiport in H. halobium cell envelope vesicles.Biochem. 15, 4608-4614.

Lanyi, J. K. & MacDonald, R. E., (1977). Light dependent proton gradients and electrical potential in H. halobium cell envelope vesicles. Fed. Proc. 36, 1824-1827.

Larsen, H., (1967). Biochemical aspects of extreme halophilism. pp. 97-132. In Rose, A. Y. & Wilkinson J. (eds) Advances in Micro. Physiol. 1, Academic Press, Inc.

Lee, A., (1975). Functional properties of biological membrane: A physico-chemical approach. Progress in Biophysics and Mol. Biol. 29, 3-56.

Lewis, A., (1976). Primary photochemical and photophysical processes in visual transduction. Biophysical J. 16, 204a.

Lewis, A., Marcus, M. A., Ippen, E. P., Shank, C. V., Mirsch, M. D. & Mahr, M., (1977). Sub-picosecond and picosecond dynamics of the conversion of light energy in chemical energy by bacteriorhodopsin. Biophysical J. 17, 75a.

Lewis, A., Spoonhower, J. P., Marcus, M. A. & Lemley, A. T. (1977). Kinetic resonsnce Raman spectroscopy. Low temperature and physiological investigation of bacteriorhodopsin and bacteriorhodopsin analogs. Biophysical J. 17, 77a.

Lewis, A., Spoonhower, J. P. & Perreault, G. J., (1976). Observation of light emission form a rhodopsin. Nature 260, 675-678.

Li, Y. H., Chan, L. M., Tyer, L., Moody, R. J., Himel, C. M. & Hercules. D. M., (1975). Study of solvent effects on the fluorescence of 1-(dimethylamino)-6-naphthalelesulfonic acid and related compounds. JACS 97, 3118-3126.

Linden, C. D. & Fox. C. F., (1975). Membrane physical state and function. Accounts of Chem. Res. 8, 321-327.

Long, M. M., Urry, D. W. & Stoeckenius, W., (1977). Circular dichroism of biological membranes: purple membrane of H. halobium. BBRC 75, 735-741.

Lowery, O. H., Rosebrough, N. J., Farr, A. L. & Randall, R. J., (1951). Protein measurement with the folin-phenol reagent. J. Biol. Chem. 193, 265-275.

Lozier, R. H. & Niederberger, W., (1977). The photochemical cycle of bacteriorhodopsin. Fed. Proc. 36, 1805-1809.

MacDnald, R. E.& Lanyi, J. K., (1975). Light-induced lucine transport in H. halobium envelope vesicles: A chemiosmotic system. Biochem. 14, 2882-2889.

Mantulin, W. W. & Hubert, J. R., (1973). Measurement of the temperature dependendence of the fluorescence quantum yield of organic molecules in solution. Photochem. Photobiol. 17, 139-143.

Marcus, M. A. & Lewis, A. (1977). Kinetic resonance Raman spectroscopy: Dynamics of deprotonation of the Schiff base of bacteriorhodopsin. Science 195, 1328-1330.

Marshall, C. & Brown, A., (1968). The membrane lipids of H. halobium. Biochem J. 110, 441-448.

Mendelsohn, R., (1973). Resonance Raman spectroscopy of the photoreceptor-like pigment of H. halobium. Nature 243, 22-2 22-24.

Mescher, M. F., Hansen, U. & Strominger, J. L., (1976). Formation of lipid-linked compounds in H. salinarium. Presumed intermediate in glycoprotein synthesis. J. Biol. Chem. 251, 7289-7294.

Mescher, M. F. & Strominger, J. L.,(1976). Purification and characterization of a procaryotic glycoprotein from the cell envelope of H. salinarium. J. Biol. Chem. 251, 2005-2014.

Michel, H. & Oesterhelt, D., (1976). Light induced changes of the pH gradient and the membrane potential in H. halobium. FEBS Letters, 65, 175-178.

Milder, S. J. & Kliger, D. S., (1977). Solvent effects on the spectra of retinal Schiff bases-II Model for convergence and clustering of visual pigment spectra. Photochem. Photobiol. 25, 287-291.

Mortonosi, A., (1976) (eds) The enzymes of biological membranes: physical and chemical techniques. Plenum Press.

Naqvi, R. K., Gonzalez-Rodriguez, J., Cherry, R. J. & Chance, B., (1973). A spectroscopic technique for studying protein rotation in membranes. Nature New Biol. 245, 249-251.

Nicolson, G. L., (1976). Transmembrane control of the receptors on normal and tumor cells. I. cytoplasmic influence over cell surface components. BBA 457, 57-108.

Oesterhelt, D., (1974). Bacteriorhodopsin as allight driven proton pump. Azzone (eds) Membrane proteins in transport and phosphorylation. North Holland.

Oesterhelt, D. & Hess, B., (1973). Reversible photolysis of the purple complex in the purple membrane of H. halobium. Eur. J. Biochem. 37, 316-326.

Oesterhelt, D., Meentzen, M. & Schumann, L., (1973). REversible dissociation of the purple complex in bacteriorhodopsin and identification of 13-cis and all-trans retinal as the chromophores. Eur. J. Biochem. 40, 452-463.

Oesterhelt, D. & Schuhmann, L., (1974). Reconstitution of bacteriorhodopsin. FEBS Letters, 44, 262-265.

Oesterhelt, D. & Stoeckenius, W., (1971). Rhodopsin like protein from the purple membrane of H. halobium. Nature New Biol. 233, 149-152.

Oesterhelt, D. & Stoeckenius, W., (1973). Functions of a new photoreceptor membrane. PNAS 70, 2853-2857.

Oesterhelt, D. & Stoeckenius, W., (1974). Isolation of the cell membrane of H. halobium and its fractionation into red and purple membrane. Methods in Enzymology, 31, Biomembranes, part A, Fleisher, S. & Packer, L., (eds) Academic Press, 667-678.

Oldfield, L., Keough, K. & Chapman, D., (1972). The study of hydrocarbon chain mobility in membrane system using spin-lable probes. FEBS Letters, 20, 344-348.

Overath, P., Thilo, L. & Trauble, H., (1976). Lipid phase transition and membrane function. TIBS 1, 186-189.

Packer, L., Konishi, T. & Shieh, P., (1977). Conformational changes in bacteriorhoodpsin accompanying ionophore activity. Fed. Proc. 36, 1819-1823.

Pettei, M., Yudd, A. P., Nakahashi, K., Henselman, R. & Stoeckenius, W., (1977). Identification of retinal isomers isolated from bacteriorhodopsin. Biochem. 16, 1955-1959.

Plachy, H., Lanyi, J. K. & Kates, M., (1976). Lipid interactions in the membrane of extremely halophilic bacteria. Electron spin resonance and dialometric studies of the bilayer. Biochem, 13, 4906-4913.

Platt, J. R., (1949). Classification of spectra of catacondensed hydrocarbons. J. CP. 17, 484-496.

Potts. W. J., (1952). Purification of hydrocarbon for use in spectroscopy. JCP, 20, 809-811.

Racker, E. & Stoeckenius, W., (1974). Reconstitution of purple membrane vesicles catalyzing light-driven proton uptake and ATP formation. J. Biol. Chem. 249, 662-663.

Racker, E., (1974). Mechanism of ATP formation in mitochondria and ion pumps. BBA 13 th Congress, pp. 269-281.

Renthal, R. & Lanyi, J. K., (1976). Light induced membrane potential and pH gradient in H. halobium envelope vesicles. Biochem. 15, 2136-2144.

Rothman, J. & Lenard, J., (1977). Membrane asymmetry. Science, 195, 743-753.

Salton, M. R. J., (1971). The bacterial membranes. Manson, L. A., (eds) Biomembranes Vol. 1, Plenum Press.

Schellman, J. A., (1968). Symmetry rules for optical rotation. Accounts of Chem. Res. 1, 144-151.

Sehgal, S. N. & Gibbons, N. E., (1960). Effects of some metal ions on the growth of H. cutirubrum. Can J. Micro. 6, 165-169.

Seliskar, C. J. & Brnad, L., (1971). Electronic spectra of 2-aminonaphthalene-6-sulfonate and related molecules. II. Effects of solvent medium on the absorption and fluorescence spectra. JACS 93, 5414-5420.

Shieh, P. & Packer, L., (1976). Photoinduced potentials across a polymer stabilized planar membrane, in the presence of bacteriorhodopsin. BBRC 71, 603-609.

Shimshick, E. & McConnell, H. M., (1973). Lateral phase separations in phospholipid membranes. Biochem. 12, 2351-2360.

Singer, S. J., (1974). The molecular organization of membra membranes. Ann. Rev. Biochem. 43, 805-833.

Singer, S. J. & Nicolson, G. L., (1972). The fluid mosaic model of the structure of cell membrane. Science 175, 720-731.

Steck, T. L., (1976). The organization of proteins in the human red bllod cell membrane. A review. J. Cell Biol. 62, 1-19.

Stier, A. & Sackmann, E., (1973). Spin labels as enzyme substrates. Heterogeneous lipid distribution in liver microsomal membranes. BBA 311, 400-408.

Stoeckenius, W., (1976). The purple membrane of salt-loving bacteria. Sc. American. 234, 38-46.

Stoeckenius, W. & Kanau, W. H., (1968). Further characterization of particular fractions from lysed cell envelopes of H. halobium and isolation of gas vacuole membranes. J. Cell Biol. 38, 337-357.

Stoeckenius, W. Lozier, R. H., (1974). Light energy conversion in H. halobium. J. Supramol. Structure 2, 769-774.

Stoeckenius, W. & Rowen, R., (1967). A morphological study of H. halobium and its lysis in media of low salt concentrations. J. Cell Biol. 34, 365-393.

Sumper, M. & Herrmann, G., (1976a). Biogenesis of purple membrane: regulation of bacteriorhodopsin synthesis. FEBS letters 69, 149-152.

Sumper, M. & Herrmann, G., (1976b). Biosynthesis of purple membrane: control of retinal synthesis by bacterio-opsin. FEBS Letters 71, 333-336.

Tinoco, I., (1963). The exciton contribution to the optical rotation of polymers. Rad. Res. 20, 133-139.

Tokunaga, F., Iwata, T. & Yoshizawa, T., (1977). Synthetic pigment analogs of the purple membrane protein. Biophysical J. 17, 76a.

Vanchermeulen, D. C. & Govindjee, R., (1971). 12-(9-anthroyl) stearic acid and atebrin as fluorescent probes for energatic states of chloroplasts. FEBS Letters, 45, 186-191.

VanHolde, K. M., (1971). Physical Biochemistry. Foundation of Modern Biochemistry series. Hager, L. & Wold, F. (eds). Prince-Hall.

Vanderkooi, J., (1972). Temperature sensitivity of fluorescent probes in the presence of model membranes and mitochondria. pp. 359-365 im Thaer, A. & Sernetz (eds) Fluorescence Techniques in cell biology. Springler-Verlog.

Vanderkooi, J., Fischkof, S., Chance, B. & Cooper, R. A., (1974). Fluorescence probe analysis of lipid architecture of natural and artificial cholesterol-rich membranes. Biochem. 13, 1589-1595.

Waggoner, A. S. & Stryer, L., (1970). Fluorescent probes of biological membranes. PNAS 67, 579-589.

Wallach, D.,& Winzler, R. J., (1974). Evolving strategies in themembrane research, Ch. 9. Springler-Verlog.

Ware, W., Doemeny, L. J. & Nemzek, T. L., (1973). Deconvolution of fluorescence nad phosphorescence decay curves: A least square method. JPC. 77, 2038-2042.

Weller, H. & Haug, A., (1977). Effects of Ca^{2+} and K^{+} on the physical state of membrane lipids in T. acidophila. J. Gen. Micro. 99, 379-382.

Wisnieski, B. & Iwata, K., (1977). Electron spin resonance evidence for vertical asymmetry in animal cell membrane. Biochem. 16, 1321-1326.

Wunderlich, R., Ronai, A., Speth, V., Seeling, J. & Blume, A., (1975). Thermotropic lipid clustering in tetrahymena membranes. Biochem. 14, 3730-3735.

Ygerabide, J. & Stryer, L., (1971). Fluorescence spectroscopy of an oriented model membrane. PNAS 68, 1217-1226.